unclassified

SECURITY CLASSIFICATION OF THIS PAGE

(2)

DTIC ELECTE D
16 1990
B

DTIC FILE COPY

REPORT DOCUMENTATION PAGE

1a. REPORT SECURITY CLASSIFICATION: Unclassified	1b. RESTRICTIVE MARKINGS
2a. SECURITY CLASSIFICATION AUTHORITY	3. DISTRIBUTION/AVAILABILITY OF REPORT: Approved for Public Release Distribution is unlimited
AD-A229 007 R(S)	5. MONITORING ORGANIZATION REPORT NUMBER(S): AFOSR-TR- 90 1131
6a. NAME OF PERFORMING ORGANIZATION: University of Arizona; 6b. OFFICE SYMBOL (If applicable):	7a. NAME OF MONITORING ORGANIZATION: AFOSR/NA
6c. ADDRESS (City, State and ZIP Code): Aerospace & Mechanical Engineering, Building No. 16, Tucson, Arizona 85721	7b. ADDRESS (City, State and ZIP Code): Building 410, Bolling AFB, DC 20332-6448
8a. NAME OF FUNDING/SPONSORING ORGANIZATION: AFOSR; 8b. OFFICE SYMBOL (If applicable): N/A	9. PROCUREMENT INSTRUMENT IDENTIFICATION NUMBER: AFOSR - 88 - 0163
8c. ADDRESS (City, State and ZIP Code): Building 410, Bolling AFB, DC 20332-6448	10. SOURCE OF FUNDING NOS.

PROGRAM ELEMENT NO.	PROJECT NO.	TASK NO.	WORK UNIT NO.
6110F	2307	A3	

11. TITLE (Include Security Classification): COMPUTATIONAL STUDIES OF COMPRESSIBILITY EFFECTS ON DYNAMIC STALL

12. PERSONAL AUTHOR(S): K.-Y. Fung, Associate Professor

13a. TYPE OF REPORT	13b. TIME COVERED	14. DATE OF REPORT (Yr., Mo., Day)	15. PAGE COUNT
Final Scientific	FROM 6/01/88 TO 8/31/90	90/09/27	94

16. SUPPLEMENTARY NOTATION

17. COSATI CODES			18. SUBJECT TERMS (Continue on reverse if necessary and identify by block number)
FIELD	GROUP	SUB. GR.	
	20.04		Dynamic Stall, Airfoils, numerical, experiments

19. ABSTRACT (Continue on reverse if necessary and identify by block number)

The dynamic stall characteristics of several airfoils in sinusoidal pitch oscillations as well as in constant rate pitch ramps over a wide range of unsteady flow conditions have been investigated. It is found that the flow before the onset of stall can be considered quasi-steady and predicted using inviscid theory, that the effect of unsteadiness on the onset of dynamic stall depends on the airfoil geometry and whether the flow has become locally supersonic, and that the effect of the freestream Mach number on the onset is rather insensitive to the airfoil geometry. Our analysis on both experimental and numerical results predicts the presence of a separation bubble at the leading edge. It also suggests that the bursting of the bubble, or failure to reattach after the initial separation, is the onset mechanism for most of the dynamic stall cases being studied here. The effects of transition on bubble bursting (the onset of massive separation or dynamic stall) are studied numerically by choosing the location at which the turbulence model is switched from molecular to turbulent eddy viscosity in the numerical code. It was found that at angles of attack close to the static stall angle, minor movements in the transition point could cause a separation bubble to burst, and that bubble bursting is more susceptible to transition point location in a locally supersonic flow than a subsonic flow. Keywords: Pitch motion/oscillation; Flow separation; Mathematical models; Eddies; Fluid mechanics; Model tests. (EDC)

20. DISTRIBUTION/AVAILABILITY OF ABSTRACT	21. ABSTRACT SECURITY CLASSIFICATION
UNCLASSIFIED/UNLIMITED ☐ SAME AS RPT. ☒ DTIC USERS ☐	Unclassified

22a. NAME OF RESPONSIBLE INDIVIDUAL	22b. TELEPHONE NUMBER (Include Area Code)	22c. OFFICE SYMBOL
Capt. Henry E. Helin	(202) 767-0471	N/A

DD FORM 1473, 83 APR EDITION OF 1 JAN 73 IS OBSOLETE.

unclassified

Final Scientific Report

AFOSR Grant No. 88-0163

June 1, 1988 to August 31, 1990

COMPUTATIONAL STUDIES OF COMPRESSIBILITY EFFECTS ON DYNAMIC STALL

Submitted to:

Air Force Office of Scientific Research

Submitted by:

K.-Y. Fung, Associate Professor
Department of Aerospace &
Mechanical Engineering

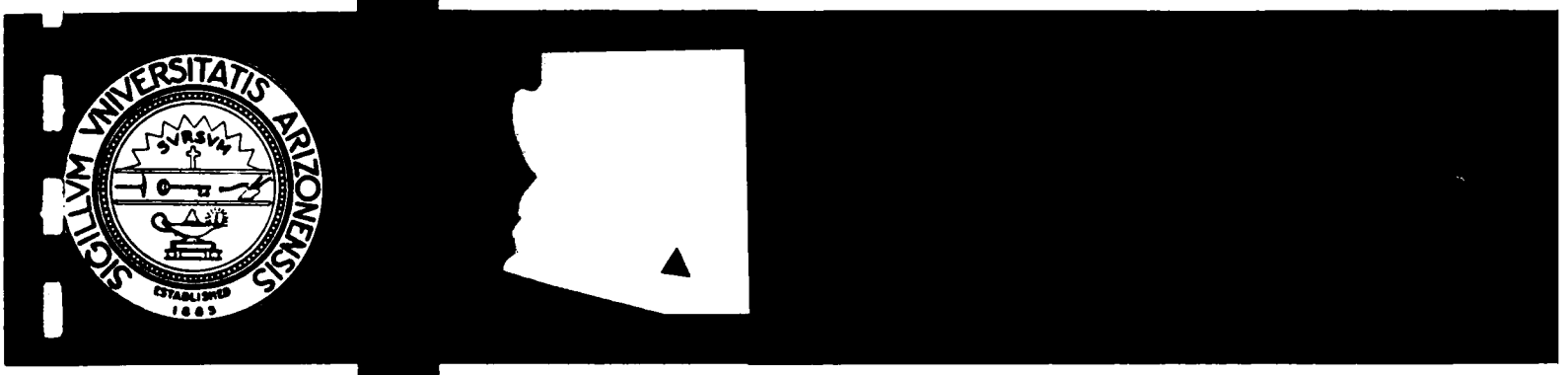

ENGINEERING EXPERIMENT STATION
COLLEGE OF ENGINEERING AND MINES
THE UNIVERSITY OF ARIZONA
TUCSON, ARIZONA 85721

1.0 SYNOPSIS

This final report summaries the activities and results of an investigation on the onset mechanism of dynamic stall supported on the grant AFOSR-88-0163 for the period from June 1, 1988 to August 31, 1990. Results of this research have been presented at the NASA/AFOSR/ARO workshop, Ames Research Center, April 17-19, 1990, and will be presented formally as AIAA paper 91-0003 at the January Aerospace Sciences Meeting, Reno. Two students were supported on this grant. One received the Masters and the other is anticipating his PhD.

The dynamic stall characteristics of several airfoils in sinusoidal pitch oscillations as well as in constant rate pitch ramps over a wide range of unsteady flow conditions have been investigated. It is found that the flow before the onset of stall can be considered quasi-steady and predicted using inviscid theory, that the effect of unsteadiness on the onset of dynamic stall depends on the airfoil geometry and whether the flow has become locally supersonic, and that the effect of the freestream Mach number on the onset is rather insensitive to the airfoil geometry. Our analysis on both experimental and numerical results predicts the presence of a separation bubble at the leading edge. It also suggests that the bursting of the bubble, or failure to reattach after the initial separation, is the onset mechanism for most of the dynamic stall cases being studied here. The effects of transition on bubble bursting (the onset of massive separation or dynamic stall) are studied numerically by choosing the location at which the turbulence model is switched from molecular to turbulent eddy viscosity in the numerical code. It was found that at angles of attack close to the static stall angle, minor movements in the transition point could cause a separation bubble to burst, and that bubble bursting is more susceptible to transition point location in a locally supersonic flow than a subsonic flow.

2.0 NOMENCLATURE

α $\mapsto$ angle of attack

C_f $\mapsto$ skin friction Coefficient

C_ℓ $\mapsto$ lift coefficient

C_{ℓ_α} $\mapsto$ lift curve slope

C_p $\mapsto$ $(P-P_\infty)/1/2\rho U^2_\infty$, wall static-pressure coefficient

$C_{p_{min}}$ $\mapsto$ maximum suction peak, minimum pressure coefficient

c $\mapsto$ airfoil chord

δ $\mapsto$ boundary layer displacement thickness

γ $\mapsto$ ratio of specific heats

K $\mapsto$ $\frac{R_{\delta_{s'}}}{\sqrt{R}}$ Reynolds number ratio at separation

k $\mapsto$ $\omega c/2U_\infty$ reduced frequency, non-dimensional frequency, Strouhal number

Λ $\mapsto$ $\frac{\theta_s^2}{\upsilon}\frac{\Delta U}{\Delta S}$ Gaster's bubble parameter

M $\mapsto$ Mach number

R $\mapsto$ $\frac{U\,L}{\upsilon}$ Reynolds number

θ $\mapsto$ boundary layer momentum thickness

S' $\mapsto$ coordinate along airfoil contour from stagnation point

T.P. $\mapsto$ Point of transition from laminar to turbulent flow for numerical model

U $\mapsto$ velocity

u $\mapsto$ velocity in x-direction

v $\mapsto$ velocity in y-direction

$\eta, \xi, \tau \mapsto$ transformed coordinates

subscripts

0 $\mapsto$ value at stagnation point

c $\mapsto$ based on the chord

e $\mapsto$ just outside the boundary layer

∞ $\mapsto$ free-stream value

s $\mapsto$ value at laminar separation point

3.0 INTRODUCTION

Rapid upward pitching of the airfoil is an important consideration for the design of helicopter rotor blades. This upward pitching unsteady motion of the airfoil delays boundary layer separation and hence, increases the lift beyond the static stall angle. Once the angle of attach reaches a certain point a vortex separates from the leading edge. The low suction pressure associated with this separation vortex increases lift very dramatically for as long as the vortex remains on the surface of the airfoil. This process of creating lift beyond the static stall lift limit has become known as dynamic stall. Dynamic stall was first observed on helicopters when designers observed that the lift on a helicopter rotor blade in high speed flight was greater than what they had predicted by conventional aerodynamics. The shaped area in Figure 1 marks the dynamic stall area where the flow speed relative to the rotor blade is slow and the angle of attack is rapidly being pitched up. Ham and Garelick[1] observed that this extra lift could be explained if the lift on the retreating-blade, the blade moving in the opposite direction of flight, is greater, due to equivalent rapid pitching motions, than the lift predicted by steady flow theory. Harper and Flanigan[2] showed that the lift of an aircraft can be significantly increased if the aircraft is pitched at a rapid rate. Recent interests in improving the maneuverability of fighter aircraft and helicopters require an expansion of the flight envelop to include separated flow conditions. Research in dynamic stall has progressed steadily, but a lack of understanding about the mechanisms of static stall compounded with the numerous parameters of dynamic stall has kept dynamic stall an incomplete research topic.

In absence of dynamic effects, the flow over an airfoil at angles of attack beyond the static stall value must have been massively separated. The process of separation, however, depends on the condition of the flow preceding the flow at stall.

According to McCullough and Gault[3], there are three types of static stall: trailing-edge stall, thin-airfoil stall, and leading-edge stall. Trailing-edge stall is characterized by the movement of the turbulent separation point forward from the trailing edge. Thin-airfoil stall is preceded by laminar flow separation at the leading edge with laminar or turbulent reattachment at a point downstream which move rearward with increasing angle of attack. The body streamline that bifurcates at the separation point and merges at the reattachment point encompasses a region commonly referred to as a long separation bubble, since its length can be comparable to the chord. Leading-edge stall is also preceded by laminar flow separation near the leading edge but with almost immediate reattachment due to rapid transition to turbulent flow. The size of the region between separation and reattachment is comparable to the thickness of the boundary layer, and grows shorter as the stall angle is approached. At stall, immediate reattachment is no longer favorable, resulting in a massive separation of the boundary layer, or bursting of the separation bubble.

The occurrence of a stall for a pitching airfoil may be delayed, or in some cases totally avoided, to a much higher angle than the static stall value. Ericsson and Reding[4] reviewed the various delay mechanisms found in a wide range of dynamic stall experiments and presented heuristic models for their prediction. As commented in the review paper by Carr[5], the process of dynamic stall involves many events (Figure 2) and a large number of parameters. The dynamic stall events can be divided into three flow regimes: (1) the attached flow regime, in which the boundary layer remains thin despite the static stall angle is exceeded; (2) the separated flow regime, in which the boundary layer has broken down into a vortex dominated flow; (3) the reattachment regime, the recovery to attached flow after most of the vortexes have moved downstream of the trailing edge while the airfoil is returning to an angle below the static stall value. The key feature is, however, the development and downstream convection of a so-called dynamic stall vortex when the boundary layer is massively

separated, causing large changes in the aerodynamic forces on the airfoil. The formation of the dynamic stall vortex signals the end of the attached flow regime beyond which analytic techniques are less likely to be successful, since a separated flow is far more complex than an attached flow.

Here, an attempt is made to study the attached flow regime for airfoils undergoing oscillatory and ramp-type motions about the static stall angle and characterize the conditions of the boundary layer before the onset of separation and the formation of the dynamic stall vortex.

4.0 ORGANIZATION OF EXPERIMENTAL DATA

In order to study the onset mechanism of dynamic stall, two experimental data sets were examined. The first of these sets was preformed at NASA Ames Research Center by McCroskey, McAlister, Carr and Pucci[6]. A listing of the data sets from this experiment is presented in Appendix A. This data set includes experiments on eight airfoils: NACA 0012, Ames A-01, Wortmann FX-098, Sikorsky SC-1095, Hughes HH-02, Vertol VR-7, NLR-1, and NLR-7301. For each of these eight airfoils, pressure histories were recorded for sinusoidal pitch oscillations. These oscillations varied in mean angle as well as amplitude of oscillation and pitching frequency. During the oscillation, 200 averaged pressures were recorded on 26 pressure transducers. The free-stream Mach number was varied from as low as 0.035 to 0.302. In total the McCroskey data comprises 1226 cases for an average of 153 cases per airfoil. Figure 3 shows three different types of lift cycles obtained from the McCroskey data. Figure 3a shows a sudden increase in C_{ℓ_α} which is called the dynamic overshoot. The dynamic overshoot is created by the suction peak of the separation vortex traveling down the airfoil chord. Figure 3b shows a quasi-steady, very low k, lift cycle where the flow separates at the static stall angle. At this low frequency, the pressure and lift behave as for static airfoil. The low frequency cases

are useful as base cases in order to compare dynamic cases to static cases. Figure 3c shows a fully attached case where the static stall angle is exceeded and the lift exceeds the maximum static C_ℓ yet the flow remains attached throughout the entire dynamic cycle. For many practical applications this dynamic stall effect is preferred. This case has the advantage of nearly a forty percent increase in lift past the static stall value without the adverse effect of a sudden loss in lift, as in Figure 3a.

The second set of data was collected at United Technologies Research Center by Lorber and Carta[7]. A listing of the data sets from this experiment is presented in Appendix B. The Lorber and Carta data was collected on a Sikorsky SSC-A09 airfoil section in both sinusoidal pitch oscillations as well as constant pitch rate ramps. For constant rate pitching, the airfoil was held at a constant angle of attack. Then using a constant pitching rate, the airfoil was pitched past the static stall angle. The airfoil was then held constant at this angle of attack for some time after stall. A representative case of a lift curve is presented in Figure 4. Lorber and Carta used eighteen primary pressure transducer locations and took 1000 time samples. The advantage of this data set is that there are 5 times the number of time steps per case compared to the McCroskey data. On the other hand, there are only 19 cases compared to the 1226 cases in the McCroskey data.

5.0 SUCTION PEAK ANALYSIS

This study began by examining the existing dynamic stall data. The amount of pressure data was enormous, so a plan was created to examine the hundreds of pressure distributions associated with each pitch cycle. In order to view the change in the pressure distribution in real time, computer graphics were used to create a "movie" of the pressure distribution, the change in the lift, and the change in the moment. From these movies, a better understanding of the interrelationship between these three parameters was formed. This relationship is shown in Figure 5. Figure 5 was created

by a snap-shot of the screen during a run of the movie program. The three plots that appear in Figure 5 are C_p vs. chord, C_ℓ vs. α, and C_ℓ vs. C_m. The entire curve changes for each time step for the C_p vs. chord plot. The upper surface pressure distribution is indicated by the red line and the lower surface pressures by the green line. The other two plots have the entire cycle plotted and a solid red circle moves around the loop with changing time steps. Figure 5 shows the pitching cycle at $C_{p_{min}}$. Notice the lift has not yet reached its maximum value, but is at a plateau. This is the time step just before the vortex is shed from the leading edge. Shedding occurs in the next time step. What is not shown in Figure 5 is the time scale involved, but the movie program does provide a clear and insightful study of the time scale involved in the dynamic stall process. From the time of maximum suction peak, it was observed that the vorticity shed from the leading edge travels at about one third the speed of the free-stream flow. The vorticity being shed is evident. It clearly shows that this vorticity packet flowing over the airfoil is responsible for the sudden increase in the slope of the lift curve past the static stall angle. With the aide of the movie program, all of these cycles can be examined by viewing the time dependent pressure distribution. Viewing the pressure distribution in this way gives the investigators excellent insight into the flow field of the entire oscillating airfoil, but gives little information about the local effects near the leading edge where the vortex was shed.

From an examination of extensive experimental data, it was found that the maximum suction peak $C_{p_{min}}$ attainable in a course of upward pitching motions past the static stall angle is a good indicator of the onset of the dynamic stall process. For the frequency and pitch rate range in these experiments and if the flow remains attached, the suction peak should lag behind α_{max}. A sudden drop in suction peak suggests that the boundary layer has separated. The pressure at the point of maximum lift would not provide any insight into the mechanism of stall because this is the point where the vortex has left the trailing edge of the airfoil and the flow is fully separated

already. By examining $C_{p_{min}}$, the parametric dependency of stall onset can be characterized at the time the mechanism of stall is present.

Figure 6 shows the dependency of the maximum suction peak on the free stream Mach number for all the dynamic stall experiments of Reference 6 on the NACA 0012 airfoil. The solid line in Figure 6 represents the critical C_p at which the local flow velocity equals the speed of sound, or mathematically defined as:

$$C_{P,cr} = \frac{2}{\gamma M_\infty^2}\left[\left(\frac{1+\left[(\gamma-1)/2\right]M_\infty^2}{1+(\gamma-1)/2}\right)^{\gamma/(\gamma-1)} - 1\right] \qquad [1]$$

The square symbols represent suction peaks for static stall cases at various Mach numbers, and other symbols represent maximum suction peaks for different reduced frequency ranges. Except for a few cases in which the flow is fully attached throughout the oscillation cycle, all maximum peak suction values for nonzero pitching frequencies are above the static values, the squares, for a Mach number. For values below the critical C_p, a general trend can be observed that the higher the frequency, the higher the suction peak overshoot above the static stall value. However, values above the critical C_p, become almost insensitive to the pitching frequency. Hence, the lift is less sensitive to change in frequency at higher Mach numbers and the dynamic effect vanishes. This insensitivity was first pointed out by Fung and Carr[8]. Figure 7 shows the same relationship for the Vr7 airfoil. In this case, the overshoot is much more pronounced showing the Vr7 airfoil to be much more sensitive to frequency. Another way to see this effect is by examining the local Mach number as a function of the free-stream Mach number. The local Mach number on the airfoil surface can be found using the following equation.

$$M_a = \left\{ \frac{2}{(\gamma-1)} \left[\frac{1+[(\gamma-1)/2]M_\infty^2}{\left(\frac{\gamma M_\infty^2}{2} C_{p,a} + 1\right)^{\frac{\gamma-1}{\gamma}}} - 1 \right] \right\}^{\frac{1}{2}} \qquad [2]$$

Where a is a point on the airfoil surface. Thus when surface Mach number is plotted against free-stream Mach number, the C_p limit appears as a straight line in Figure 8, showing a limit on the local Mach number attainable without separation.

Suction peak values of the Lorber and Carta[7] data set are plotted in Figure 9. The Lorber and Carta data have values for a higher Mach number, 0.4, and constant rate pitching instead of sinusoidal pitching. Figure 9 shows that even with a different pitching scheme and a higher Mach number, the same phenomenon that led Fung and Carr to suggest that shocks are involved in the onset of separation exists.

The effect of unsteadiness on the maximum suction peak, or the onset of stall is examined further in Figure 10. Five cases based on two airfoils from Reference 6 were carefully chosen to isolate effects from other parameters. Figure 10 shows that two different airfoils do not respond to increasing frequency the same way. Of particular interest is the slope, which characterizes the degree to which the onset of stall can be delayed with increased favorable unsteadiness. Both airfoils appear to be relatively independent of frequency at the high Mach number, 0.301, but for the lower Mach numbers, the maximum suction peak increases with increasing frequency although not at the same rate. The dramatic differences of these slopes drove much of this study to concentrate on these two airfoils to see just how the Vr7 airfoil gets such an advantage in lift despite having similar static values.

The effect of Mach number on the stall onset is investigated by comparing two cases of the same pitching scheme but different airfoils. Figure 11 shows how Mach number affects the maximum suctions peak. Although the two curves in Figure 11 are different, they are simply offset by the camber created lift of the Vr7 airfoil. Since the

offset remains constant with increasing Mach number, the Mach effect is independent of airfoil geometry. Another interesting characteristic of Figure 11 is the change in sign of the slope near M=0.2. The change in slope is caused by the transition from a subcritical Mach number to a supercritical Mach number case.

At this point there are two questions that needed to be answered. The first question is what exactly are the differences between subcritical and supercritical cases? Secondly, although the effect the frequency has on the suction peak is known, what is the effect of the frequency on the entire pressure distribution? An approach to the answers was accomplished by plotting the pressure distribution as a function of chord position and angle of attack. The results were displayed as color 2-D contour plots. When viewed as slides projected side by side on a large screen, differences between supercritical and subcritical cases were evident as were the effects of frequency. Contours for Mach=0.185 and Mach=0.301 are plotted in Figure 12. Figure 12 shows the pressure coefficient over the entire chord as a function of change in angle of attack. The initial angle of attack is shown in the upper right hand corner of each plot. The amplitude as well as the reduced frequency is shown under the title of each plot. From Figure 12 and the information gathered by viewing many similar contours, a great deal can be learned about the differences between supercritical and subcritical cases. It was observed that the pressure gradients for the lower Mach number cases were much greater, that the separation process occurs much more quickly in the high Mach number cases, and that there was very little change in the pressure distributions when the frequency was changed from a high value to a higher value. This is the same phenomenon that was observed when just the suction peaks were examined, but here the down stream and time dependent effects are more clear. A great number of cases were examined in this fashion. Figures 13-17 are all black and white examples of the types of plots of the pressure coefficient as a function of chord and the instantaneous angle of attack for the NACA 0012 airfoil. Note that in Figures 13-17, the Y-axis is

labeled from the initial angle of attack. Thus y=0 indicates the initial angle of attack which is denoted in the upper right hand corner. The Y-axis scale is one degree change in angle of attack. From the initial angle of attack, α then increases by the amount of the amplitude, denoted below the plot title, and then decreases. Figures 13 and 14 show the effect of increasing the frequency for a low Mach number separated flow. In Figure 13 where the reduced frequency, k, is 0.099 separation occurs at about α=8 degrees, but in Figure 14 where k=0.149 separation occurs at about α=9 degrees. In comparison, Figure 15 show a fully attached case where there is no flow separation. Figures 16 and 17 are the high Mach number analogy for Figures 14 and 15. In Figure 16, where k=0.024 separation begins at α=4.5 degrees, but in Figure 17 where k=0.145 separation doesn't begin until α=7 degrees. These figures show the dynamic effect in a way that the frequency effect is easily seen.

6.0 BOUNDARY LAYER ANALYSIS

After examining the experimental data sets, it became evident a better understanding of the conditions of the boundary layer before the onset of stall was needed. Of particular interest is the region near the leading edge where the onset of stall begins. Figure 18 shows the locations of the pressure transducers for the McCroskey[6] data set. Since there are only two or three transducers in the first two or three percent of the chord, the resolution of the experimental data near the leading edge is not fine enough for an analysis to be performed to determine the conditions of the boundary layer. To remedy this inadequacy, a computational approach was adopted and a sequence of numerical calculations was performed.

The NACA 0012 and the Vr7 were chosen for their most distinctive dynamic stall behaviors amongst the seven airfoils tested in Reference 6. Two Mach numbers, 0.185 and 0.301, were chosen for most of the test cases were performed at these values.

The ARC2D code originally programmed by J. L. Steger and modified by Thomas Pulliam[9] was chosen for the study here. ARC2D is an implicit finite difference code for solving the two-dimensional Euler and Navier-Stokes equations. The formulation for ARC2D begins with the strong conservation law form of the two-dimensional Navier-Stokes equations in Cartesian coordinates. The equations in non-dimensional form are written as follows.

$$\partial_t Q + \partial_x E + \partial_y F = R^{-1}\left(\partial_x E_v + \partial_y F_v\right) \qquad [3]$$

where

$$Q = \begin{bmatrix} \rho \\ \rho u \\ \rho v \\ e \end{bmatrix} \quad , \quad E = \begin{bmatrix} \rho u \\ \rho u^2 + p \\ \rho uv \\ u(e+p) \end{bmatrix} \quad , \quad F = \begin{bmatrix} \rho v \\ \rho uv \\ \rho v^2 + p \\ v(e+p) \end{bmatrix}$$

$$E_v = \begin{bmatrix} 0 \\ \tau_{xx} \\ \tau_{xy} \\ f_4 \end{bmatrix} \quad , \quad F_v = \begin{bmatrix} 0 \\ \tau_{xy} \\ \tau_{yy} \\ g_4 \end{bmatrix}$$

$$\tau_{xx} = \mu\left(4u_x - 2v_y\right)/3$$
$$\tau_{xy} = \mu\left(u_y + v_x\right)$$
$$\tau_{yy} = \mu\left(-2u_x + 4v_y\right)/3$$

$$f_4 = u\tau_{xx} + v\tau_{xy} + \mu \Pr^{-1}(\gamma - 1)^{-1}\partial_x\left(\left\{\frac{\gamma P}{\rho}\right\}^2\right)$$

$$g_4 = u\tau_{xy} + v\tau_{yy} + \mu \Pr^{-1}(\gamma - 1)^{-1}\partial_x\left(\left\{\frac{\gamma P}{\rho}\right\}^2\right) \qquad [4]$$

The equations are then transformed from Cartesian coordinates to general curvilinear coordinates with the variables τ, ξ and η.

$$t=\tau,\ \xi=\xi(x,y,t),\ \eta=\eta(x,y,t) \qquad [5]$$

The graphical representation of the transformation from Cartesian coordinates to generalized curvilinear coordinates is shown in Figure 19. To represent the Cartesian

derivatives ∂_x and ∂_y of Equation [3] in terms of the curvilinear derivatives, the chain rule is used.

$$\begin{bmatrix} \partial_t \\ \partial_x \\ \partial_y \end{bmatrix} = \begin{bmatrix} 1 & \xi_t & \eta_t \\ 0 & \xi_x & \eta_x \\ 0 & \xi_y & \eta_y \end{bmatrix} \begin{bmatrix} \partial_\tau \\ \partial_\xi \\ \partial_\eta \end{bmatrix} \qquad [6]$$

Applying the chain rule to Equation [3] the Navier-Stokes equations can be written in the form as Equation [7]

$$\partial_\tau Q + \xi_t \partial_\xi Q + \xi_x \partial_\xi E + \eta_x \partial_\eta E + \xi_y \partial_\xi F + \eta_y \partial_\eta F = R^{-1}\left(\xi_x \partial_\xi E_v + \eta_x \partial_\eta E_v + \xi_y \partial_\xi F_v + \eta_y \partial_\eta F_v\right) \qquad [7]$$

Pulliam's code was modified to run on both the Cray 2 and the Cray-YMP super computers for this study. Also, input/output changes were made to improve post-processing capabilities. Although ARC2D can be run in many modes, for this first series of runs it was set to calculate steady, inviscid, 2D solutions for a C-grid. The inviscid C-grid for the Vr7 airfoil is shown in Figures 20 and 21. The hyperbolic C-grid was generated with a program developed by Tim Barth at NASA Ames Research Center. The grid used for the NACA 0012 calculations is similar to the Vr7 grid. Both grids are 249 by 67 for a total of 16,683 intersections. The results of these runs are summarized in Table 1. The angle of attack, α, was chosen to range from 7.0 degrees to the point at which a shock induced unsteadiness caused the steady calculation not to converge. These results give a detailed description of the pressures on the airfoil surface. This description could then be compared with that of the experimental cases to determine if viscous and unsteady effects are important.

Typical computational and experimental results are shown in Figures 22 and 23. Surprisingly good agreement are found between the computed and experimental

pressure distributions for the same C_ℓ up to the value at which the maximum suction peak or onset of stall occurs. Which suggests that the attached flows before stall onset are quasi-steady and viscous effects are unimportant to the pressure distribution. These pressure distributions were then used to estimate the velocity at the edge of the boundary layer on the airfoil surface.

The laminar separation bubble has been mentioned several times so far in this report, but now it will be carefully defined and investigated. Near the leading edge of an airfoil at a high angle of incidence the adverse pressure gradient just past the maximum suction peak can become large enough for the flow to separate from the airfoil. After separation, if the critical Reynolds number is exceeded, the flow may become turbulent. If this happens close enough to the point of separation, the increased mixing of the turbulent flow may be sufficient to reattach the flow. In the region between the separation and the reattachment a region of reversed flow exists. This region is commonly referred to as a laminar separation bubble. A sketch of a laminar separation bubble appears in Figure 24. In Figure 24, a closed bubble is shown so that the zero streamline leaves the body at S and reattaches at A. Streamlines from infinity stay outside this boundary. The reattachment is caused by a transition from a laminar boundary layer to a turbulent boundary layer at the point B. In literature separation bubbles have been characterized by the Reynolds number at separation, $R_{\theta s}$ or $R_{\delta s}$. Owen and Klanfer[10] analyzed tests in which bubbles were observed to form two distinct types of bubbles. First, a short bubble for which $R_{\delta s}$ is always greater than 500 and whose length is of the order of 1 percent of chord. A short bubble contracts with increasing angle of attack. Secondly, a long bubble for which $R_{\delta s}$ is always less than 500 and whose length is of the order of 2 or 3 percent of the chord. A long bubble grows with increasing angle of attack. Owen and Klanfer also stated that the bubble must be of one kind only, with no intermediate state. Gaster[11] stated that if the flow is laminar at separation, the downstream behavior of the

flow can only depend on the local Reynolds number and pressure distribution. Also, since the flow is almost stationary inside the separated region, the perturbation of the potential flow is such that the pressure is constant under the laminar shear layer. From this Gaster concluded, the shape of the bubble is dependent on the pressure distribution of a fully attached flow. Thus the proper pressure gradient parameter to describe bubble behavior must be based on the unseparated potential flow.

In order to characterize the bubbles involved in dynamic stall, analytical methods were used. The first of these methods required calculating the momentum thickness at separation. Since the inviscid numerical results provide the velocity at the surface, we adopted Tani's[12] separation prediction procedure, which is based on Prandtl's equation of motion for two-dimensional boundary layer flow, i.e,

$$\frac{u\partial u}{\partial x}+\frac{v\partial v}{\partial y}=U_e U_e'+\upsilon\frac{\partial^2 u}{\partial y^2} \qquad [8]$$

then the momentum thickness is defined as

$$\theta=\int_0^\infty \frac{U}{U_\infty}\left(1-\frac{U}{U_\infty}\right)dy \qquad [9]$$

and the displacement thickness is defined as

$$\delta=\int_0^\infty \left(1-\frac{U}{U_\infty}\right)dy \qquad [10]$$

and the momentum thickness is computed using Thwaites[13] formula, which combined with the definition of the momentum thickness yields an expression for the momentum thickness at separation as a function of the surface velocities from the stagnation point to the point of separation, i.e.,

$$\left(\frac{\theta}{c}\right)^2 R = 0.441\left(\frac{U}{U_\infty}\right)^{-6}\int_0^{S'}\left(\frac{U}{U_\infty}\right)^5 d\left(\frac{S'}{c}\right) \qquad [11]$$

As Tani suggested, the displacement and momentum thicknesses can be related as $\frac{\delta_{s'}}{\theta_{s'}} = 3.7$, where s' denotes separation. This assumption does not affect our result as will be shown, because this factor simply becomes a constant in front of the final expression. Applying this constant to [11] yields a formula for the displacement thickness at separation,

$$\delta_{s'} = 3.7\sqrt{\frac{0.441}{R}\left(\frac{U}{U_\infty}\right)^{-6}\int_0^{S'}\left(\frac{U}{U_\infty}\right)^5 d\left(\frac{S'}{c}\right)} \qquad [12]$$

Now K is introduced as the ratio of the Reynolds number at separation over the square root of the free-stream Reynolds number. This ratio is,

$$K = \frac{R_{\delta_{s'}}}{\sqrt{R}} \quad \text{where} \quad R_{\delta_{s'}} = \frac{U_{s'}\delta_{s'}}{\upsilon} \qquad [13]$$

After simplification,

$$K = \frac{3.7U_{s'}}{U_\infty}\sqrt{0.441\left(\frac{U}{U_\infty}\right)^{-6}\int_0^{S'}\left(\frac{U}{U_\infty}\right)^5 d\left(\frac{S'}{c}\right)} \qquad [14]$$

K is calculated by integrating the computed inviscid pressure distribution from the stagnation point to the assumed separation point. The assumed separation point is the point where velocity has fallen six percent from its maximum value. The integration is performed with a trapezoidal integration routine. In addition, the location of the stagnation, maximum velocity, and separation points are quadratically interpolated to smooth out the grid effects. Now K is plotted in Figure 25 against C_ℓ in the form suggested by Curle and Skan[14]. They observed that K drops fairly sharply to a minimum as C_ℓ increases, and than increases with further increase in C_ℓ. It was

determined that the minimum value of K was a possible explanation of bubble breakdown. Their theory states that as C_ℓ increases beyond the critical value, laminar separation will take place. If the value of K is large enough and R_{δ_s} is greater than 500, the separation will be short. As C_ℓ increases K decreases, and if it decreases sufficiently, the short bubble may burst. Figure 25 shows this relationship. The interesting points of Figure 25 include the differences between the low and high Mach numbers, the effect of locally supersonic flow, and different airfoils. The two curves for M=0.301 are very close to those for the lower Mach number until just before the flow is locally supersonic, indicated by the arrows. They descend, reach a minimum, and then increase. The increase is shortly after the flow becomes locally supersonic and the static stall is exceeded. Thus for the higher Mach number cases, bubble bursting is likely to be the stall onset mechanism, and the sudden decrease in slope just before the flow becomes locally supersonic is due to the compressibility effect which moves the separation point further upstream to a more laminar location than in incompressible flow. On the other hand, the curves for M=0.185 descend, reach a minimum, increase, and then descend again. The cause for this second descent is, again shown by the arrows, the change from subcritical to supercritical flow. Since the angle of attack at the first minimum is below 11 degrees for both airfoils and the static stall angle is 13.4 degrees, the bubble will not burst at the first minimum. If the bubble does not burst at or before the first minimum, bursting is unlikely to occur after since the flow is increasingly more turbulent as the lift increases. Therefore, the type of static stall is trailing edge, which agrees with the data in Reference 6. At the local maximum of the K curves, the suction peak location begins to move faster, due to compressibility, upstream than the downstream movement of the stagnation point as the angle of attack increases, resulting in a decrease in K, a momentum thickness at separation. For the lower Mach number cases, unsteady effects delay boundary layer

separation until, even at this low free-stream Mach number, the flow becomes locally supersonic, suggesting that compressibility effects cause the bubble to burst.

Gaster[11] made a correlation between the momentum thickness and the length of the separation bubble. He stated that since the momentum thickness varies only slowly near separation and C_f is small, it is a better length parameter than the rapidly changing displacement thickness. He then theorized that if the two parameters R_{θ_s} and $\frac{\theta_s^2}{\upsilon}\frac{\Delta U}{\Delta S}$ do in fact control bubble behavior, bursting should yield a unique relationship between them. Gaster combined his data with McGregor's[15] and Crabtree's[16] work and plotted the relationship shown in Figure 26. Figure 26 shows two important features. First, all symbols shown are to the right of Owen's[10] bursting criterion. This implies bubble existence. Also, all the points, except for one, are in the short bubble region. Since Owen and Klanfer stated that all bubbles must be of one kind only, for these airfoils the bubble form must be short. Thus a short bubble burst would lead to the leading edge stall.

7.0 EFFECTS OF TRANSITION

Since bubble bursting or failure to reattach is likely to be the onset mechanism of leading edge stall, the effect of transition on reattachment is assessed numerically here. The Baldwin and Lomax[17] turbulence model is chosen for this study. The way an algebraic turbulence model works in a code is the addition of an eddy viscosity to the flow starting from an user-specified point on along the down stream coordinates. The location of this point mimics, in some sense, the transition from laminar to turbulent process, and is critical to the calculation of lift values and the identification and classification of laminar separation bubbles. The case where the transition point is at the leading edge of the airfoil would correspond to tripping the boundary layer at the leading edge in an experiment. In this case, there would be turbulent flow over the

entire airfoil and there would be no laminar separation bubble. Alternately, if the transition point was placed at the trailing edge, the calculation may not approach a steady state since the flow will be unable to reattach under laminar conditions. In order to calculate the proper lift and the corresponding flow, an appropriate transition point needs to be chosen before any calculation can proceed. Table 2 lists a series of computational experiments we conducted to study the effect of the transition point placement on flow reattachment.

For a free-stream Mach number of 0.185 and a moderate angle of attack, 10.0 degrees, the flow is relatively insensitive to transition point placement. With a T.P. of 0.01 or 0.02 the computed lift value reaches rapidly an asymptotic value and the residual is low suggesting a converged solution. The flow fields for these two cases appear as Figures 27 and 28. When the T.P. is moved to 0.1, the residual reflects a solution that is not converged, but the lift value is still reasonable, noting that there is much more laminar flow than would physically exist for the given Reynolds number. The flow field for this case is shown in Figure 29. If the T.P. is moved to 0.5, the flow is massively separated as shown in Figure 30. These results show that good lift values can be predicted with extremely high transition points(0.1) and converged solutions can be obtained with moderately high transition points(0.02).

The sensitivity to transition point placement near stall increases significantly. Since the static stall angle is 15.9 degrees for M=0.185, several runs were made at α=15.5. Figures 31 and 32 show fully converged solutions with reasonable lift values for transition points of 0.01 and 0.015 respectively. Interestingly, if the transition point is moved to 0.016, the flow becomes moderately separated as shown in Figure 33. Moving the transition point for 0.015 to 0.016 corresponds to moving the T.P. one grid line. This shows that the transition point is sensitive to the fine measurement of one grid line near stall.

In order to examine the effects of Mach-supercritical flow on transition point sensitivity, several runs were made for M=0.301. A couple of runs were made at the moderate angle of attack of 10.0 degrees, but the angle was not sufficient to produce supercritical flow, so the results behaved like the M=0.185 cases. Since the static stall angle for M=0.301 is 13.43, the angle for calculation was chosen to be 13.25. For this Mach number, calculations were made with transition points up to 0.0125 and produced good lift values with converged solutions. Results for transition points of 0.01 and 0.0125 are shown in Figures 34 and 35. When the transition point was moved to 0.0135, which corresponds to moving one grid line, the calculation produced negative densities during the run. Since ARC2D was being run in non-time-accurate mode, the time step is scaled by the Jacobian. In this case, a vortex forms at the leading edge as the flow develops. The separation vortex develops rapidly, and the non-time-accurate method is too crude for a meaningful prediction. In order to see this effect more clearly, a time accurate run was performed. The run was started from the converged solution of M=0.301, T.P.=0.0125, and α=13.25. With the T.P. set at 0.0135, 500 iterations with a time step of 0.001 were calculated. The 500^{th} iteration corresponds to the flow traveling one-half of a chord length from the time of the converged solution. The solution from this run is shown in Figure 36. Although the lift value did not change significantly from the previous calculation, the sonic line on the down stream side, or shock, has moved to almost one grid line down stream and is closer to the transition point. With more time steps, the flow separates because the shock is close to the laminar region. Figures 37 and 38 show this massive separation. This again support the conjectures that the dynamic stall onset mechanism may be compressibility effect related and the reattachment of a separating boundary layer, or failure to reattach, is an important part of the separation process.

8.0 CONCLUSIONS

The results in this report clarify, support, and extend the analysis and observation reported in Fung and Carr[8] for higher Mach numbers, up to 0.4. and constant rate pitching cases. Both the frequency and Mach effects were examined for dynamic stall cases. It was determined that although the lift values for different airfoils can be different due to camber, the effect of changing Mach number is the same for different airfoils. Conversely, the response to changing frequency can be vastly different for different airfoils. It is believed that the difference in frequency effect is due to the shape of the leading edge of the airfoils.

In the analysis of the experimental data, several interesting features of the flow field were examined. First, the time the separated vortex takes to travel the length of the airfoil is related to one-third of the free-stream velocity. Also observed were some differences between Mach-supercritical and subcritical cases. The pressure gradients for subcritical cases are much higher than for supercritical cases. The separation process is more abrupt for the high Mach number or supercritical cases. Finally, as the Mach number increases the flow becomes more and more insensitive to increases in pitching frequency.

In order to investigate possible dynamic stall mechanisms, an inviscid numerical code was used to determine the pressure distribution on the airfoil surface. After computing the inviscid flow field for two airfoils at two different Mach numbers and several different angles of attack, it was shown that quasi-steady inviscid theory could be used to determine the pressure distribution just before the onset of stall. These inviscid pressure distributions were then used to compute the growth of the boundary layer and determine the momentum thickness at separation. This analysis supports the existence of a laminar separation bubble, which is prone to burst as the airfoil undergoes dynamic stall motions. In the case of M=0.185, an interesting result was found. At low angles of attack the flow is subcritical, the boundary layer calculations

suggest that bubble bursting would not occur. Whereas, at high angles of attack the boundary layer calculations suggest that bubble burst would occur soon after the flow becomes Mach-supercritical. This further suggests that the mechanism of dynamic stall is compressibility effect related.

To study the effects of transition on flow reattachment, a Navier-Stokes code with an algebraic turbulence model was used to calculate flow fields of different Mach numbers, transitions points, and angles of attack. The results from these runs show that at low angles the transition point placement is not critical. However, near stall the transition point placement becomes very sensitive. Moving the transition point one grid line down stream, from where a converged solution with an attached flow field was obtained, can produce a separated flow. In a supercritical flow, the transition point placement is even more critical. Moving the transition point one grid line down stream, from where a converged solution with an attached flow field was obtained, can cause a steady solution to become unstable. In the Mach-supercritical case, the shock plays a major role. If the shock is in the turbulent region, then the turbulent mixing will cause the flow to reattach. If the shock is in the laminar region, there will be no mixing to aide reattachment, and the flow will separate. Hence, the reattachment process is an important feature of dynamic stall.

In order to more clearly understand the mechanism of dynamic stall, the most ambitious scheme would be to fully and accurately model the onset mechanism with some computational technique. However, the use of any type of turbulence model always casts some doubt on the validity of the solution. Thus a study based on an algebraic model can at best give qualitative features of the dynamic stall process, until more rigorous techniques become available.

9.0 REFERENCES

1. Ham, N.D. and Garelick, M.S., "Dynamic Stall Considerations in Helicopter Rotors," *Journal of the American Helicopter Society,* Vol.13, No. 2, April 1968, pp. 49-55.

2. Harper, P.W. and Flanigan, R. E., "The Effect of Change of Angle of Attack on the Maximum Lift of a Small Model," NACA TN 2061, March 1950.

3. McCullough, G. B. and Gault, D. E., "Examples of Three Representative Types of Airfoil-section Stall at Low Speed," NACA TN 2502, Sept. 1951.

4. Ericsson L. E. and Reding J. P., "Fluid Mechanics of Dynamic Stall, Part I. Unsteady Flow Concepts," *Journal of Fluid and Structures*, Vol. 2, pp. 1-33, 1988

5. Carr, L.W., "Dynamic Stall Progress in Analyses and Prediction." *AIAA* Paper 85-1769, 1985.

6. McCroskey, W. J., et al., "Experimental Study of Dynamic Stall on Advanced Airfoil Sections," NASA TM-84245, Vols. I-III, 1982.

7. Lorber, Peter F. and Carta, Franklin O., "Unsteady Stall Penetration Experiments at High Reynolds Number," AFOSR TR-87-1202, April 14, 1987.

8. Fung, K.-Y., Carr, L.W., "The Effects of Compressibility on Dynamic Stall," First National Fluid Dynamics Congress, 1987.

9. Pulliam, T., "Euler and Thin Layer Navier Stokes Codes: ARC2D, ARC3D, Notes for Computational Fluid Dynamics User's Workshop," The University of Tennessee Space Institute, Tullahoma, Tenn., March 12-16, 1984.

10. Owen, P. R., and Klanfer, L., "On the Laminar Boundary Layer Separation from the Leading Edge of a Thin Aerofoil," ARC Current Paper No. 220, 1955.

11. Gaster, M., "The Structure and Behavior of Laminar Separation Bubbles," AGARD Conference Proceedings 4, pp. 819-854, 1966.

12. Tani, I., "Low-Speed Flows Involving Bubble Separations," Progress in Aeronautical Sciences, Vol. 5, Pergammon Press, 1964.

13. Thwaites, B., "Approximate Calculation of the Laminar Boundary Layer," *Aero. Quart.* 1, 245-280, Nov. 1949.

14. Curle, N. and Skan, S.W., "Calculated Leading-edge Laminar Separations from some RAE Aerofoils," A.R.C. CP 504, 1960.

15. McGregor, I., "Regions of Localized Boundary Layer Separation and Their Role in the Nose-Stalling of Aerofoils," Ph.D. Thesis, Queen Mary College, University of London, 1954.

16. Crabtree, L. F., "Effects of Leading-Edge Separation on Thin Wings in Two-Dimensional Incompressible Flow," *Journal of the Aeronautical Sciences*, Vol. 24, Aug. 1957, pp. 597-604.

17. Baldwin, B.S. and Lomax, H., "Thin Layer Approximation and Algebraic Model for Separated Turbulent flows," AIAA Paper No. 78-257, 1978.

10.0 FIGURES, TABLES and APPENDICES

Dynamic Stall Area on a Helicopter in Forward Flight

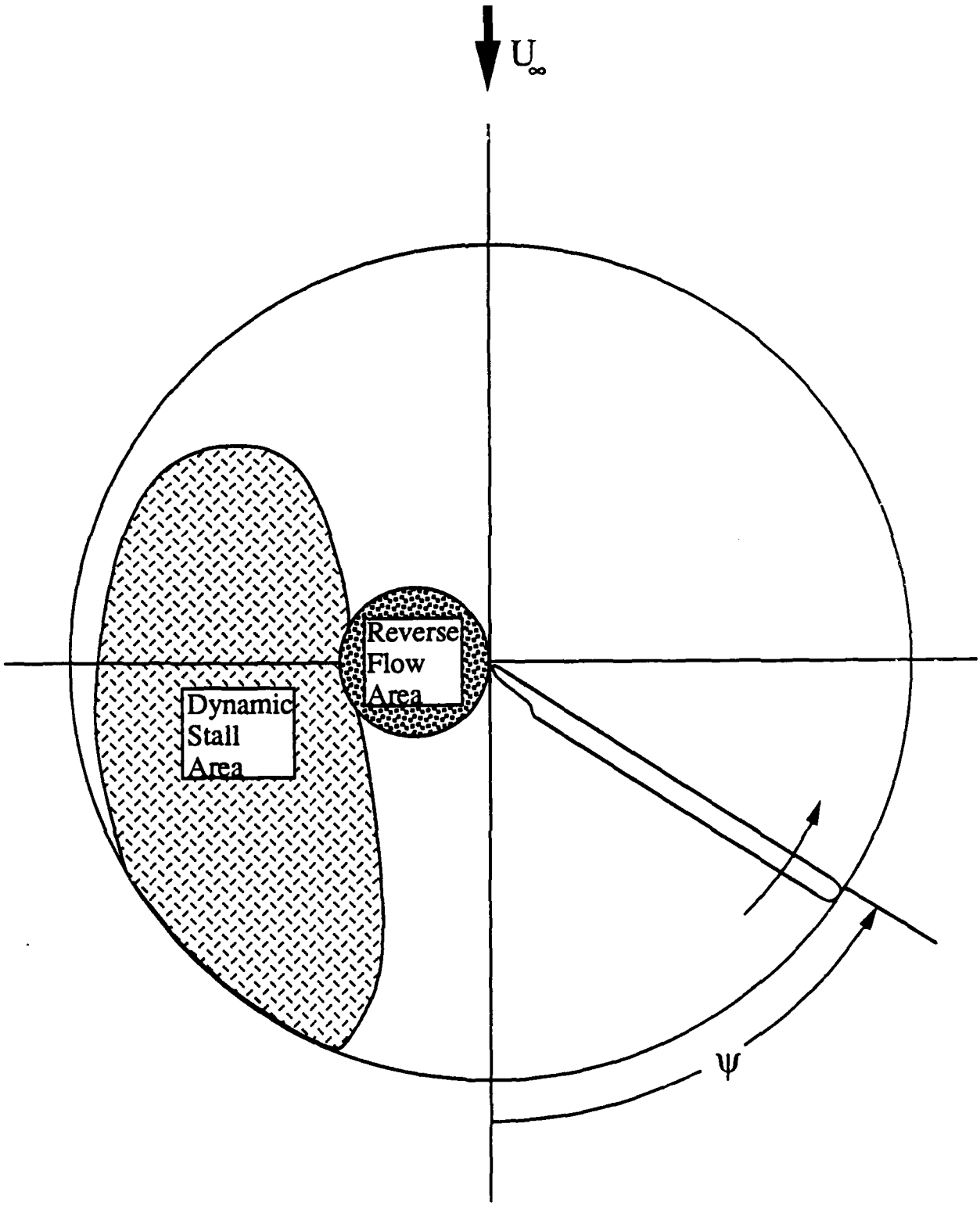

Figure 1. Dynamic stall on a helicopter.

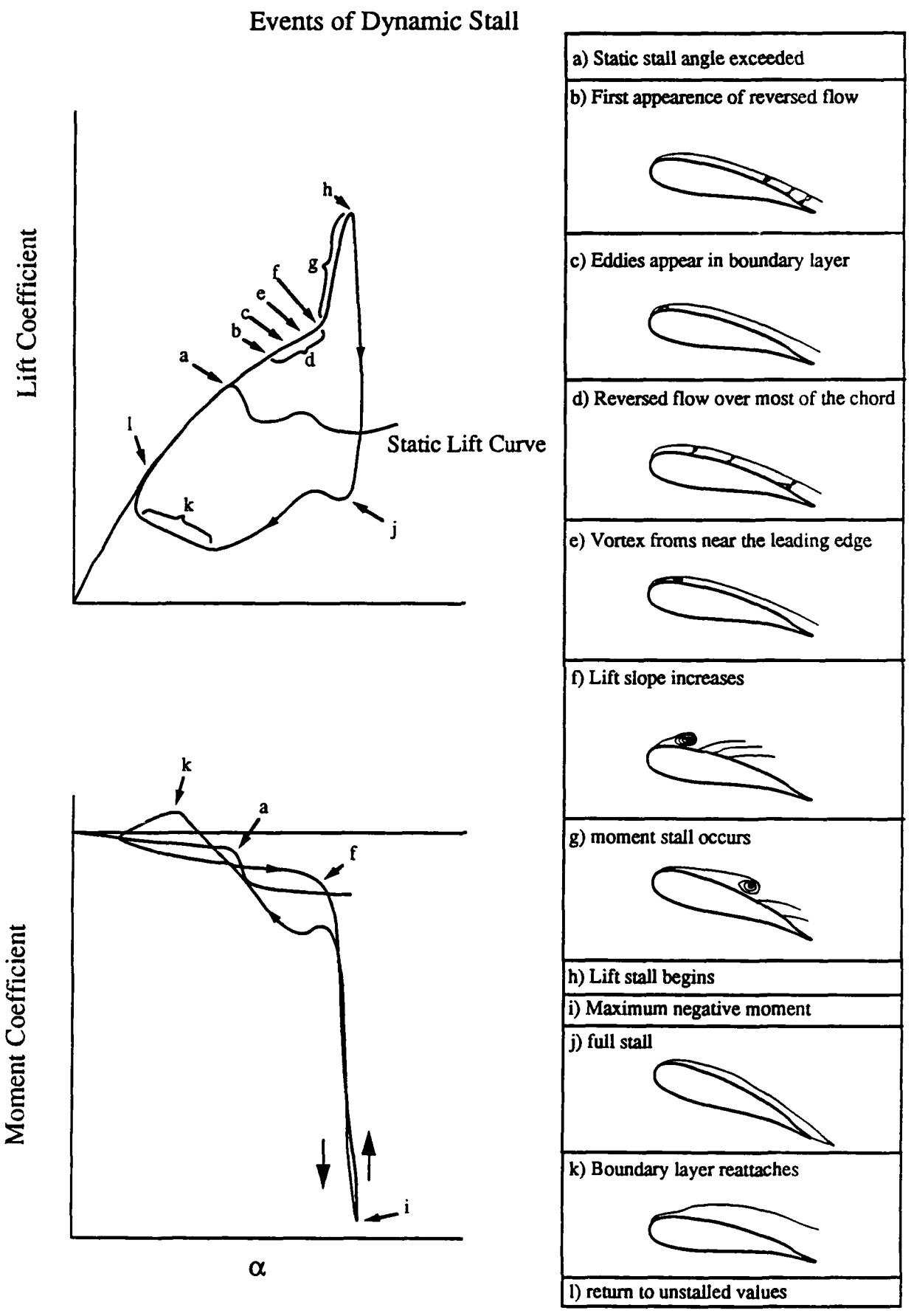

Figure 2. Events of dynamic stall.

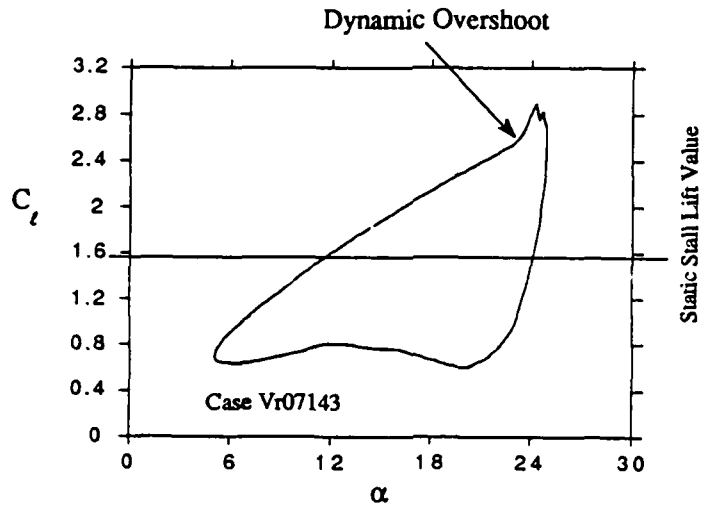

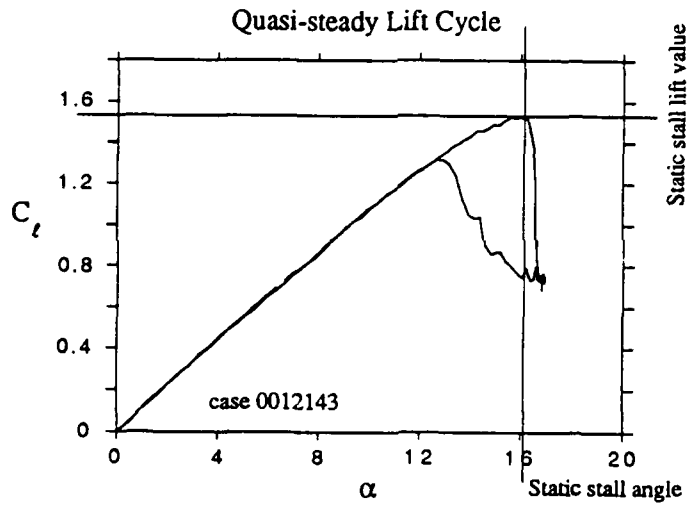

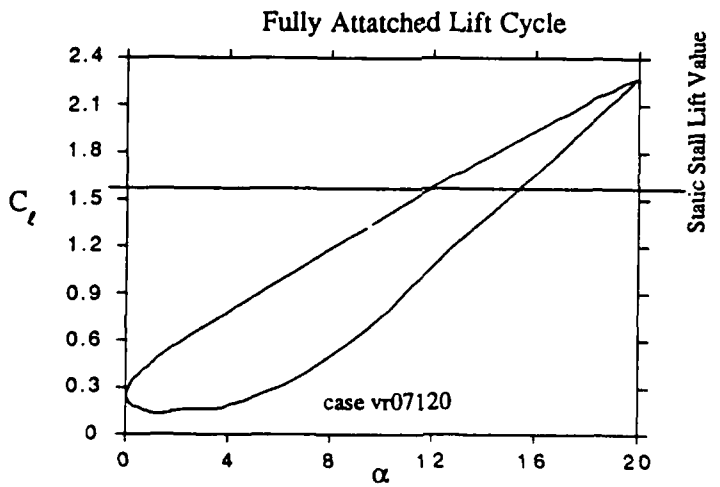

Figure 3. Typical dynamic lift cycles.

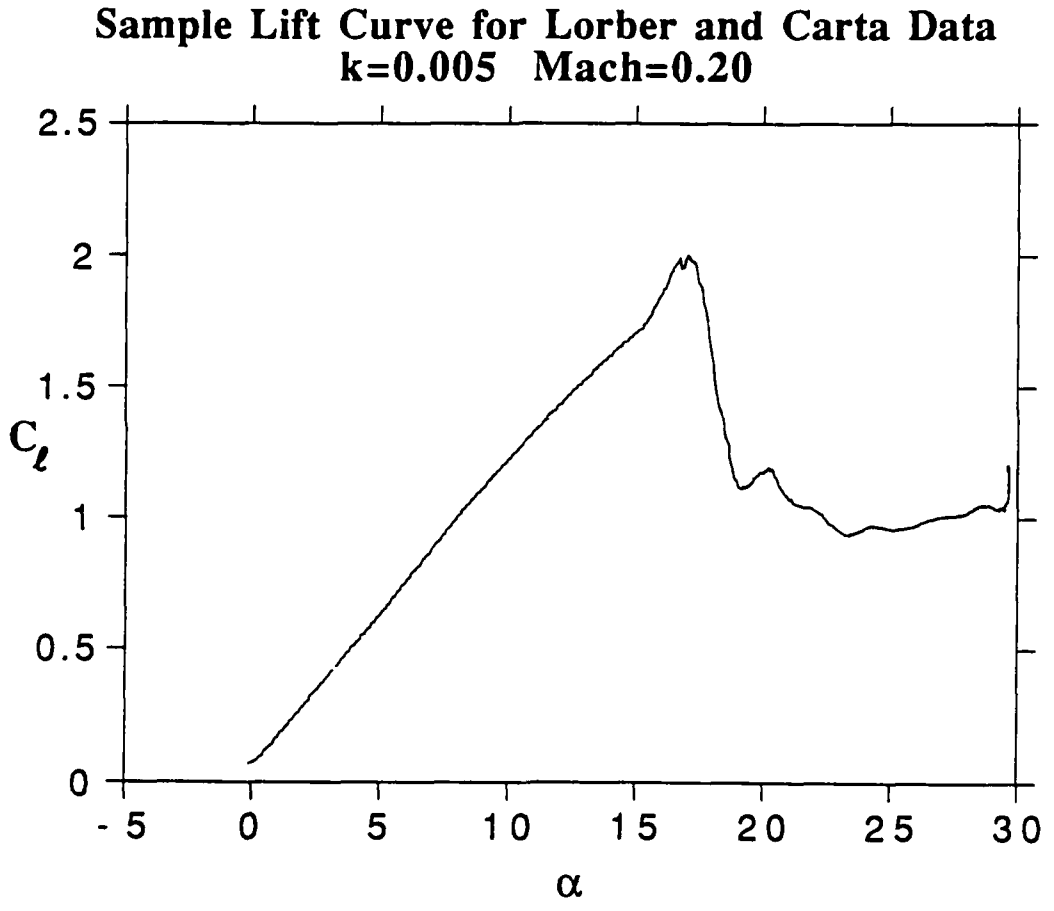

Figure 4. Sample of Lorber and Carta data.

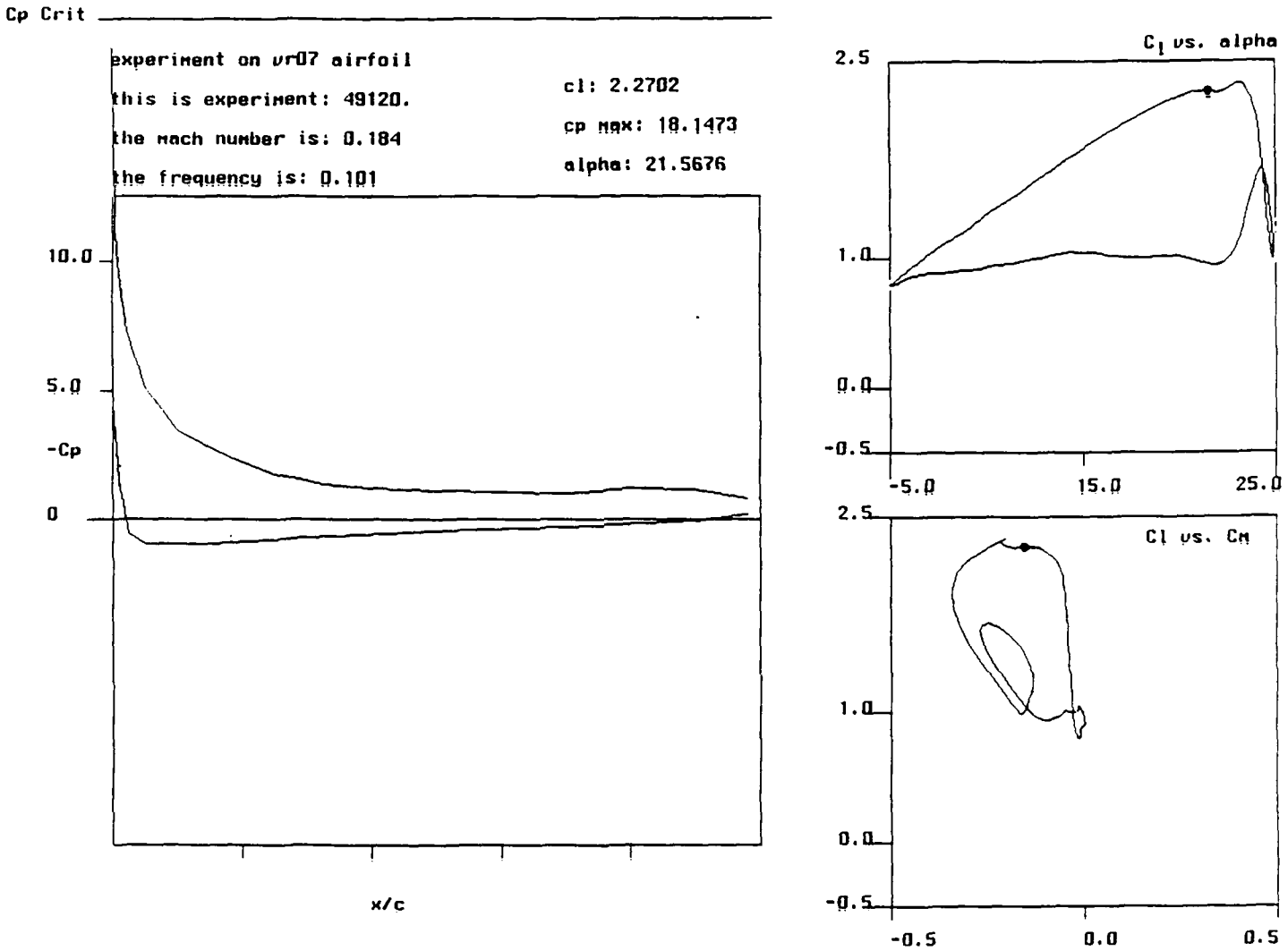

Figure 5. Still frame of "movie" program.

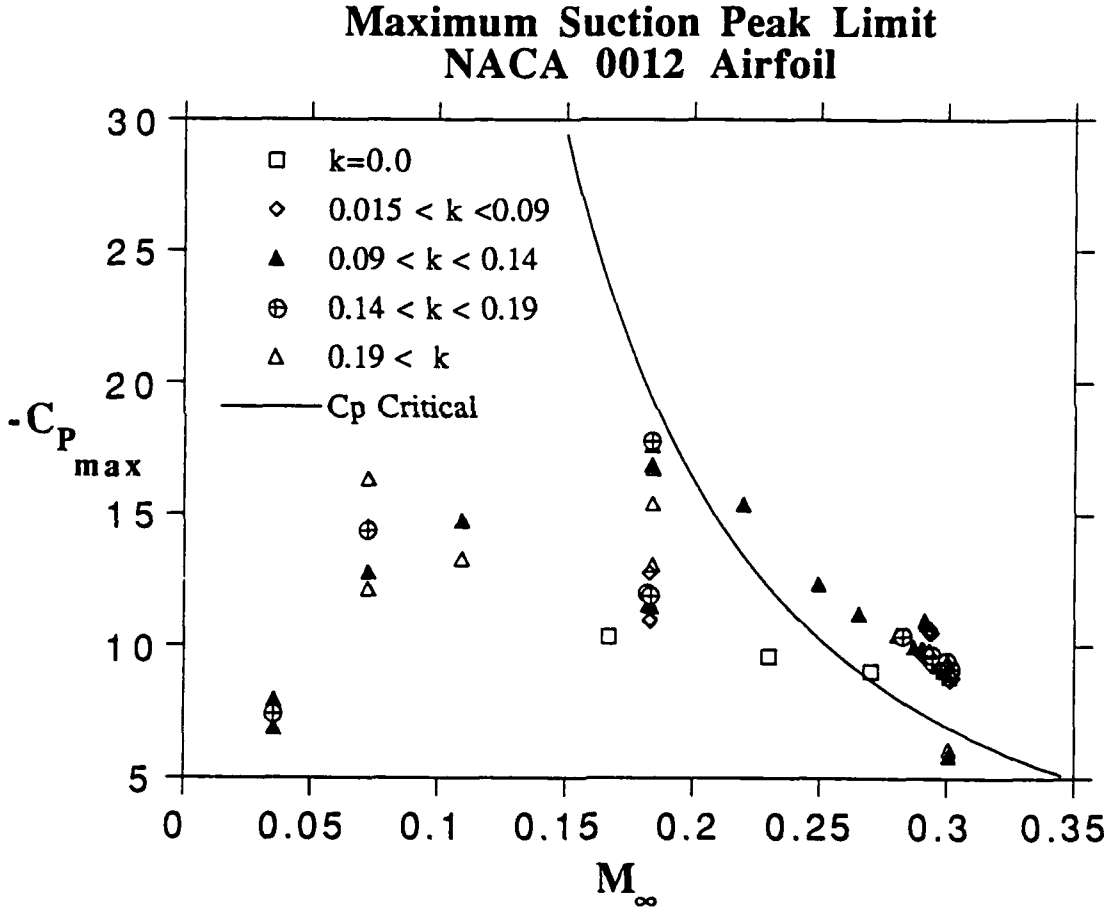

Figure 6. Maximum suction peak limit for NACA 0012 airfoil.

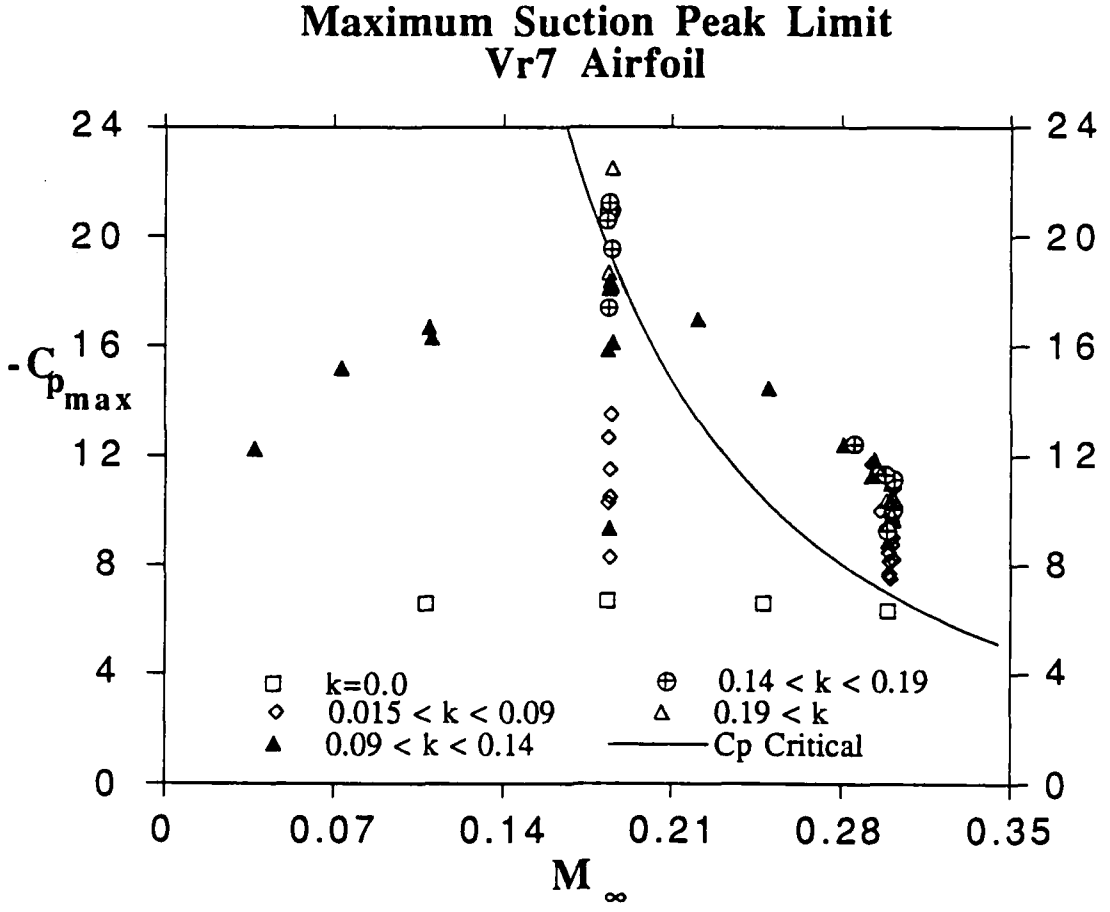

Figure 7. Maximum suction peak limit for Vr7 airfoil.

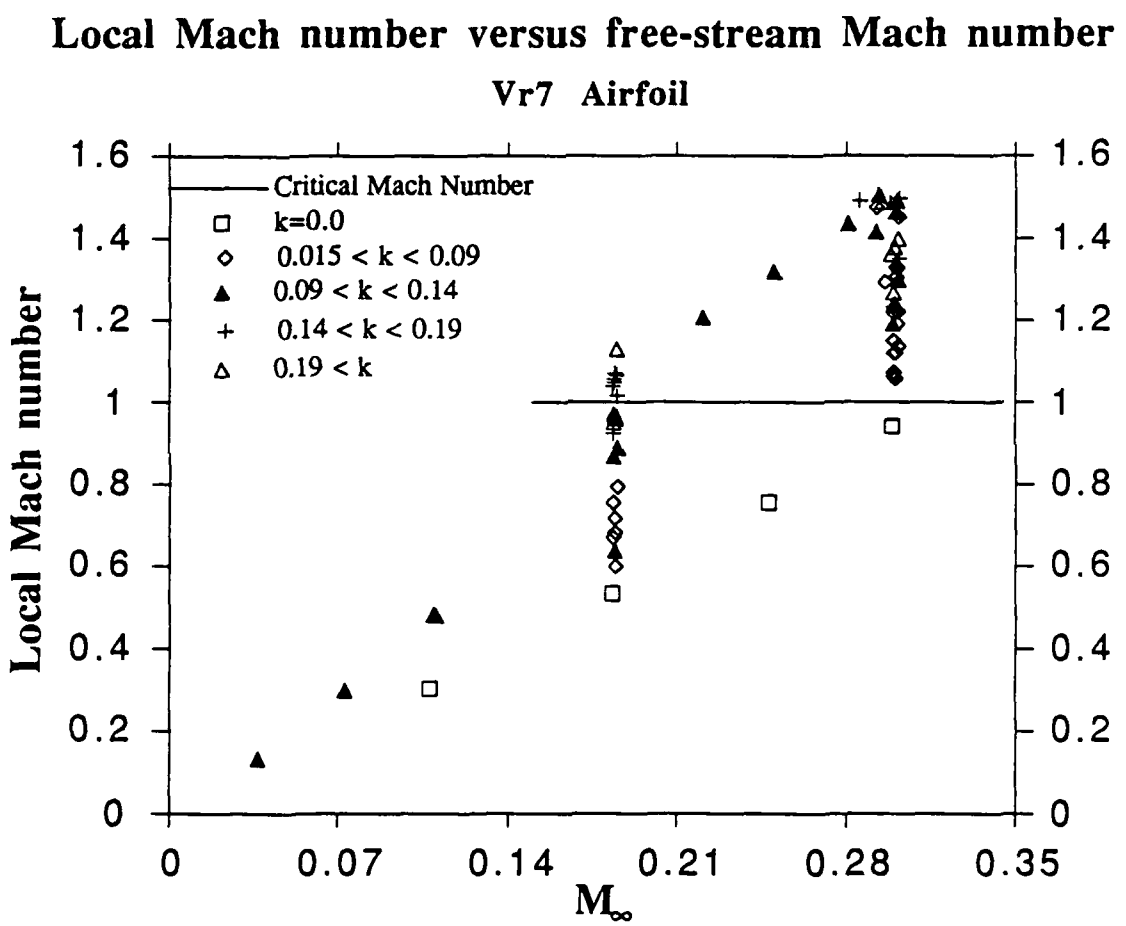

Figure 8. Local Mach number versus free-stream Mach number.

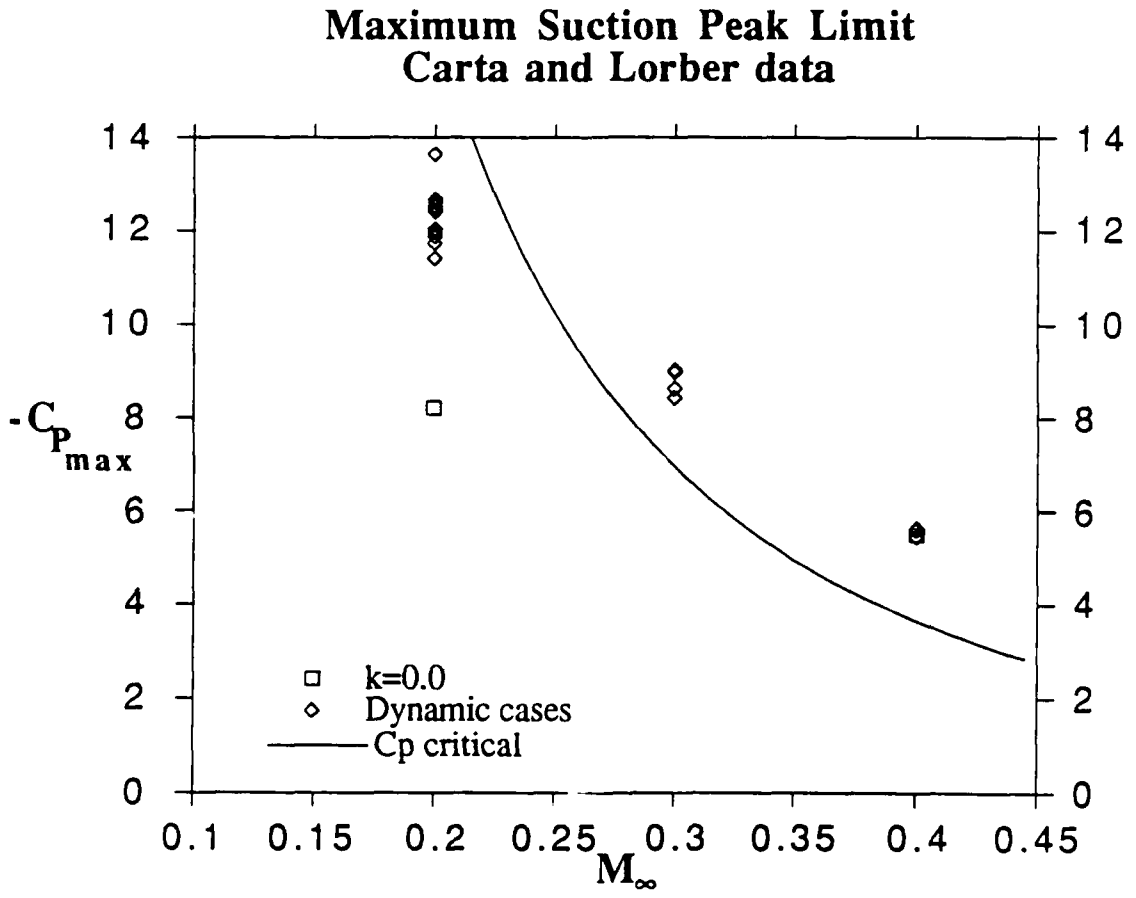

Figure 9. Maximum suction peak limit for Carta and Lorber data.

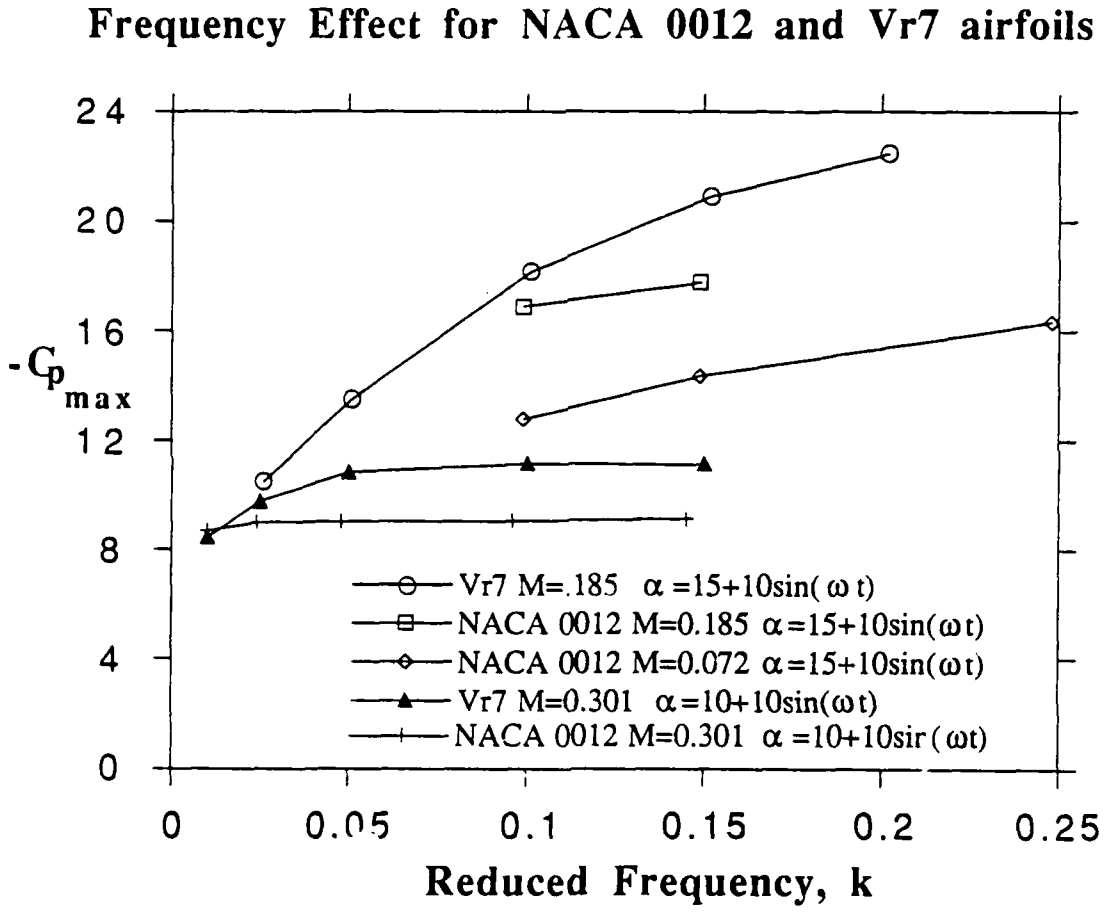

Figure 10. Frequency effect for NACA 0012 and Vr7 airfoils.

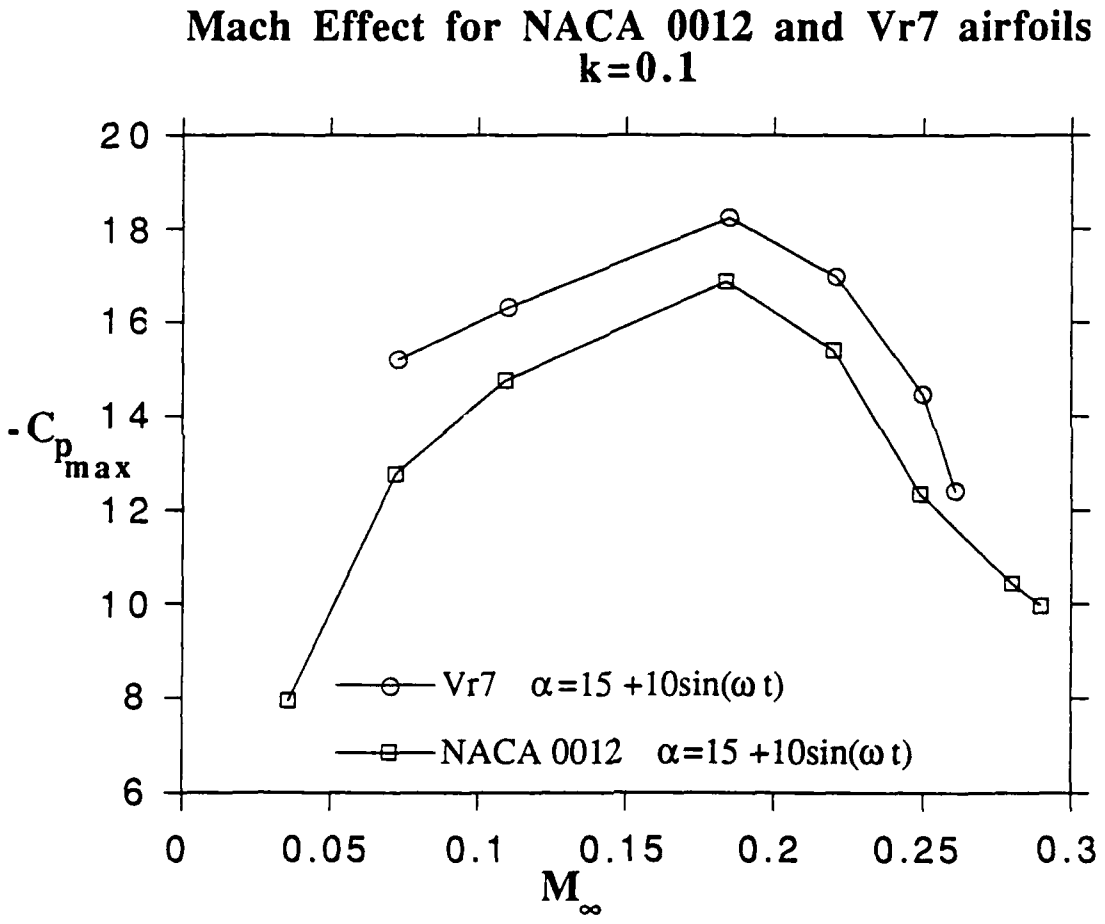

Figure 11. Mach effect for NACA 0012 and Vr7 airfoils.

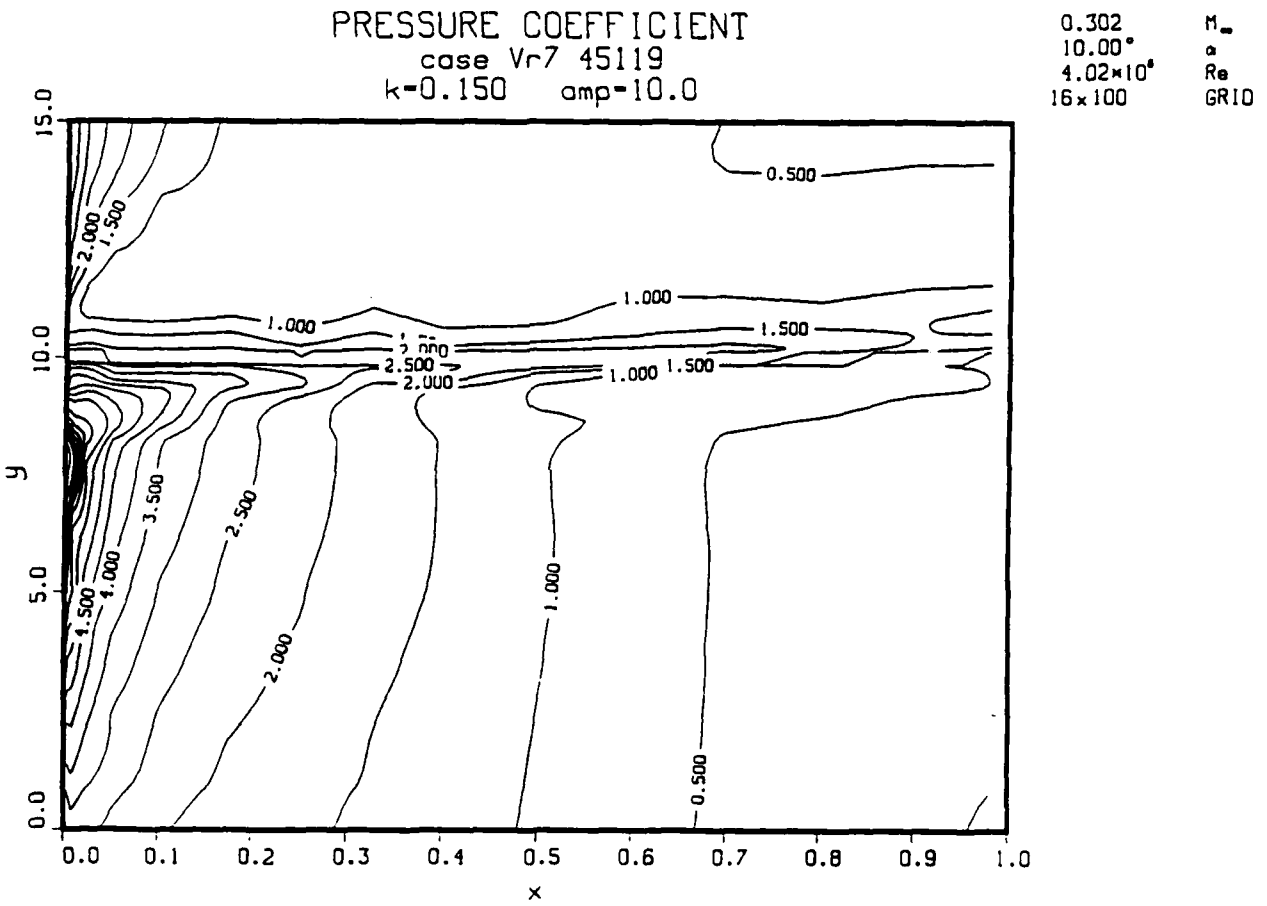

Figure 12a. Pressure coefficients contours for Vr7 at M=0.302.

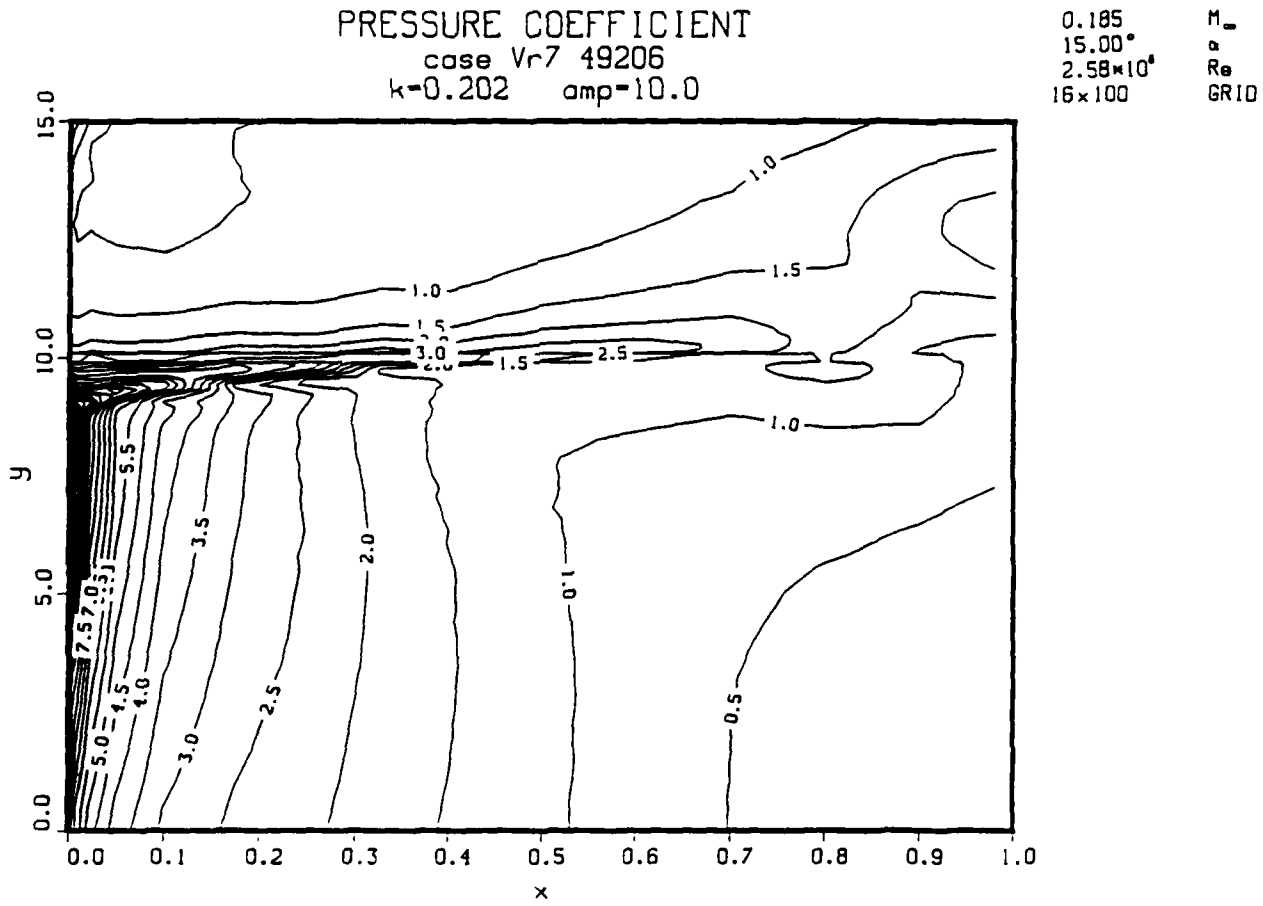

Figure 12b. Pressure coefficients contours for Vr7 at M=0.185.

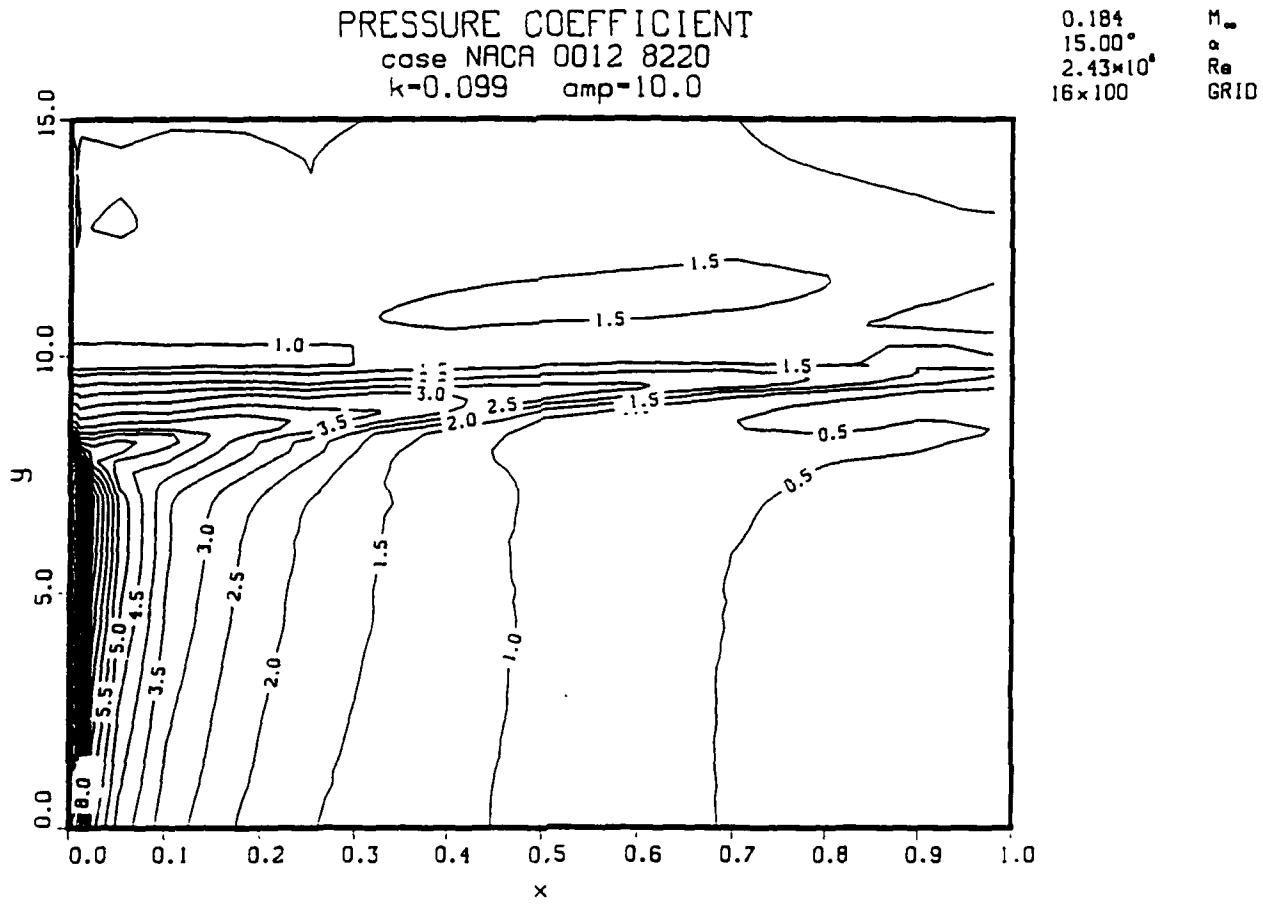

Figure 13. Pressure coefficients contours for NACA 0012 at M=0.184 and k=0.099.

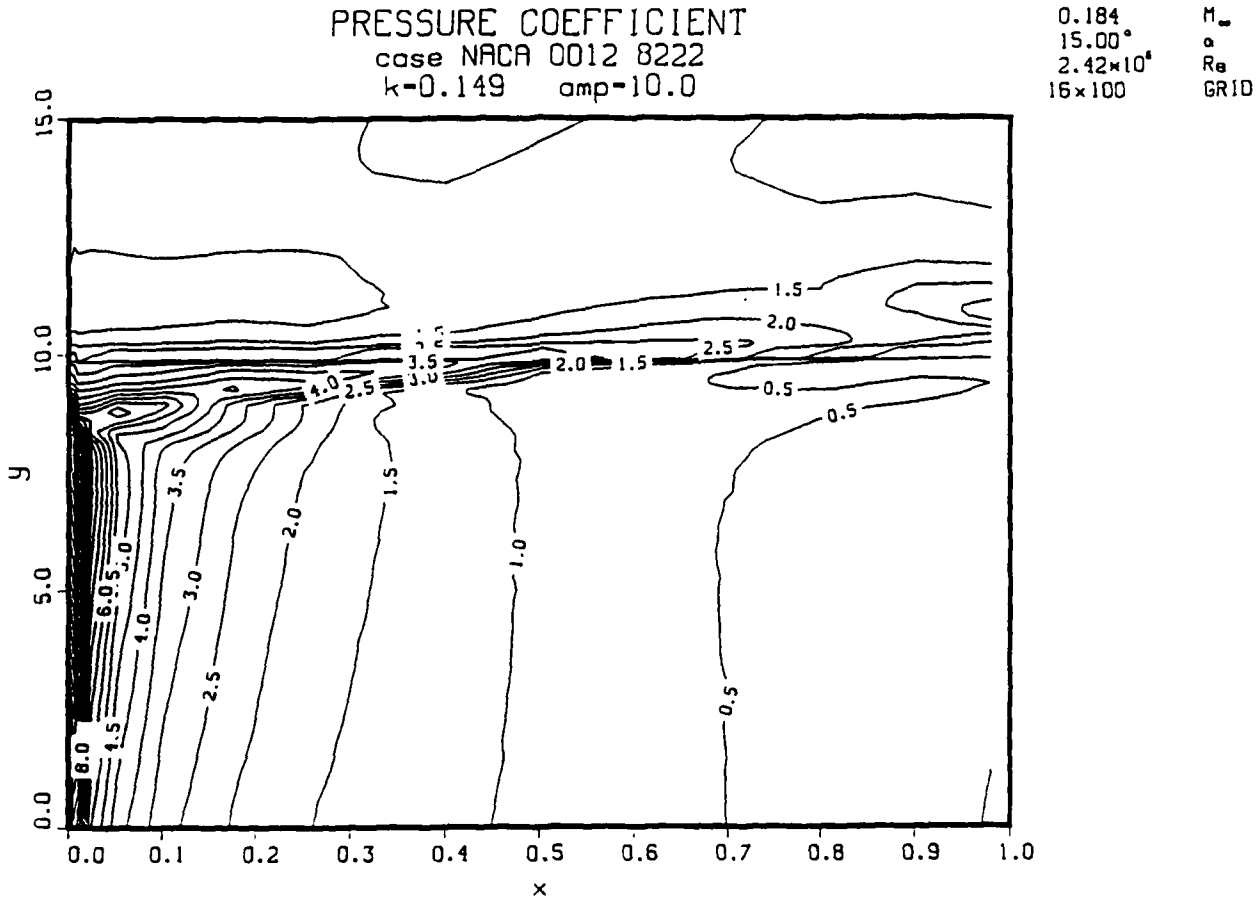

Figure 14. Pressure coefficients contours for NACA 0012 at M=0.184 and k=0.149.

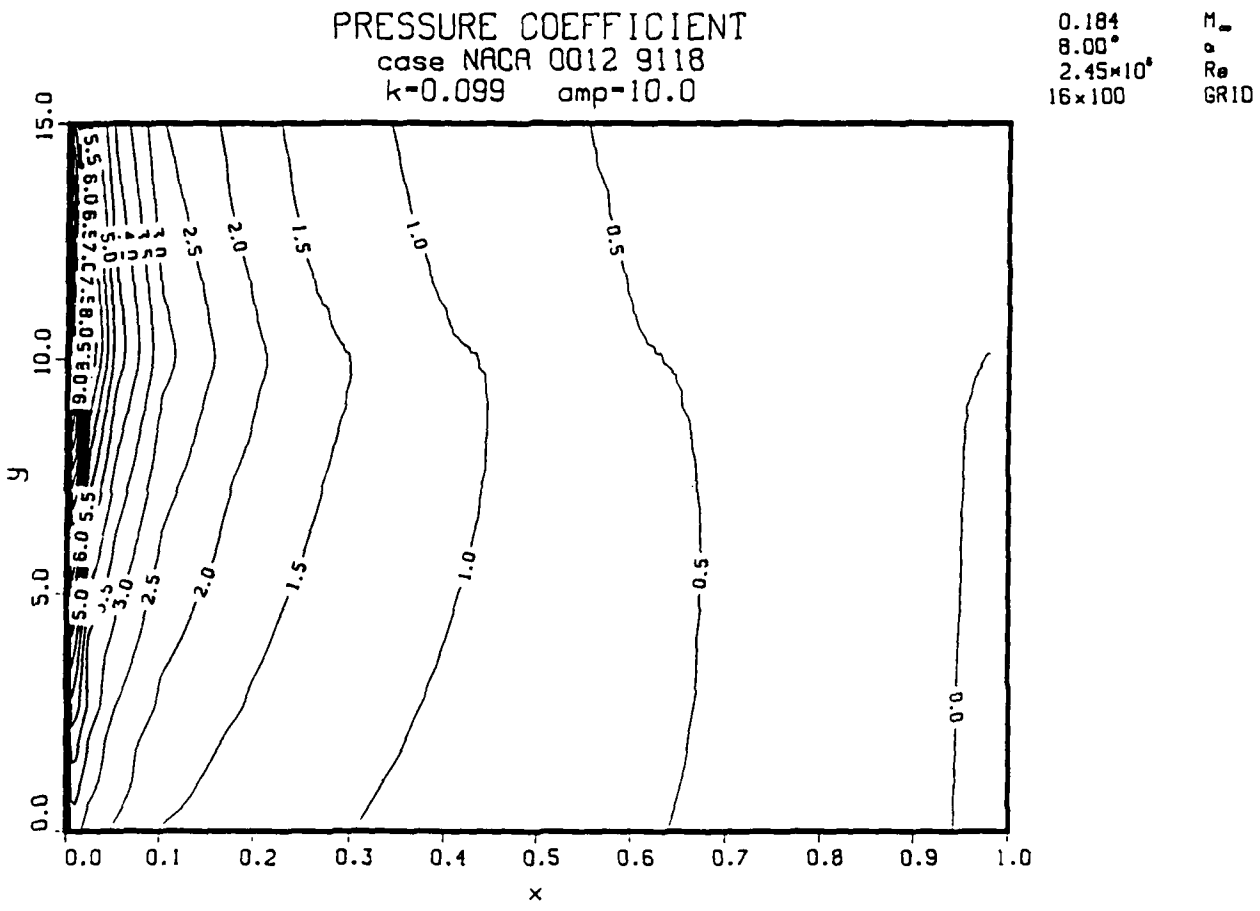

Figure 15. Pressure coefficients contours for NACA 0012 at M=0.184 and k=0.099.

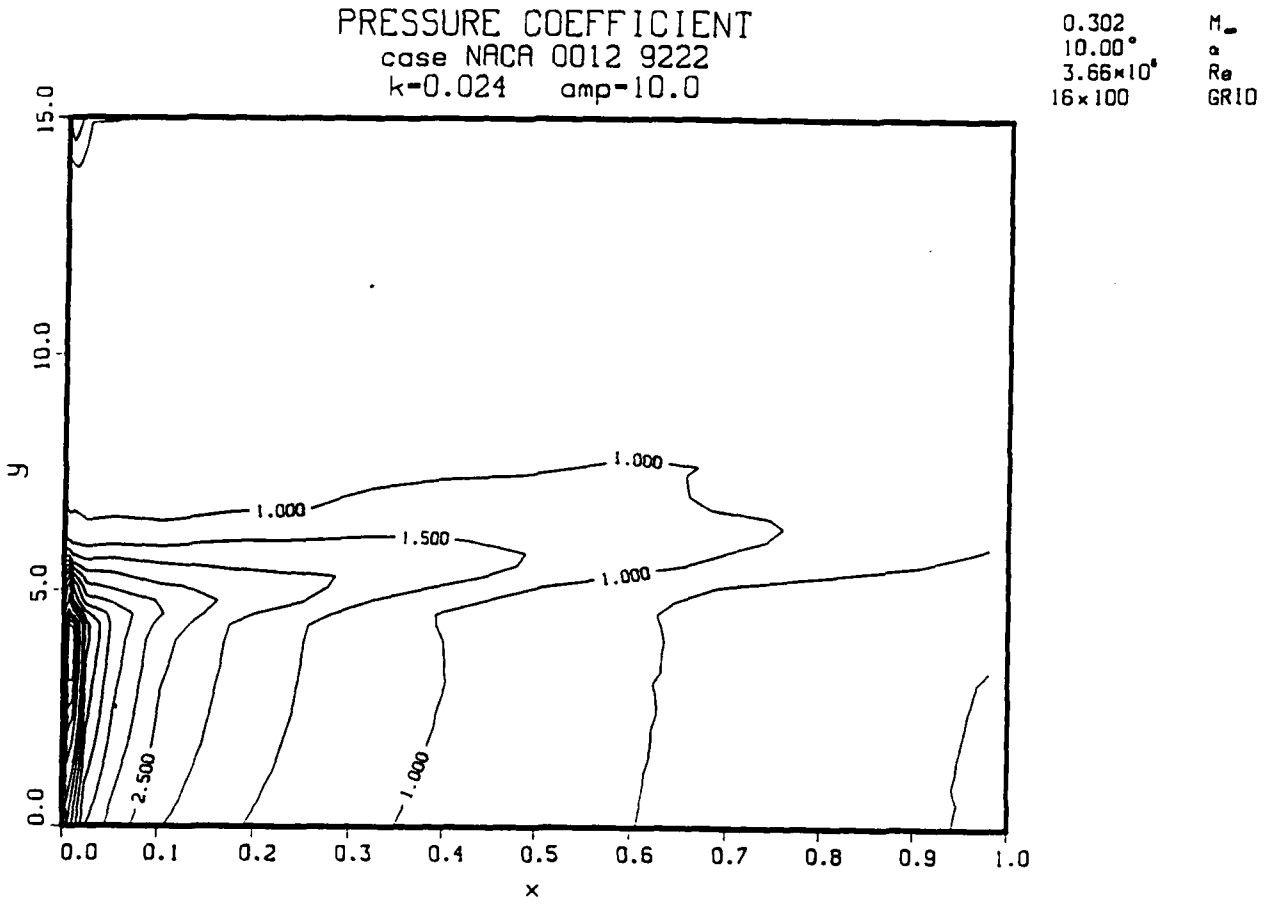

Figure 16. Pressure coefficients contours for NACA 0012 at M=0.302 and k=0.024.

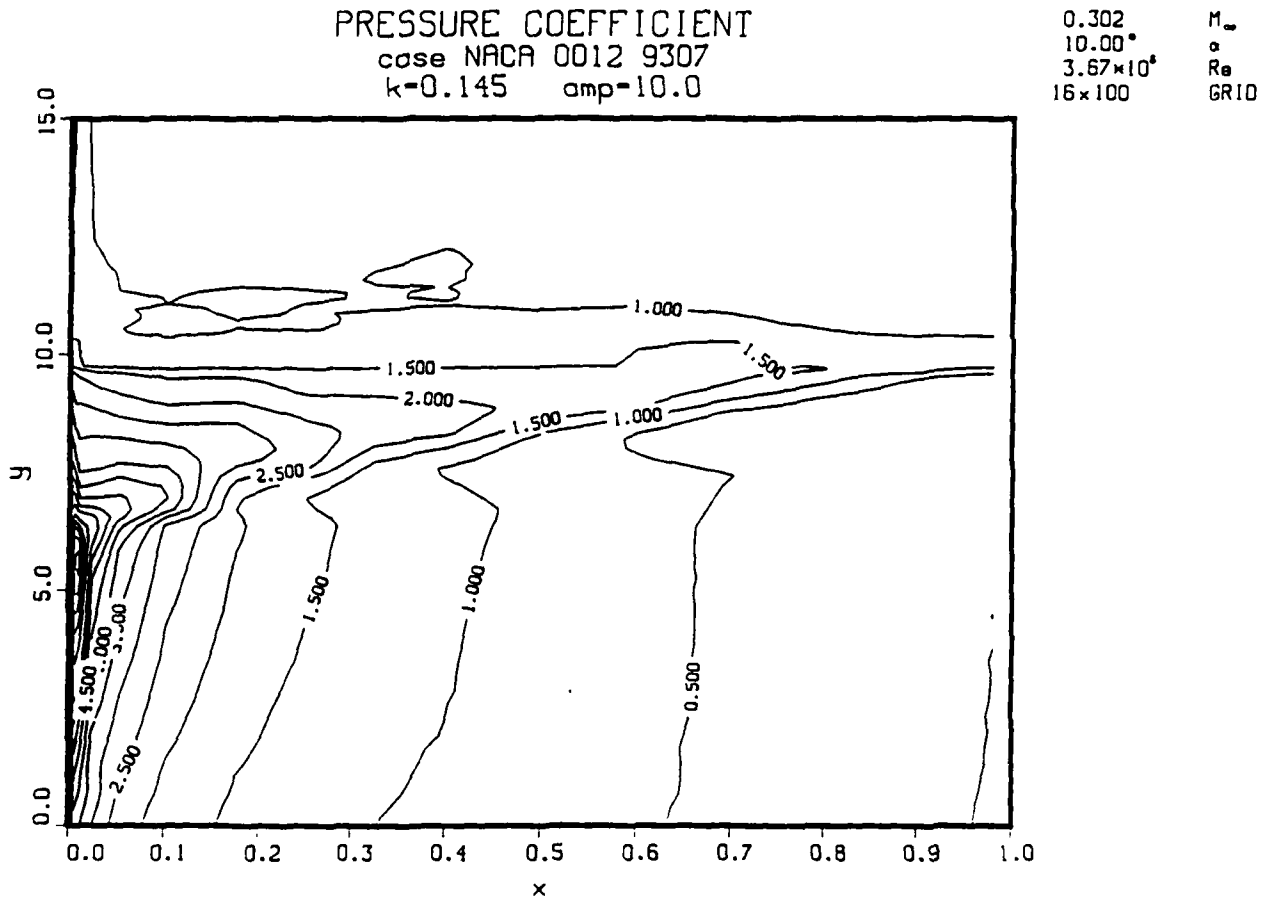

Figure 17. Pressure coefficients contours for NACA 0012 at M=0.302 and k=0.145.

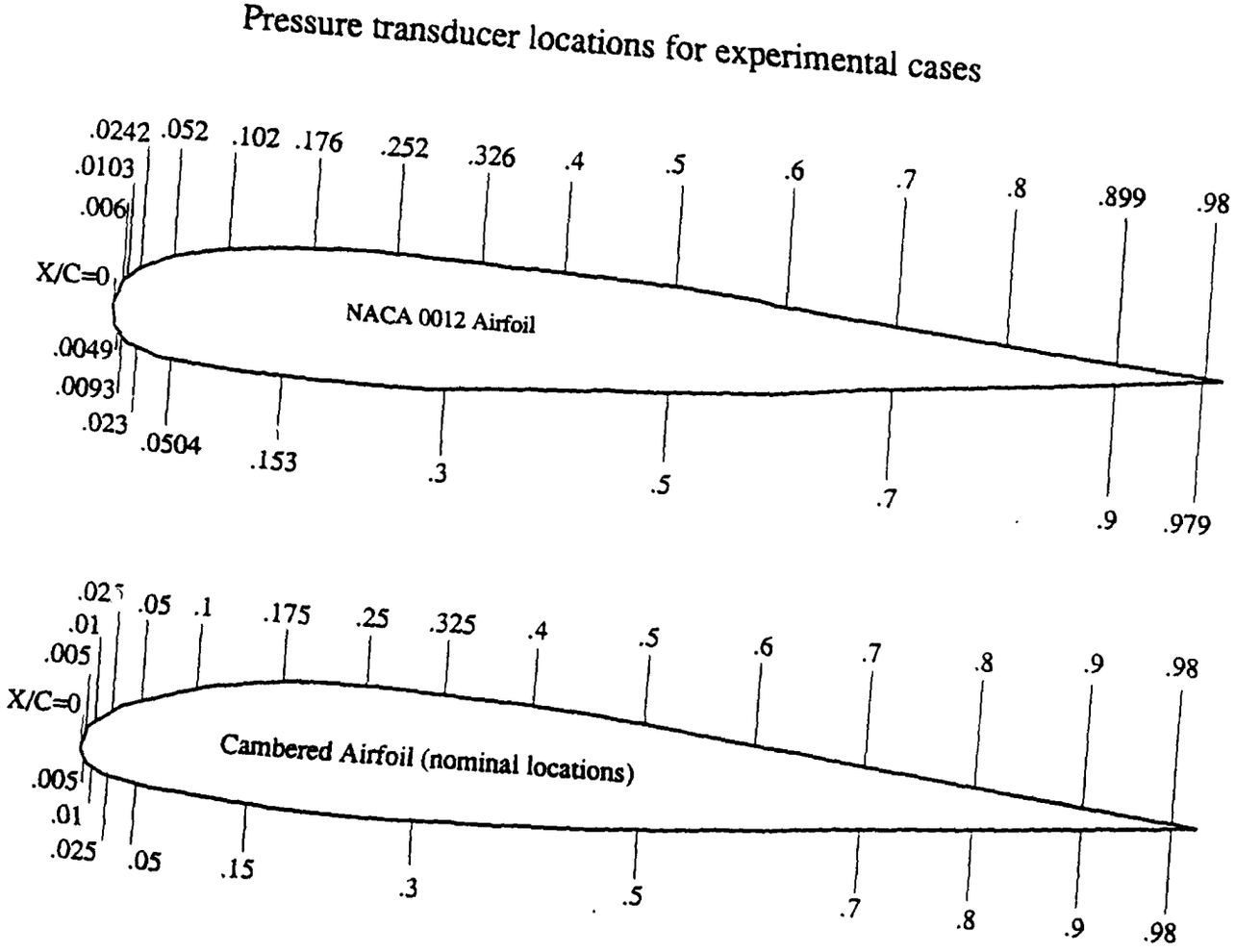

Figure 18. Experimental pressure transducer locations.

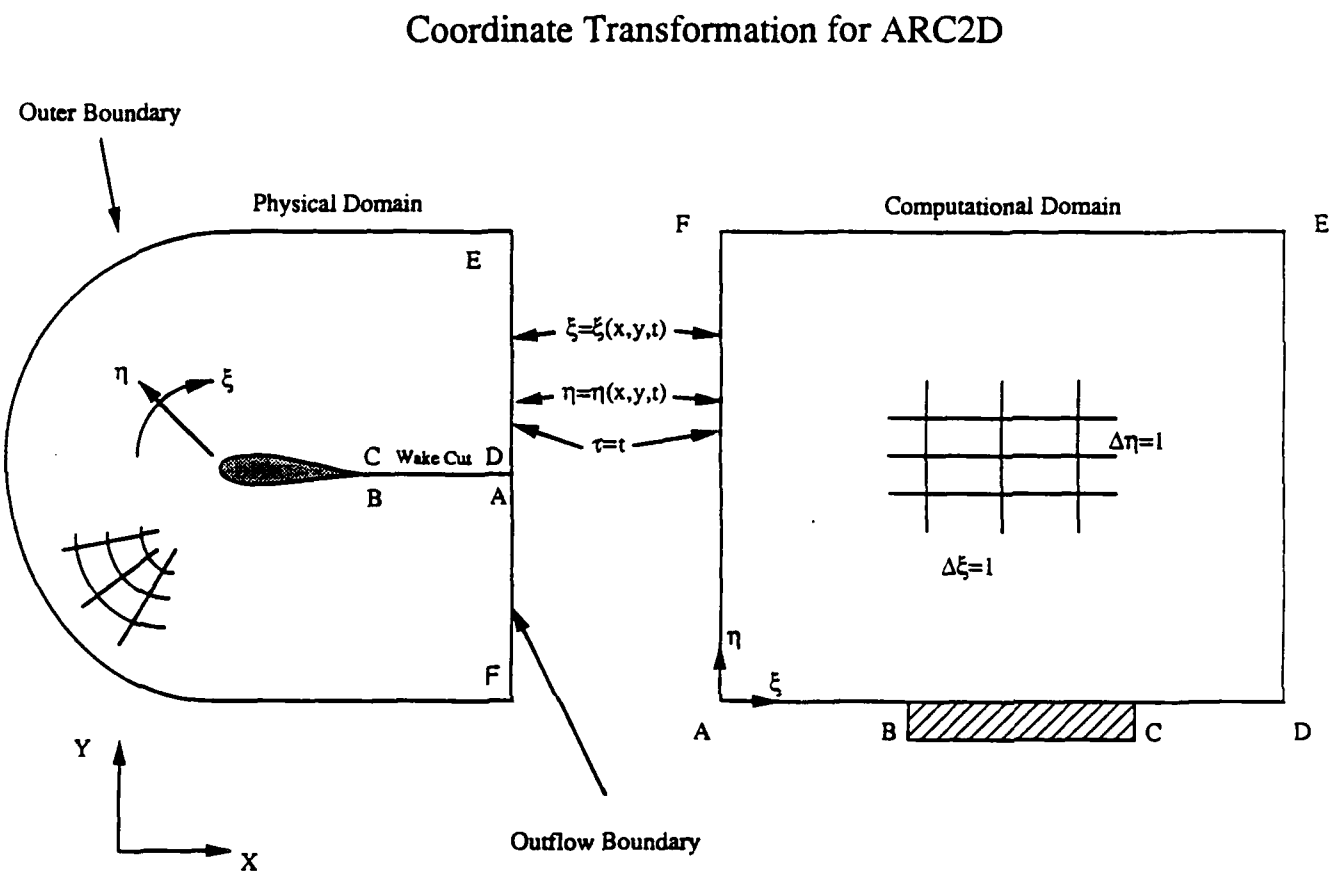

Figure 19. Generalized curvilinear coordinate transformations for ARC2D.

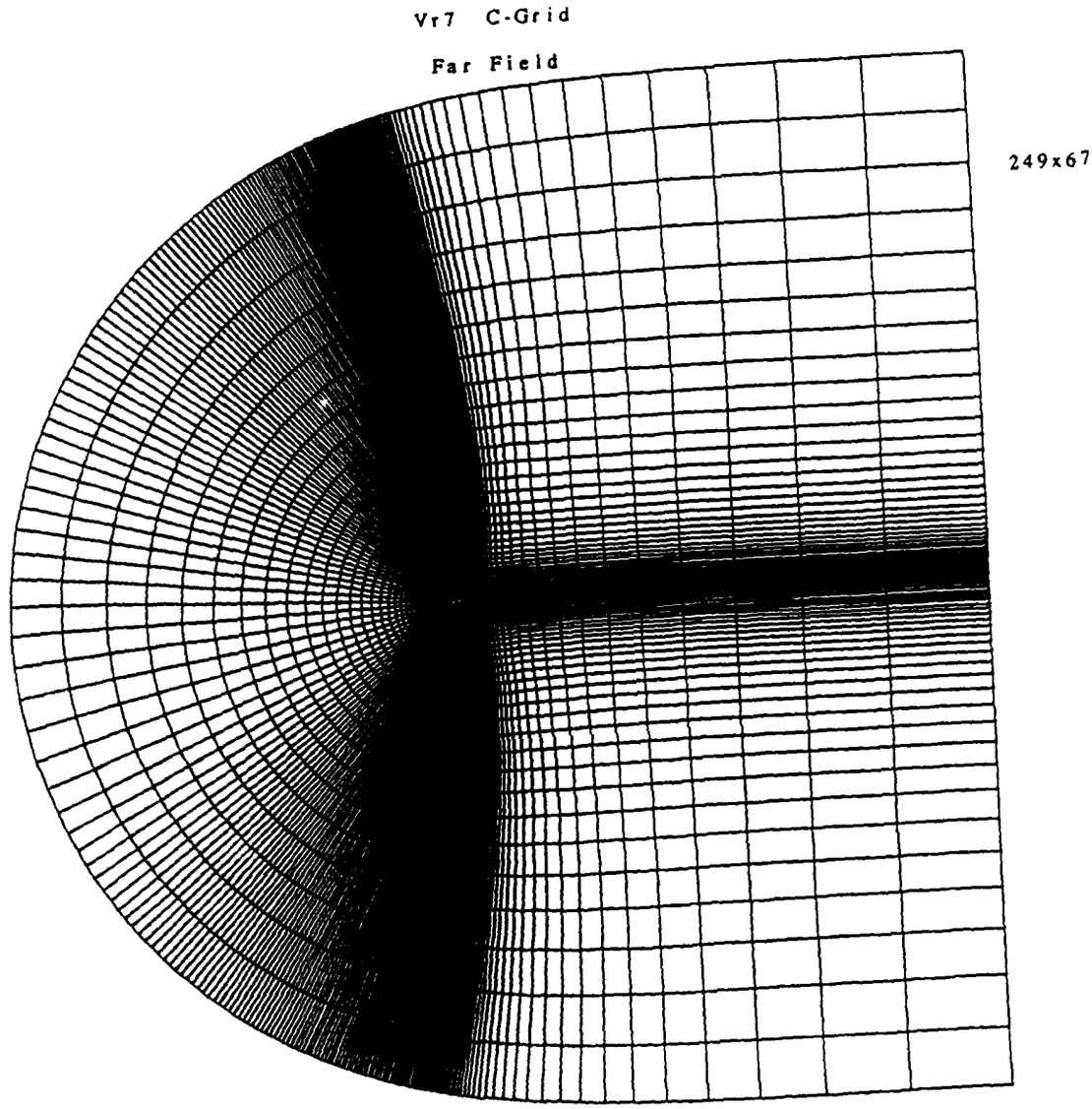

Figure 20. Vr7 inviscid C-grid, far field.

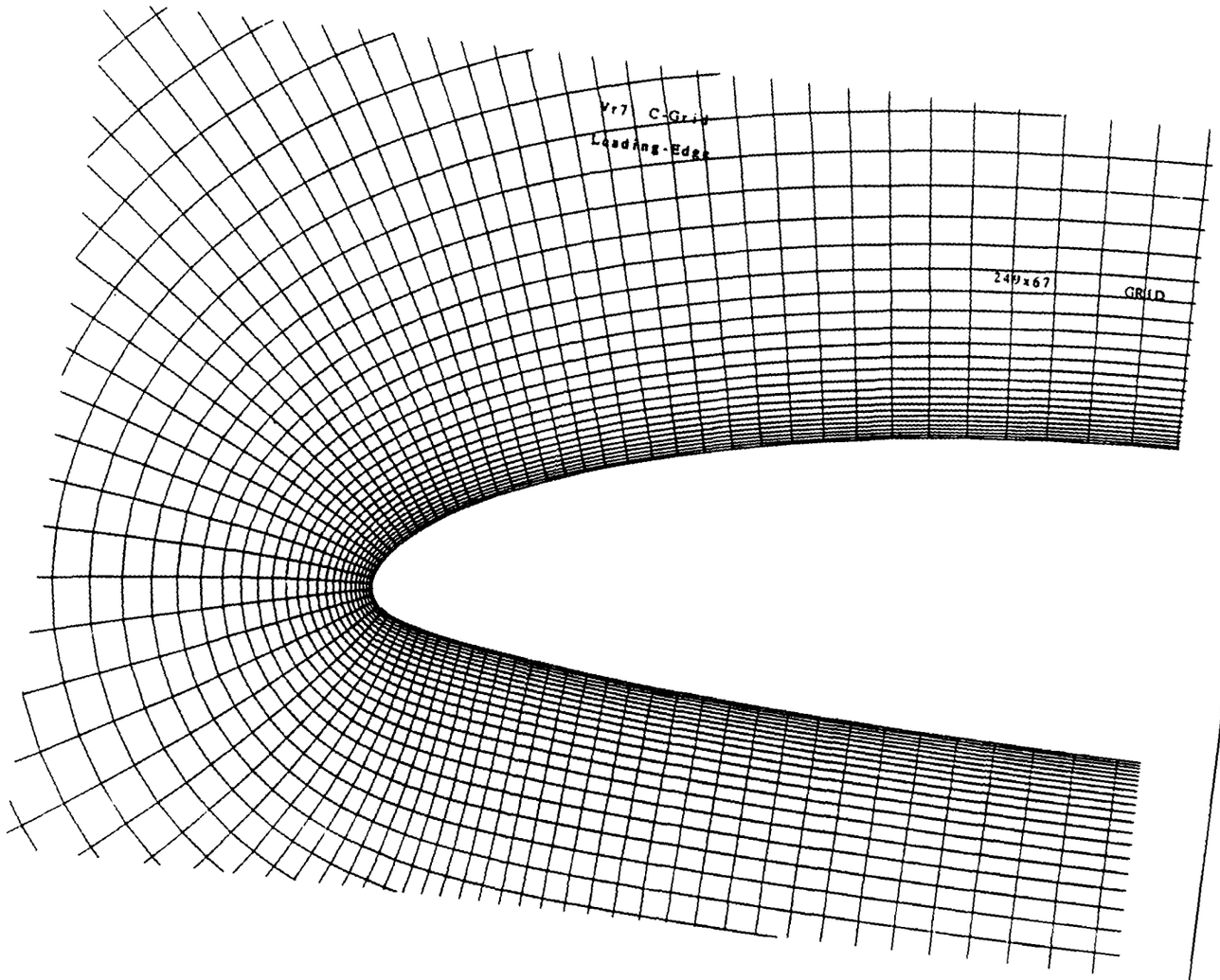

Figure 21. Vr7 inviscid C-grid, airfoil leading edge.

Table 1. Inviscid Numerical Results

NACA 0012 Low Mach Number (0.185)

angle	Iterations	C_ℓ	C_D	C_m	Resid	S-S Pts
7.0	2500	0.85117	0.00153	-0.00572	0.312E-10	0
8.0	3675	0.97191	0.00203	-0.00636	0.929E-14	0
9.0	3725	1.09231	0.00260	-0.00693	0.969E-14	0
10.0	3850	1.21235	0.00324	-0.00714	0.921E-14	0
11.0	4000	1.33199	0.00387	-0.00781	0.889E-14	0
12.0	3800	1.45118	0.00477	-0.00812	0.441E-13	0
13.0	4100	1.56987	0.00566	-0.00832	0.971E-14	0
14.0	4200	1.68800†	0.00665	-0.00840	0.768E-14	0
15.0	4250	1.80547†	0.00774	-0.00836	0.845E-14	0
16.0	4300	1.92219†	0.00894	-0.00816	0.951E-14	0
17.0	4400	2.03800†	0.01028	-0.00780	0.868E-14	0
18.0	4500	2.15267†	0.01177	-0.00725	0.829E-14	1
19.0	4600	2.26577†	0.01348	-0.00645	0.860E-14	7
20.0	4700	2.37606†	0.01554	-0.00528	0.894E-14	14
21.0	4300	2.47630†	0.01866	-0.00307	0.808E-14	24

† denotes lift greater than static stall value

NACA 0012 High Mach Number (0.301)

angle	Iterations	C_ℓ	C_D	C_m	Resid	S-S Pts
7.0	2575	0.87359	0.00206	-0.00495	0.805E-14	0
7.5	2500	0.94116	0.00240	-0.00507	0.829E-14	0
8.0	2675	1.00367	0.00277	-0.00512	0.972E-14	0
8.5	2750	1.06613	0.00316	-0.00512	0.919E-14	0
9.0	2675	1.12854	0.00360	-0.00505	0.364E-13	0
9.5	2800	1.19088	0.00407	-0.00491	0.213E-13	0
10.0	2950	1.25312	0.00458	-0.00496	0.762E-14	0
10.5	2950	1.31523	0.00515	-0.00437	0.918E-14	5
11.0	3000	1.37712†	0.00653	-0.00393	0.806E-14	13
11.5	3000	1.43850†	0.00653	-0.00335	0.827E-14	21
12.0	2800	1.49765†	0.00767	-0.00241	0.872E-14	31
12.5	2700	1.54752†	0.01003	-0.00041	0.529E-14	39
13.0	4800	1.57967†	0.01333	+0.00382	0.146E-13	49

† denotes lift greater than static stall value

Vr7 Low Mach Number (0.185)

angle	Iterations	C_ℓ	C_D	C_m	Resid	S-S Pts
7.0	3500	0.94468	0.00176	-0.00488	0.210E-11	0
8.0	4000	1.06431	0.00230	-0.00591	0.614E-11	0
9.0	4000	1.18358	0.00294	-0.00691	0.182E-10	0
10.0	5000	1.30241	0.00366	-0.00788	0.119E-11	0
11.0	5000	1.42074	0.00447	-0.00881	0.474E-11	0
12.0	5000	1.53849†	0.00539	-0.00967	0.128E-11	0
13.0	5000	1.65558†	0.00644	-0.01047	0.302E-12	0
14.0	5700	1.77191†	0.00761	-0.01119	0.985E-14	0
15.0	5200	1.88732†	0.00894	-0.01182	0.839E-14	0
16.0	4600	2.00158†	0.01046	-0.01235	0.889E-14	0
17.0	4450	2.11433†	0.01221	-0.01273	0.950E-14	0
18.0	4550	2.22498†	0.01425	-0.01293	0.944E-14	0
19.0	4600	2.33228†	0.01670	-0.01287	0.913E-14	4
20.0	4600	2.43272†	0.01980	-0.01231	0.970E-14	9
21.0	6000	2.50615†	0.02407	-0.00961	0.175E-12	15

† denotes lift greater than static stall value

Vr7 High Mach Number (0.301)

angle	Iterations	C_ℓ	C_D	C_m	Resid	S-S Pts
7.0	2675	0.97571	0.00232	-0.00451	0.881E-14	0
7.5	2975	1.03775	0.00267	-0.00487	0.854E-14	0
8.0	3300	1.09973	0.00305	-0.00520	0.926E-14	0
8.5	3500	1.16165	0.00346	-0.00549	0.902E-14	0
9.0	3825	1.22351	0.00390	-0.00573	0.941E-14	0
9.5	4050	1.28528	0.00438	-0.00542	0.867E-14	0
10.0	4200	1.34697	0.00490	-0.00606	0.968E-14	0
10.5	4250	1.40854	0.00547	-0.00614	0.995E-14	0
11.0	4300	1.46995	0.00609	-0.00615	0.841E-14	0
11.5	4300	1.53118	0.00678	-0.00607	0.997E-14	0
12.0	4300	1.59214†	0.00754	-0.00590	0.856E-14	3
12.5	4300	1.65265†	0.00840	-0.00562	0.963E-14	12
13.0	4500	1.71225†	0.00944	-0.00517	0.654E-14	18
13.5	4500	1.76864†	0.01095	-0.00439	0.730E-14	37
14.0	3100	1.81489†	0.01358	-0.00283	0.881E-14	37

† denotes lift greater than static stall value

Experimental and Computed Pressures

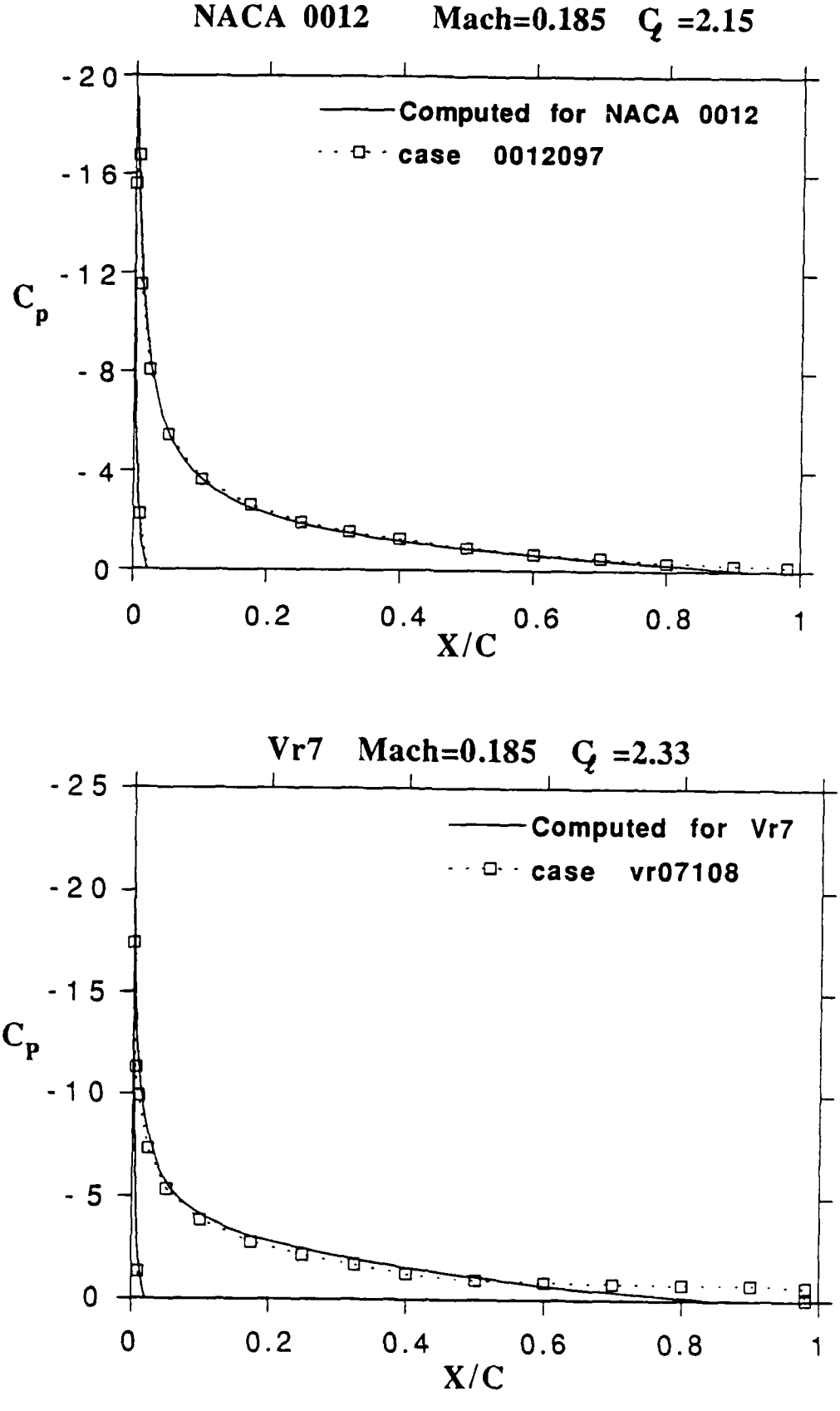

Figure 22. Experimental and computed pressures for Mach=0.185

Experimental and Computed Pressures

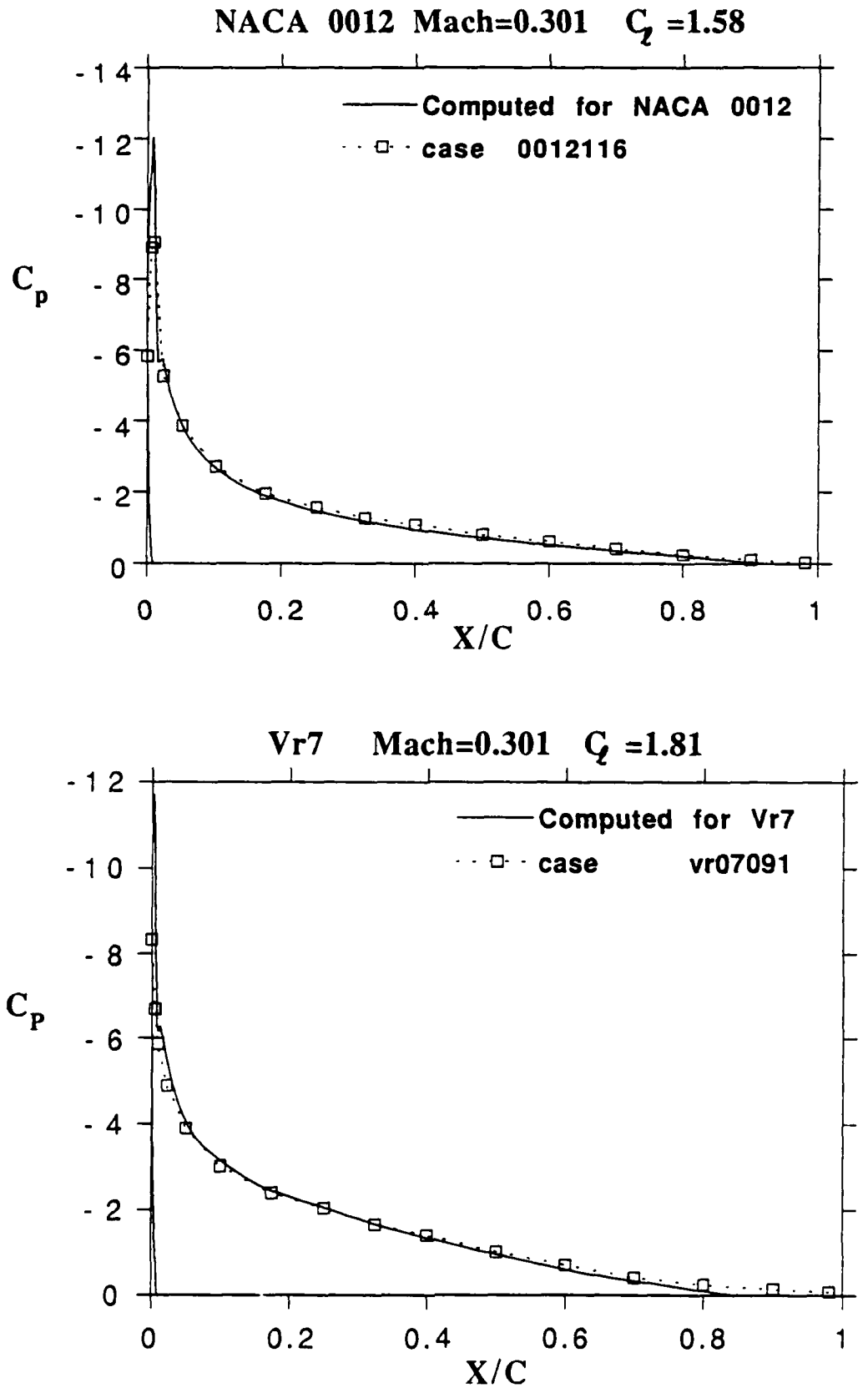

Figure 23. Experimental and computed pressures for Mach=0.301.

Laminar Separation Bubble on an Airfoil

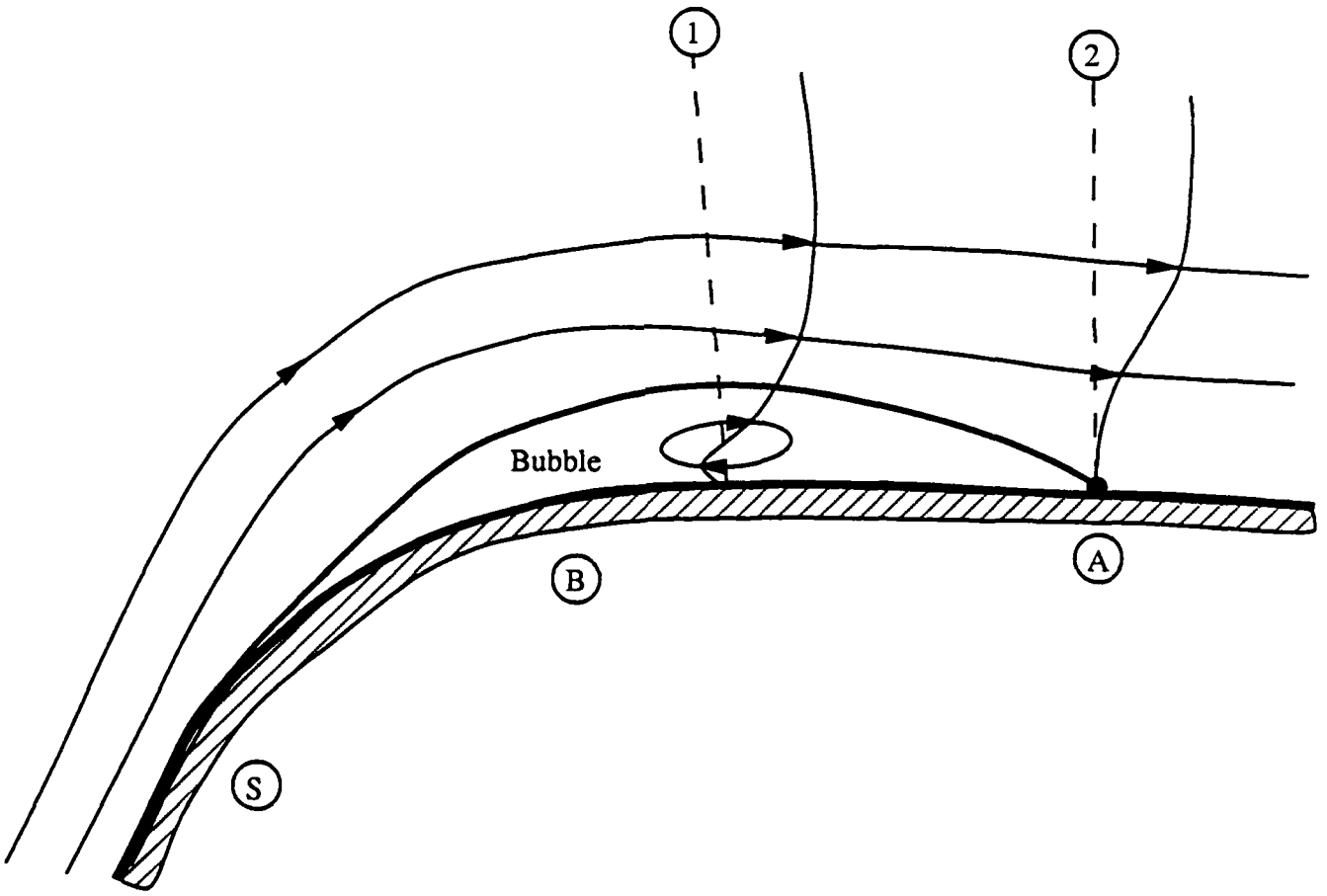

Figure 24. Laminar separation Bubble.

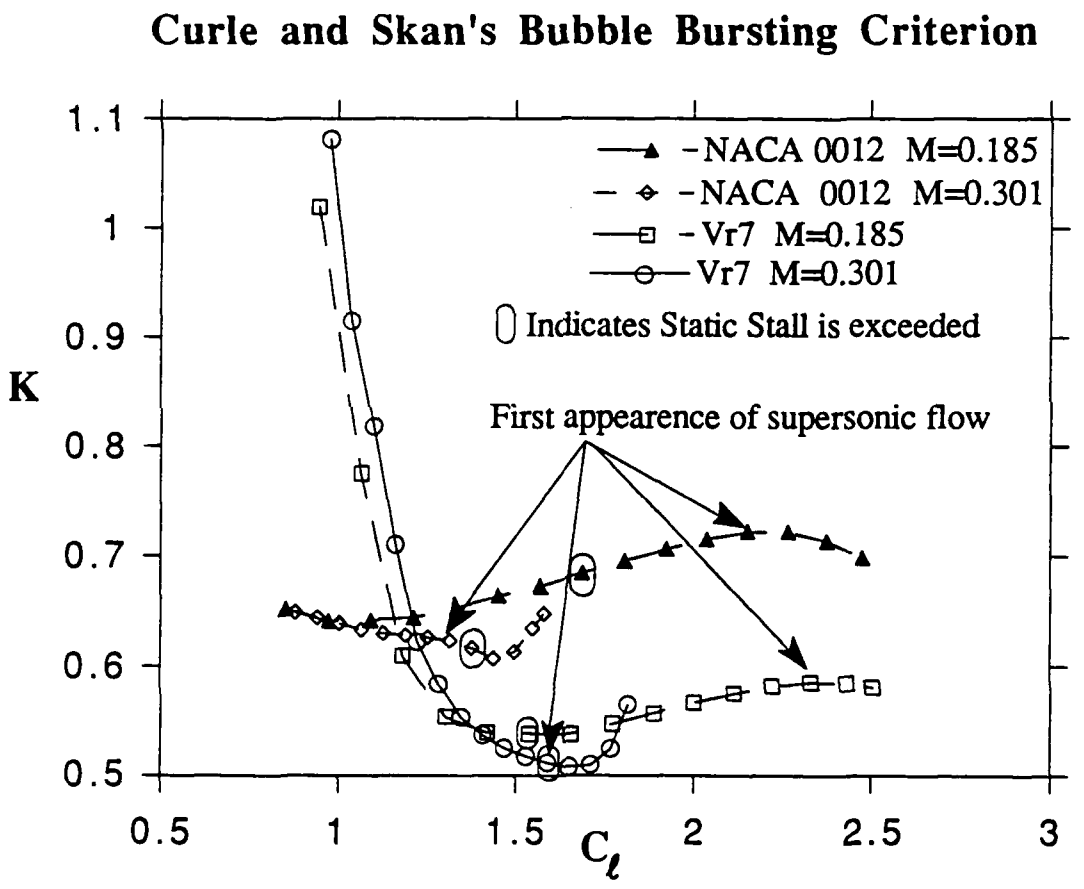

Figure 25. Curl and Scan's bubble bursting criterion.

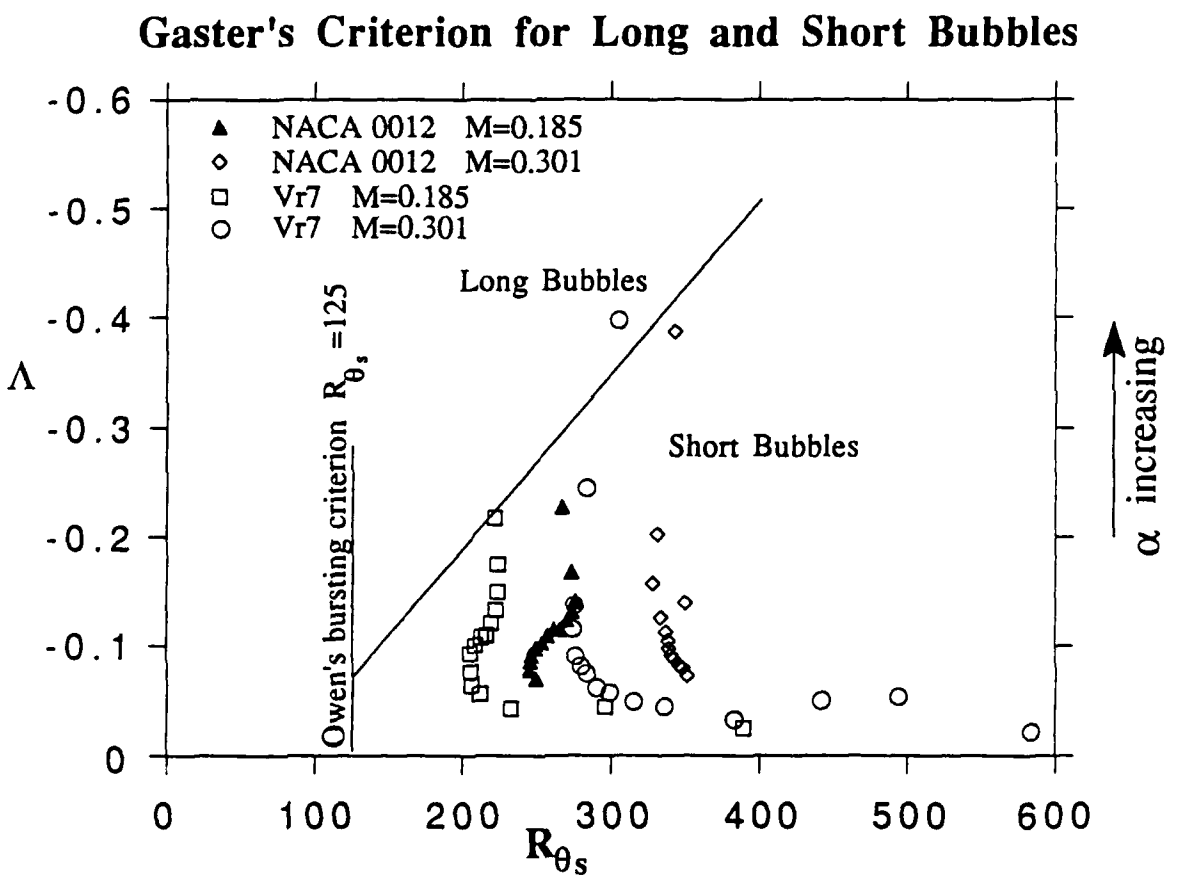

Figure 26. Gaster's criterion for long and short bubbles.

Table 2. Transition Point Study for NACA 0012.

Low Mach Number M=0.185
Re=2,370,000

α_{stall}=15.93 $C_{\ell_{ss}}$=1.59

α	T.P.	Iterations	residual	C_ℓ comp.	C_ℓ exper.	%error C_ℓ
10.00	0.0100	5000	0.183E-12	1.08408	1.08	0.38
10.00	0.0200	5000	0.183E-11	1.08800	1.08	0.74
10.00	0.1000	5000	0.610E-07	1.03494	1.08	4.17
10.00	0.5000	5000	0.265E-05	0.49959	1.08	53.7
13.25	0.0050	5000	0.693E-12	1.40177	1.38	1.58
13.25	0.0100	5000	0.403E-12	1.40763	1.38	2.00
13.25	0.0125	5000	0.840E-11	1.41054	1.38	2.21
13.25	0.0150	5000	0.408E-11	1.41064	1.38	2.22
13.25	0.0160	5000	0.534E-12	1.39451	1.38	1.05
13.50	0.0160	5000	0.323E-09	1.41439	1.39	2.44
14.00	0.0160	5000	0.685E-08	1.44385	1.43	0.96
14.50	0.0160	5000	0.594E-08	1.47493	1.46	1.02
15.00	0.0160	5000	0.651E-07	1.48368	1.49	0.42
15.00	0.0200	5000	0.165E-06	1.41001	1.49	5.37
15.50	0.0100	5000	0.110E-11	1.61433	1.52	6.21
15.50	0.0150	5000	0.160E-11	1.57660	1.52	3.72
15.50	0.0160	5000	0.108E-06	1.37093	1.52	9.81
15.50	0.0175	5000	0.108E-06	1.37093	1.52	9.81
15.50	0.0200	5000	0.955E-07	1.41203	1.52	7.10
15.50	0.0250	5000	0.138E-05	1.43104	1.52	5.85

High Mach Number M=0.301
Re=3,770,000

α_{stall}=13.43 $C_{\ell_{ss}}$=1.372

α	T.P.	Iterations	residual	C_ℓ comp	C_ℓ exper	%error C_ℓ
10.00	0.0000	5000	0.498E-09	1.11637	1.11	0.57
10.00	0.0100	5000	0.643E-13	1.12422	1.11	1.28
10.00	0.0150	4500	0.643E-14	1.12675	1.11	1.51
10.00	0.0200	5000	0.816E-13	1.12779	1.11	2.53
13.25	0.0000	5000	0.647E-13	1.42638	1.37	4.12
13.25	0.0050	5000	0.103E-11	1.43844	1.37	5.00
13.25	0.0100	5000	0.265E-11	1.44003	1.37	5.11
13.25	0.0125	5000	0.115E-11	1.43179	1.37	4.51
13.25	0.0135	5500†	0.887E-07	1.43278	1.37	4.48
13.25	0.0135	6000†	0.249E-06	1.43454	1.37	4.71
13.25	0.0135	7000†	0.173E-05	1.43771	1.37	4.94

† iterations beginning with 5001 are time accurate, not steady. These runs were started from the converged solution of the 5000 iteration for α=13.25 with a transition point of 0.0125.

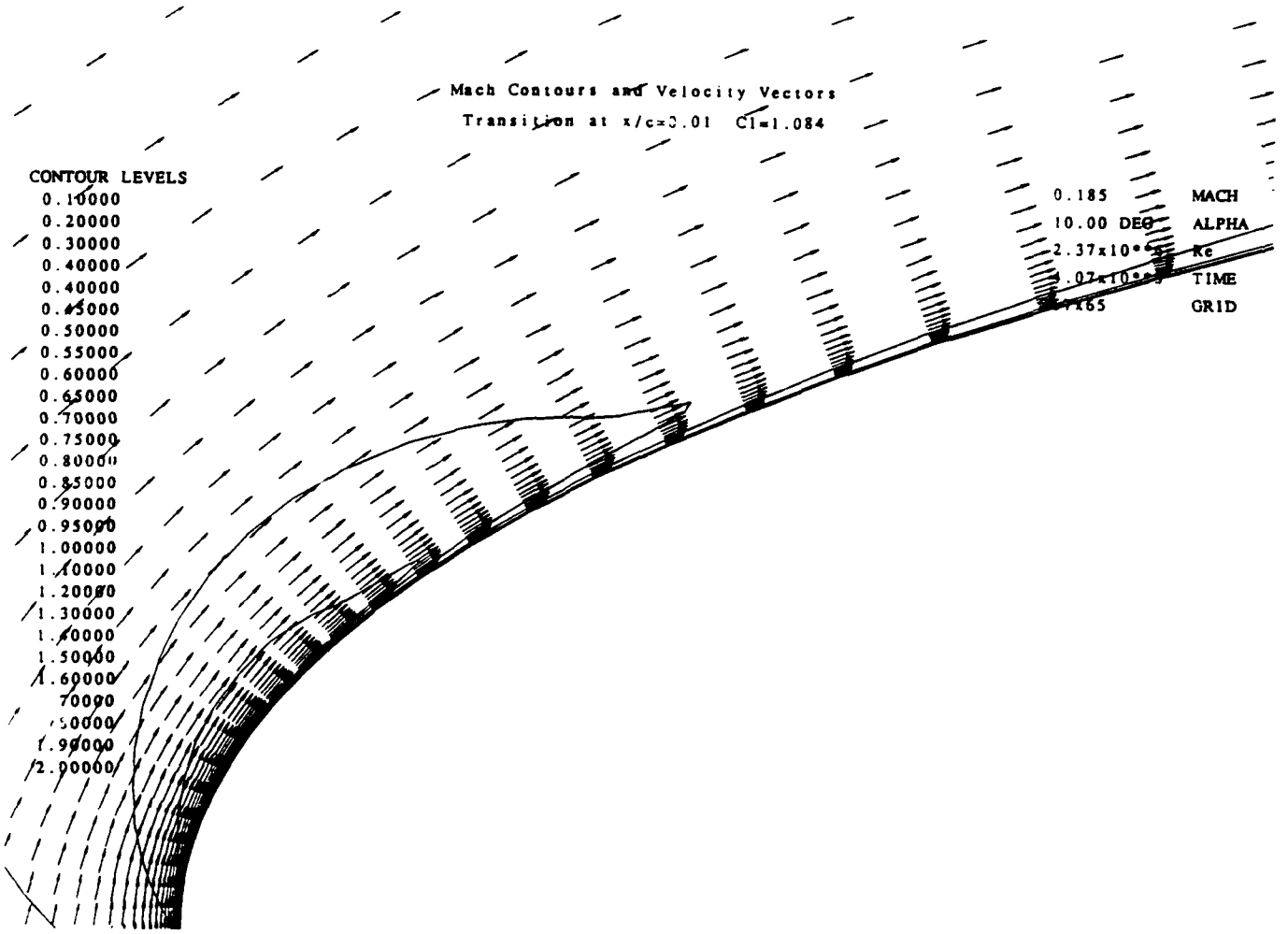

Figure 27. Navier-Stokes solution for M=0.185 α=10.00 T.P.=0.01.

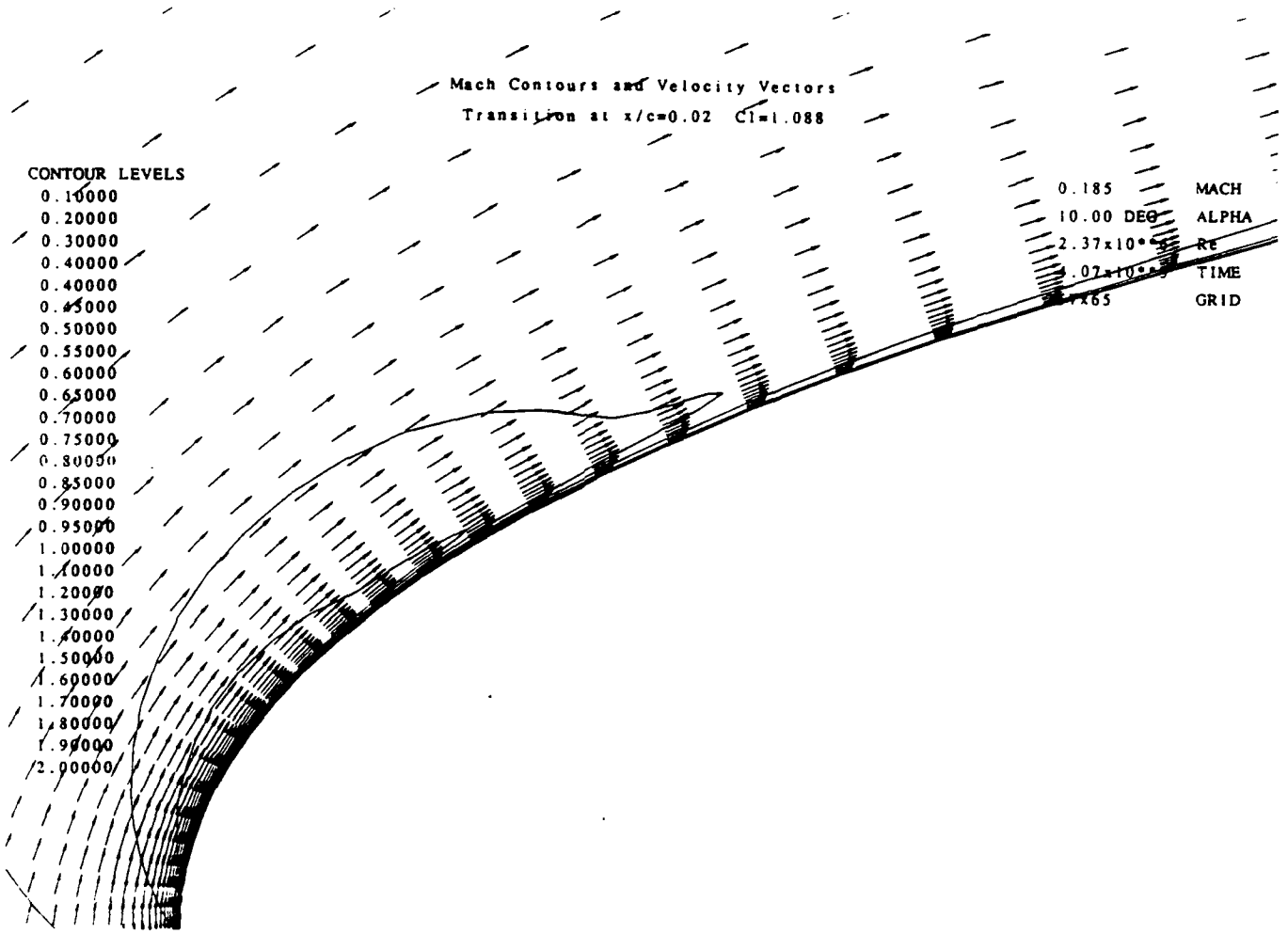

Figure 28. Navier-Stokes solution for M=0.185 α=10.00 T.P.=0.02.

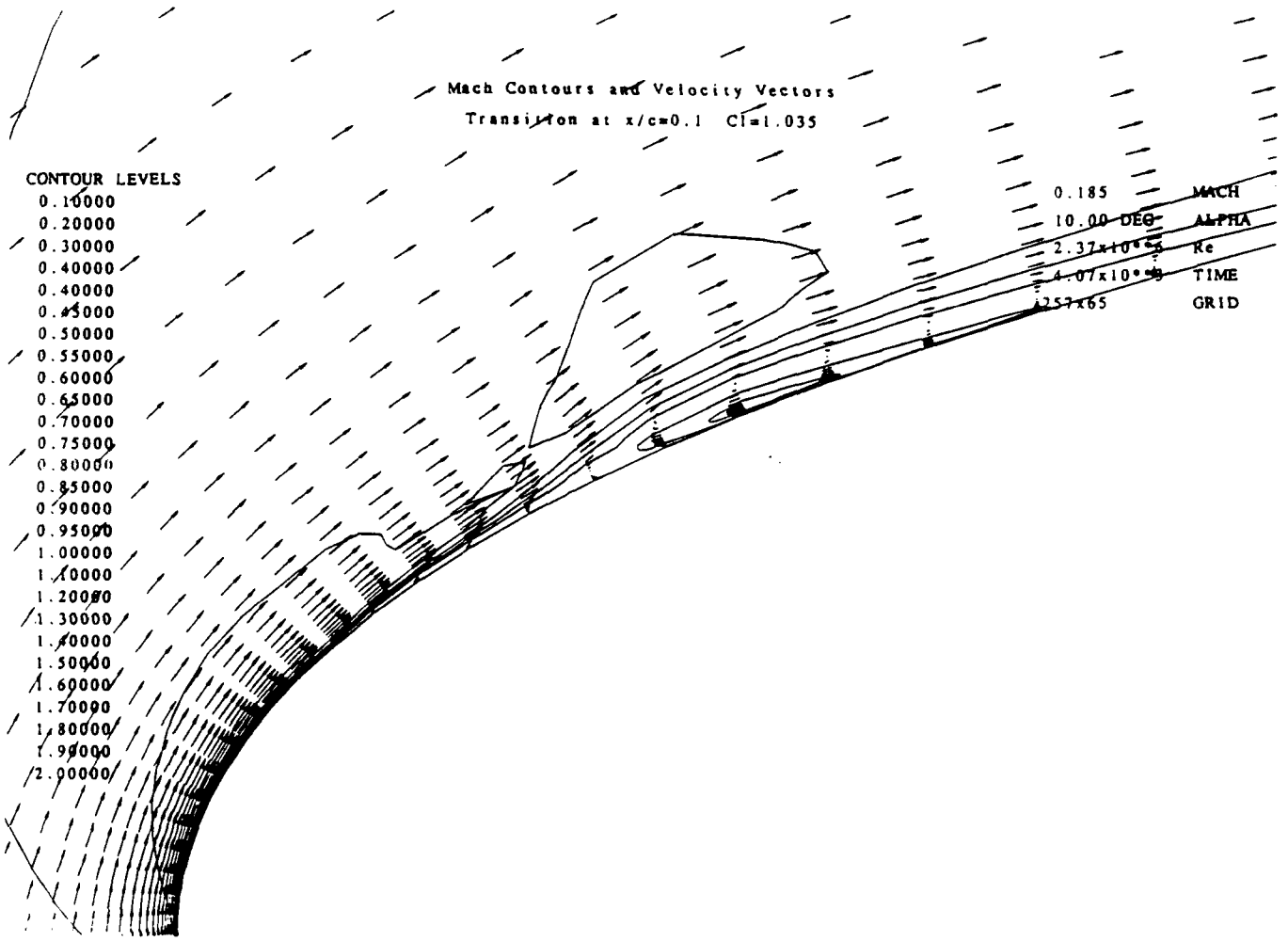

Figure 29. Navier-Stokes solution for M=0.185 α=10.00 T.P.=0.1.

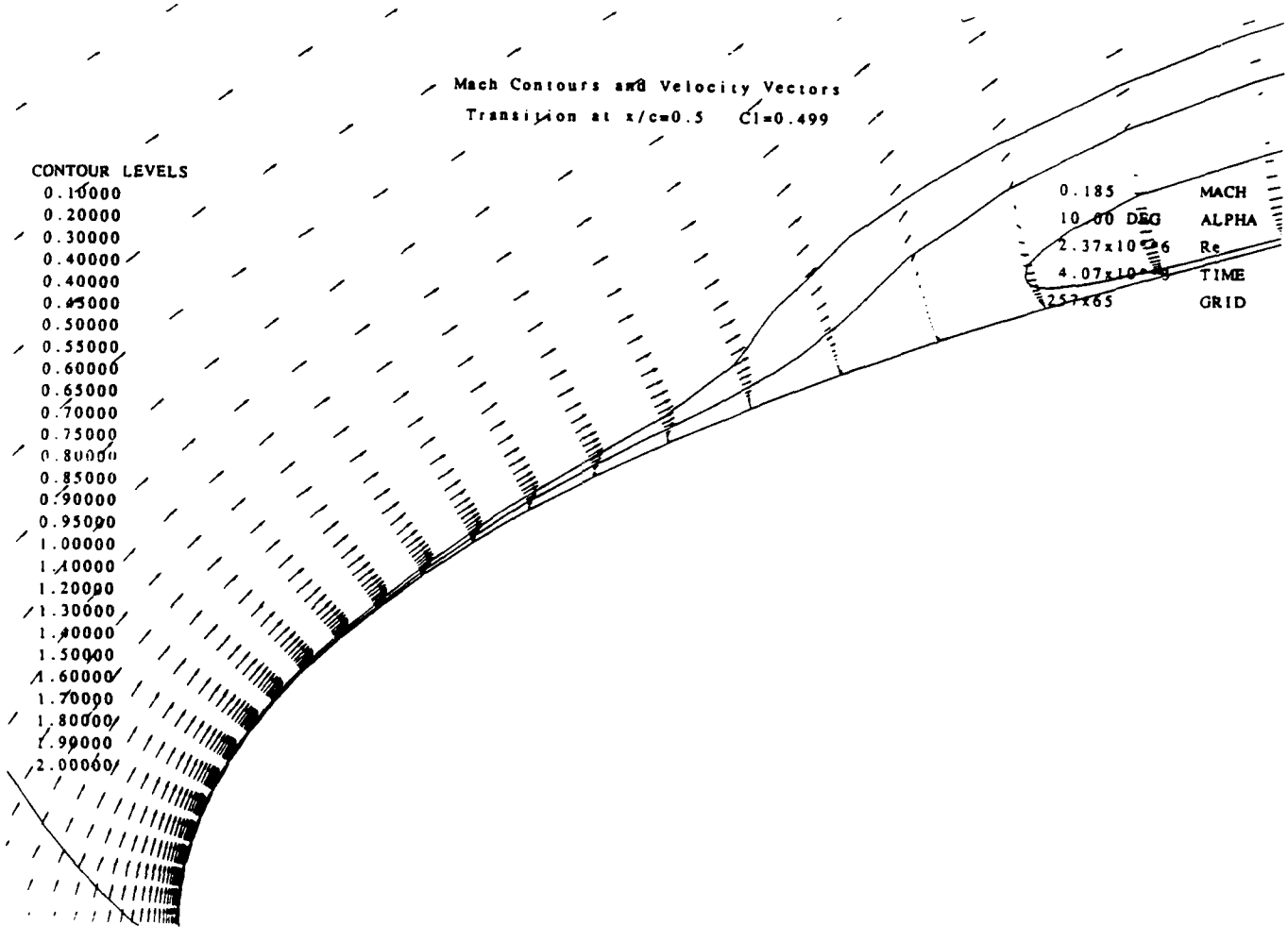

Figure 30. Navier-Stokes solution for M=0.185 α=10.00 T.P.=0.5.

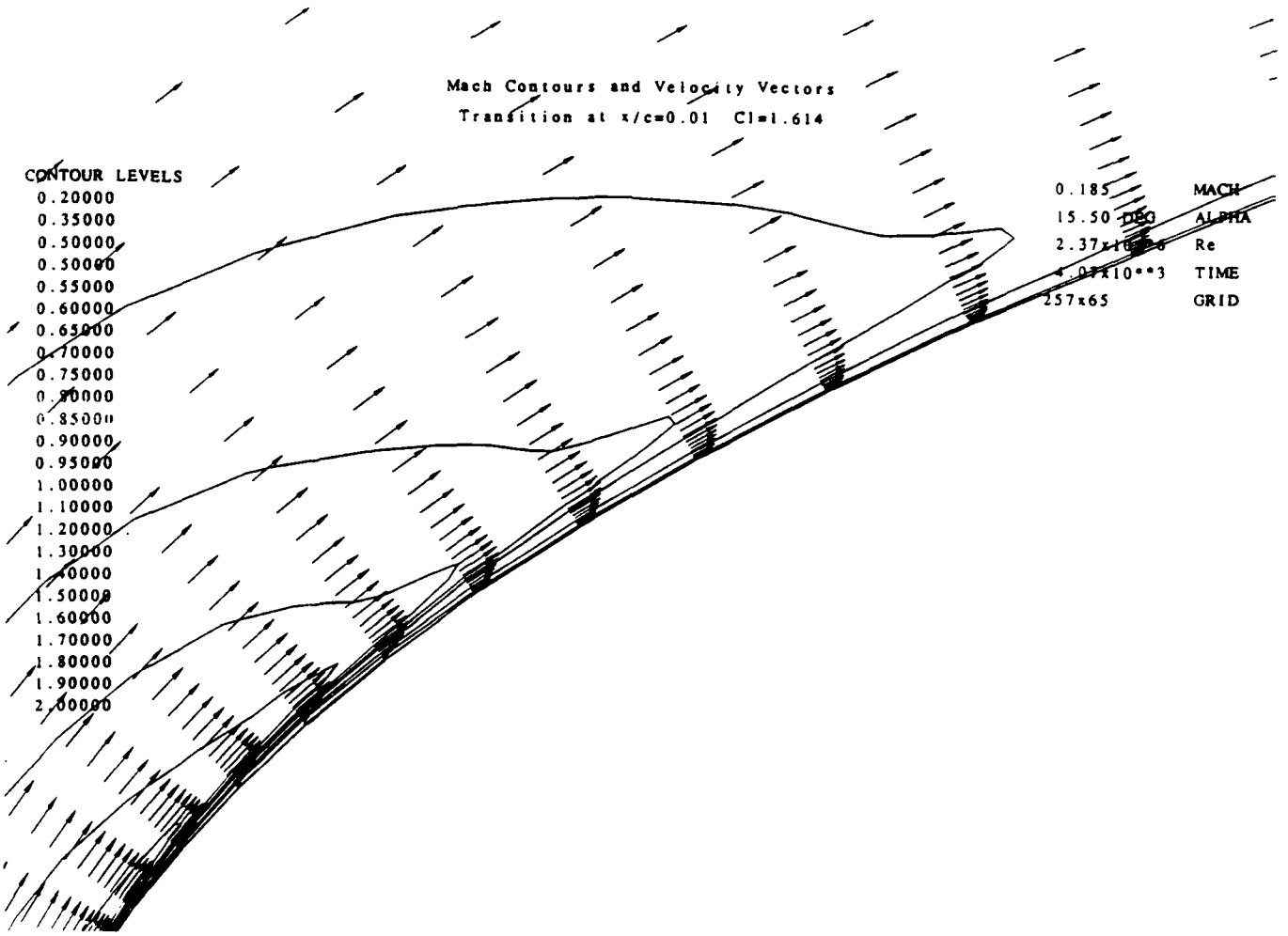

Figure 31. Navier-Stokes solution for M=0.185 α=15.50 T.P.=0.01.

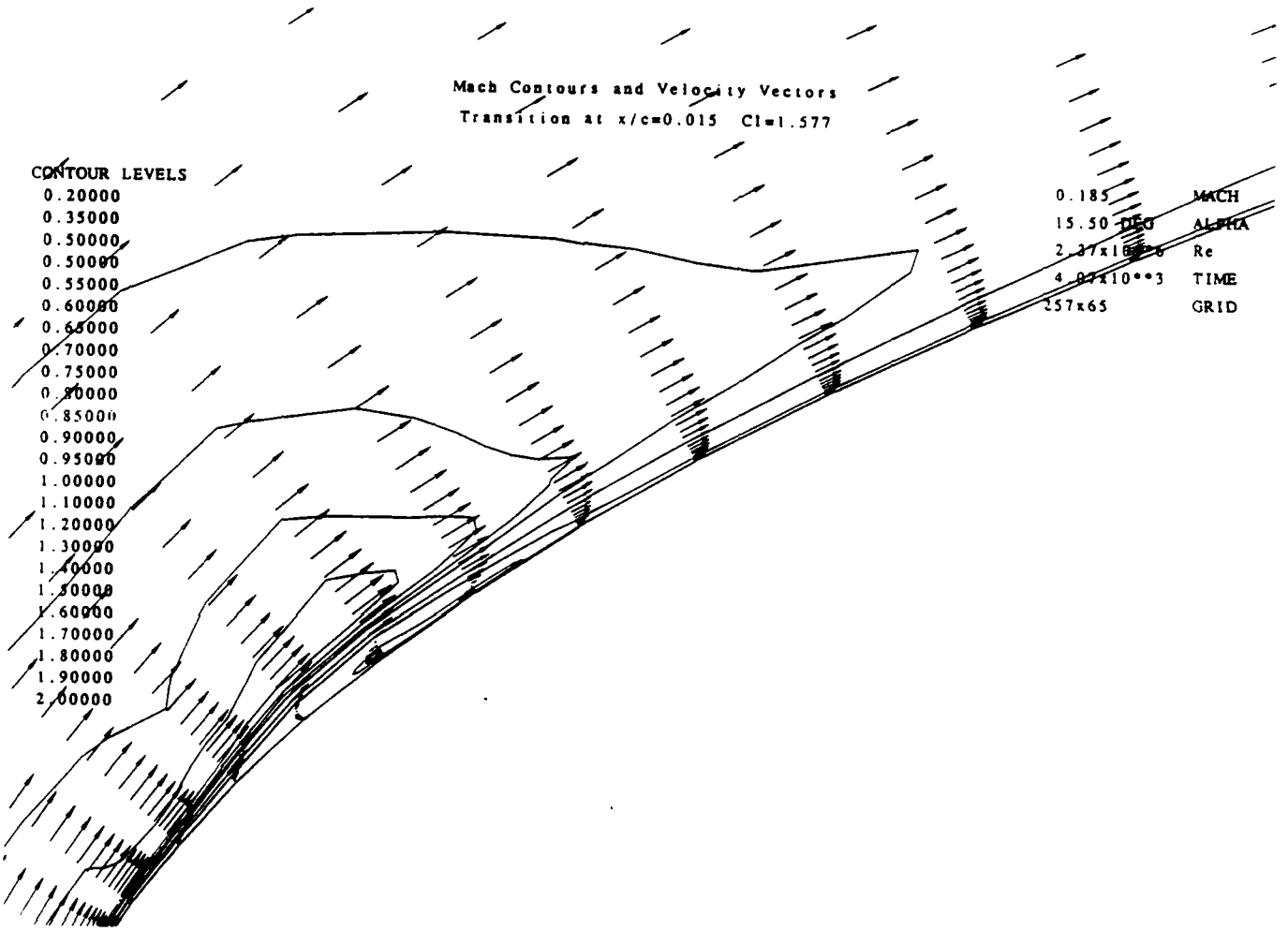

Figure 32. Navier-Stokes solution for M=0.185 α=15.50 T.P.=0.015.

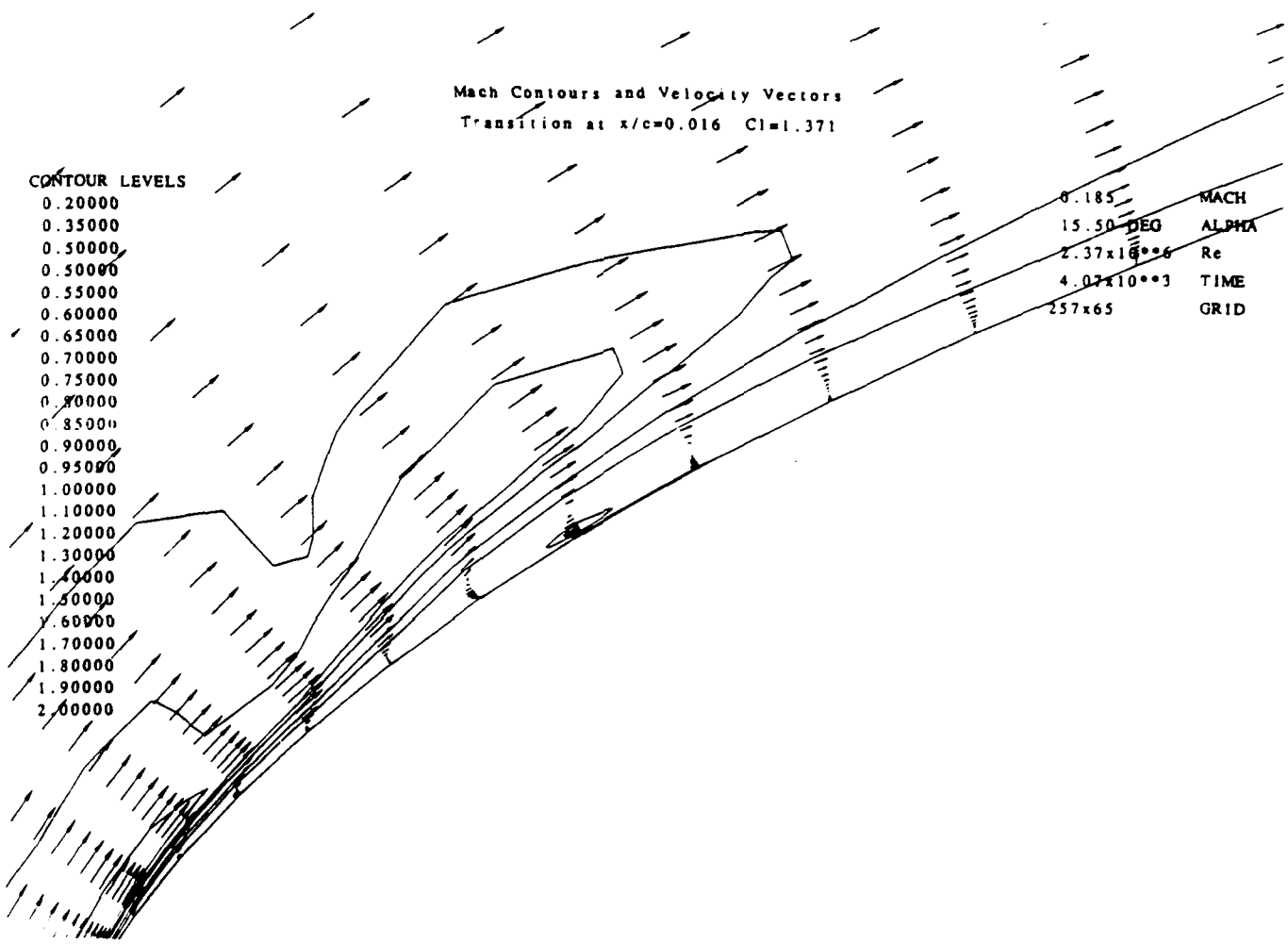

Figure 33. Navier-Stokes solution for M=0.185 α=15.50 T.P.=0.016.

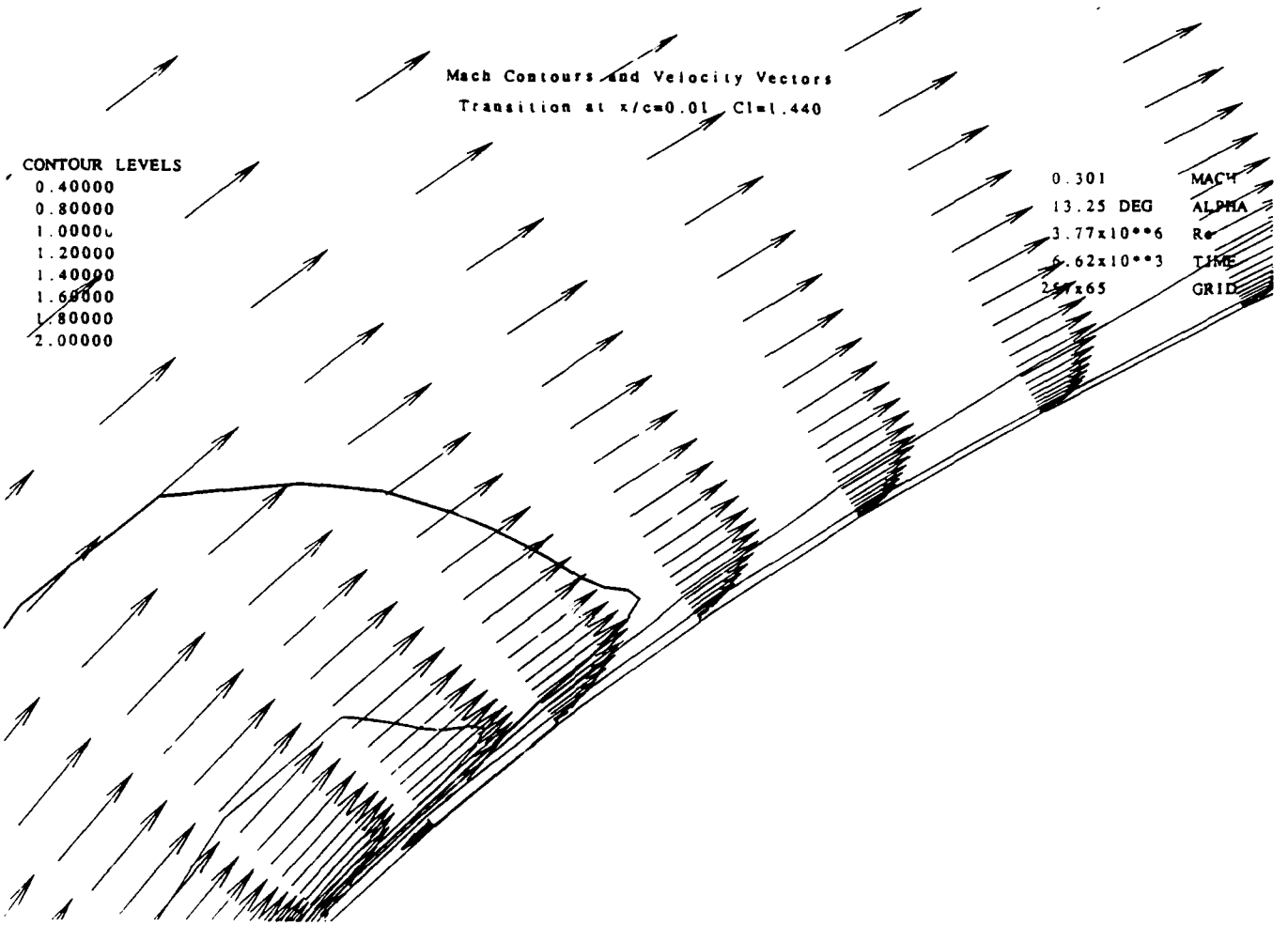

Figure 34. Navier-Stokes solution for M=0.301 α=13.25 T.P.=0.01.

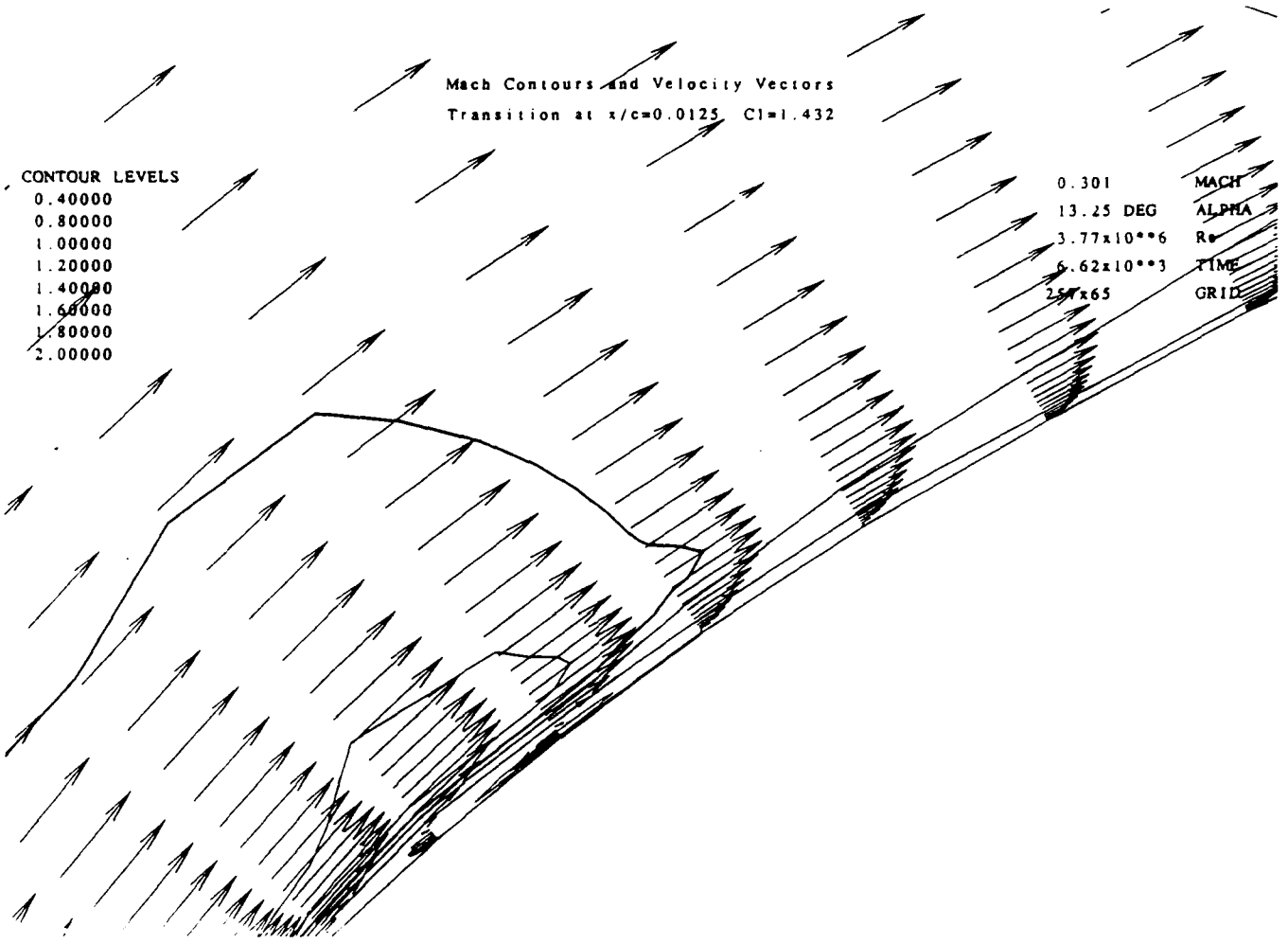

Figure 35. Navier-Stokes solution for M=0.301 α=13.25 T.P.=0.0125.

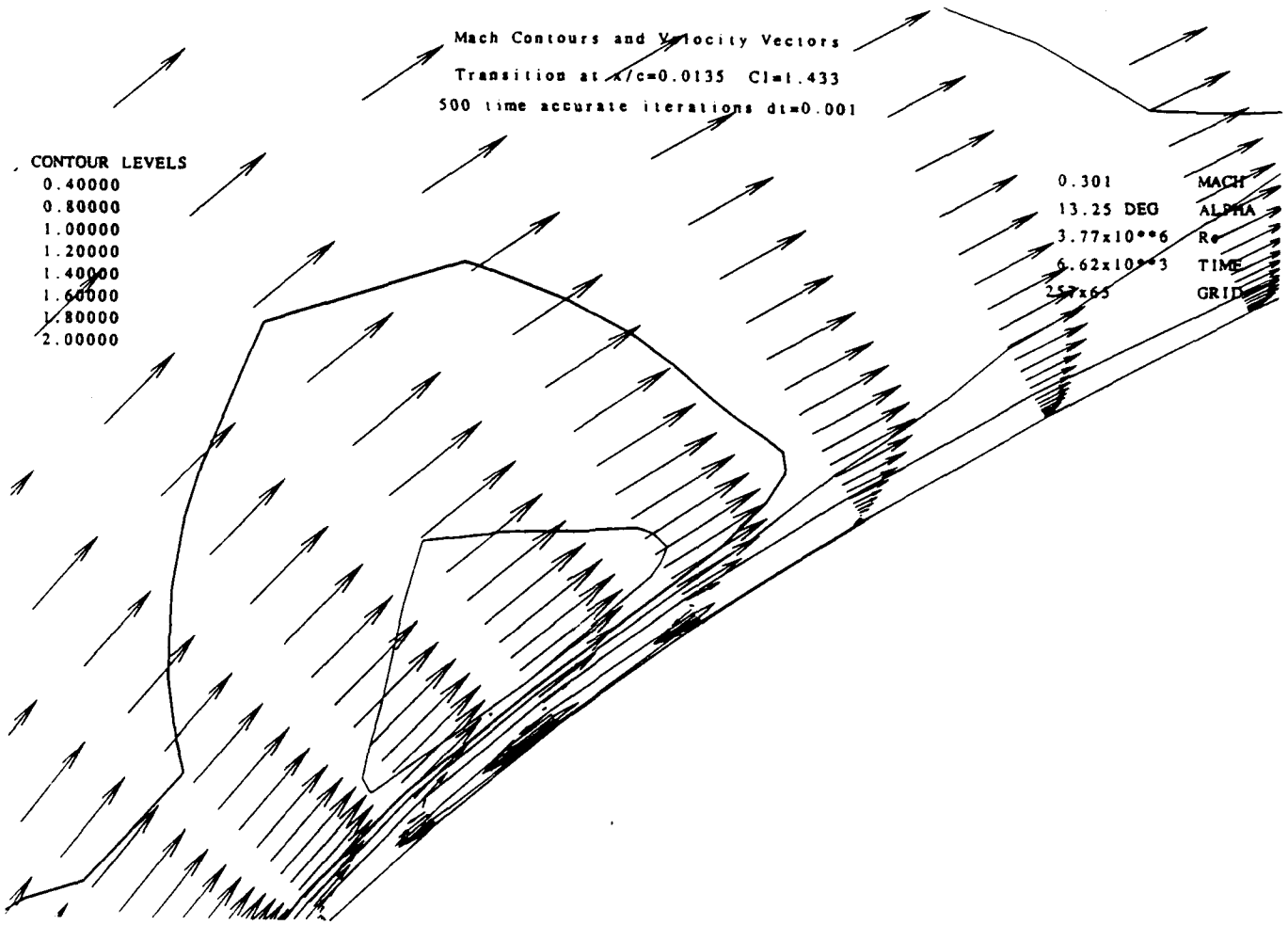

Figure 36. Navier-Stokes solution for M=0.301 α=13.25 T.P.=0.0135 Iters=500.

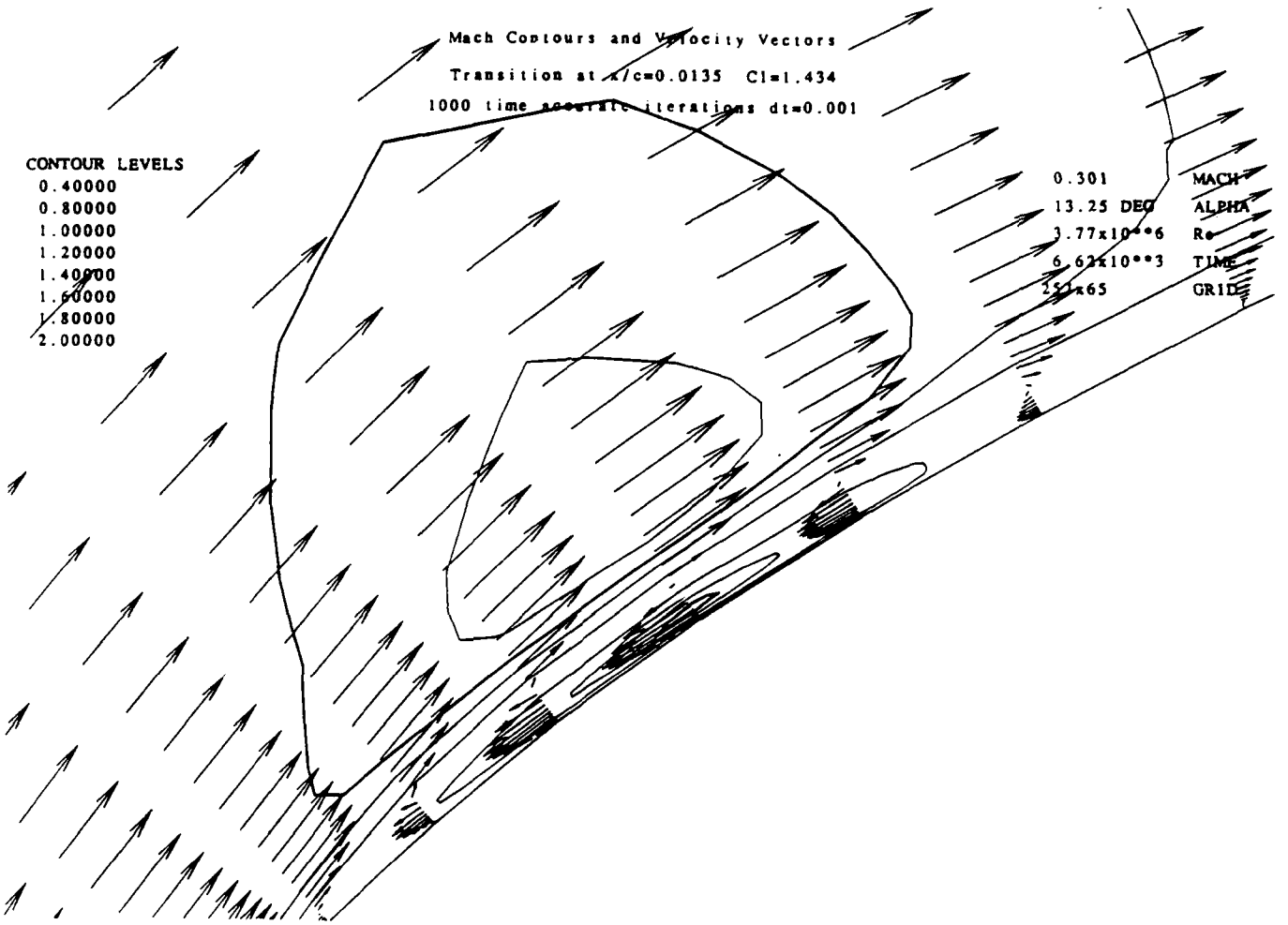

Figure 37. Navier-Stokes solution for M=0.301 α=13.25 T.P.=0.0135 Iters=1000.

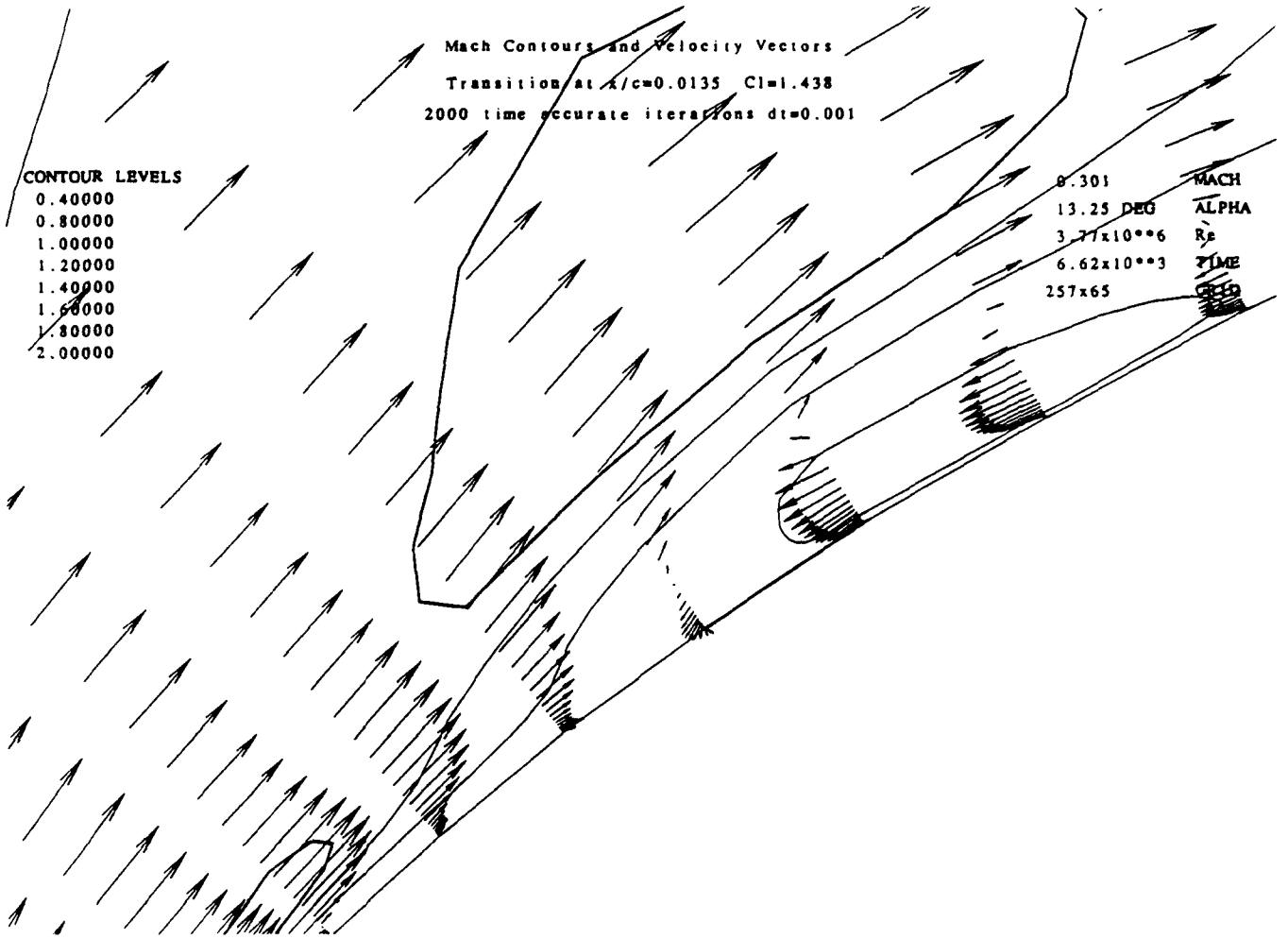

Figure 38. Navier-Stokes solution for M=0.301 α=13.25 T.P.=0.0135 Iters=2000.

Glossary:

ref#	case number for this study
case	case number from McCroskey
avem	average Mach number
k	reduced frequency
alpha0	mean angle of attack
alpha1	amplitude of oscillation
Cp max	maximum suction peak
Cl	maximum lift coefficient
Cl at	C_ℓ at maximum suction peak
Re	Reynolds number in millions
freq	frequency in Hertz
aveQ	average dynamic pressure

The NACA0012 Airfoil (0012)

ref#	case	avem	k	alpha0	alpha1	Cp Max	Cl max	Cl at	Re(mil)	freq	aveQ
1	4019	.301	.000	-5.00	.00	2.125	-.605	-.605	3.958	.000	.875
2	4100	.301	.000	-2.00	.00	.978	-.241	-.241	3.933	.000	.877
3	4102	.301	.000	.00	.00	.594	-.011	-.011	3.924	.000	.877
4	4109	.302	.000	2.00	.00	.827	.202	.202	3.910	.000	.877
5	4111	.299	.000	4.00	.00	1.416	.450	.450	3.931	.000	.885
6	4113	.302	.000	8.00	.00	4.210	.929	.929	3.898	.000	.877
7	4119	.301	.000	10.00	.00	5.874	1.123	1.123	3.901	.000	.877
8	4123	.302	.000	12.00	.00	7.726	1.312	1.312	3.876	.000	.877
9	4201	.302	.000	13.00	.00	8.501	1.370	1.370	3.871	.000	.877
10	4203	.301	.000	13.50	.00	8.827	1.384	1.384	3.867	.000	.879
11	4209	.302	.000	14.00	.00	4.892	1.045	1.045	3.861	.000	.877
12	4211	.305	.000	14.50	.00	5.009	1.044	1.044	3.823	.000	.868
13	4213	.302	.000	15.00	.00	5.121	1.060	1.060	3.843	.000	.877
14	4215	.284	.000	15.50	.00	8.394	1.339	1.339	3.629	.000	.784
15	4217	.266	.000	16.00	.00	8.716	1.396	1.396	3.398	.000	.688
16	4219	.271	.000	17.80	.00	7.464	1.246	1.246	3.463	.000	.717
17	4301	.266	.000	20.00	.00	3.101	1.141	1.141	3.448	.000	.700
18	4401	.302	.000	13.00	.00	8.498	1.350	1.350	3.795	.000	.877
19	4403	.302	.000	11.00	.00	6.769	1.222	1.222	3.784	.000	.877
20	4404	.302	.000	8.00	.00	4.031	.907	.907	3.780	.000	.877
21	4405	.302	.000	5.00	.00	1.929	.576	.576	3.781	.000	.877
22	4410	.302	.000	2.00	.00	.829	.226	.226	3.783	.000	.877
23	4411	.302	.000	.00	.00	.565	-.006	-.006	3.782	.000	.877
24	4412	.302	.000	-2.00	.00	.886	-.229	-.229	3.779	.000	.877
25	11018	.302	.000	-5.00	.00	2.004	-.584	-.584	3.999	.000	.875
26	11019	.301	.000	-2.00	.00	.876	-.234	-.234	3.990	.000	.875
27	11020	.302	.000	.00	.00	.567	-.001	-.001	3.979	.000	.875
28	11101	.302	.000	2.00	.00	.878	.234	.234	3.975	.000	.875
29	11102	.301	.000	4.00	.00	1.522	.481	.481	3.959	.000	.875
30	11105	.301	.000	8.10	.00	4.089	.918	.918	3.939	.000	.876
31	11110	.301	.000	10.00	.00	5.760	1.120	1.120	3.936	.000	.875
32	11111	.301	.000	12.30	.00	7.962	1.321	1.321	3.922	.000	.875
33	11112	.301	.000	13.40	.00	8.703	1.377	1.377	3.912	.000	.875
34	11113	.301	.000	13.80	.00	8.818	1.374	1.374	3.905	.000	.875
35	11118	.301	.000	14.00	.00	8.672	1.351	1.351	3.913	.000	.875
36	11121	.302	.000	14.60	.00	5.794	1.093	1.093	3.930	.000	.875
37	11122	.304	.000	15.00	.00	5.488	.982	.982	3.925	.000	.887
38	11123	.289	.000	15.50	.00	8.036	1.312	1.312	3.745	.000	.811
39	11200	.290	.000	16.00	.00	7.030	1.201	1.201	3.734	.000	.811
40	11201	.295	.000	17.00	.00	4.560	.868	.868	3.793	.000	.841
41	11204	.288	.000	17.90	.00	6.988	1.151	1.151	3.725	.000	.803

42	11205	.280	.000	20.00	.00	6.982	1.205	1.205	3.616	.000	.764
43	11208	.249	.000	24.90	.00	5.027	1.087	1.087	3.253	.000	.610
44	11209	.238	.000	30.00	.00	1.230	.997	.997	3.106	.000	.561
45	11210	.251	.000	25.00	.00	4.519	1.021	1.021	3.255	.000	.619
46	11211	.273	.000	20.00	.00	2.702	.850	.850	3.515	.000	.725
47	11213	.280	.000	18.00	.00	7.456	1.219	1.219	3.628	.000	.764
48	11214	.302	.000	16.00	.00	4.568	.938	.938	3.866	.000	.875
49	11215	.302	.000	15.00	.00	5.918	1.060	1.060	3.862	.000	.875
50	11216	.301	.000	14.00	.00	8.547	1.326	1.326	3.847	.000	.869
51	11221	.302	.000	13.10	.00	8.455	1.356	1.356	3.885	.000	.875
52	11222	.302	.000	11.00	.00	6.667	1.199	1.199	3.876	.000	.875
53	11223	.302	.000	8.00	.00	3.965	.904	.904	3.871	.000	.875
54	11304	.302	.000	5.00	.00	1.875	.562	.562	3.896	.000	.875
55	11305	.302	.000	2.00	.00	.812	.216	.216	3.887	.000	.875
56	11308	.301	.000	.00	.00	.557	-.009	-.009	3.871	.000	.875
57	11309	.301	.000	-2.00	.00	.841	-.229	-.229	3.871	.000	.875
58	7019	.297	.051	9.00	5.00	9.123	1.439	1.431	3.894	2.700	.878
59	7021	.299	.100	9.00	5.00	9.065	1.472	1.470	3.962	5.400	.886
60	7023	.299	.201	9.00	5.00	9.134	1.580	1.532	3.945	10.800	.886
61	7101	.301	.150	9.00	5.00	9.227	1.518	1.507	3.910	8.100	.878
62	7104	.301	.025	9.00	5.00	8.961	1.407	1.378	3.902	1.350	.878
63	7108	.301	.025	8.00	5.00	8.715	1.366	1.361	3.921	1.350	.878
64	7110	.301	.100	8.00	5.00	8.830	1.406	1.401	3.903	5.400	.878
65	7111	.301	.199	8.00	5.00	9.115	1.446	1.434	3.895	10.800	.877
66	7112	.301	.025	10.00	5.00	9.030	1.418	1.408	3.880	1.366	.877
67	7113	.301	.099	10.00	5.00	9.103	1.537	1.508	3.877	5.400	.877
68	7114	.301	.199	10.00	5.00	9.076	1.649	1.564	3.869	10.800	.877
69	7117	.301	.025	11.00	5.00	8.978	1.412	1.406	3.892	1.350	.878
70	7118	.301	.050	11.00	5.00	9.015	1.516	1.470	3.875	2.700	.878
71	7119	.301	.099	11.00	5.00	9.050	1.577	1.522	3.866	5.400	.877
72	7120	.301	.149	11.00	5.00	9.076	1.617	1.536	3.860	8.100	.877
73	7121	.301	.198	11.00	5.00	8.991	1.707	1.571	3.852	10.800	.878
74	7200	.301	.025	12.00	5.00	8.972	1.414	1.402	3.879	1.350	.878
75	7205	.302	.099	12.00	5.00	9.067	1.606	1.520	3.853	5.400	.877
76	7207	.302	.198	12.00	5.00	9.010	1.806	1.586	3.845	10.800	.877
77	7212	.302	.149	8.80	5.00	9.098	1.485	1.482	3.865	8.100	.877
78	7214	.302	.099	8.80	5.00	9.037	1.441	1.440	3.860	5.400	.877
79	7216	.302	.050	8.80	5.00	8.927	1.414	1.393	3.857	2.700	.877
80	7300	.300	.151	10.00	5.00	9.397	1.582	1.536	3.986	8.100	.877
81	7302	.300	.074	10.00	5.00	9.342	1.518	1.506	3.958	4.000	.877
82	7305	.300	.151	12.00	5.00	9.343	1.660	1.566	3.966	8.100	.877
83	8019	.035	.104	10.00	10.00	7.531	2.072	1.650	.487	.664	.013
84	8021	.035	.151	10.00	10.00	7.423	2.156	1.743	.486	.970	.013
85	8023	.035	.253	10.00	10.00	8.119	2.098	1.935	.486	1.620	.013
86	8102	.036	.103	15.00	10.00	7.944	2.118	1.495	.486	.661	.013
87	8104	.036	.153	15.00	10.00	7.387	2.116	1.538	.484	.981	.013
88	8106	.036	.104	15.00	14.00	6.889	2.214	1.528	.483	.667	.013
89	8114	.072	.099	15.00	10.00	12.775	2.192	1.983	.980	1.300	.054
90	8116	.072	.149	15.00	10.00	14.354	2.345	2.115	.980	1.950	.054
91	8118	.072	.248	15.00	10.00	16.337	2.422	2.236	.978	3.250	.054
92	8123	.072	.099	15.00	14.00	14.533	2.437	2.176	.980	1.300	.054
93	8203	.072	.248	10.00	10.00	12.141	1.805	1.801	.978	3.250	.054
94	8210	.109	.250	10.00	10.00	13.285	1.861	1.818	1.491	4.900	.122
95	8214	.109	.100	15.00	10.00	14.754	2.274	2.064	1.480	1.960	.122
96	8220	.184	.099	15.00	10.00	16.871	2.257	2.143	2.433	3.300	.339
97	8222	.184	.149	15.00	10.00	17.764	2.374	2.217	2.423	4.950	.339
98	8306	.184	.099	15.00	14.00	17.631	2.527	2.237	2.405	3.300	.339
99	9022	.184	.235	15.00	6.00	16.761	2.054	2.041	2.358	7.920	.339
100	9101	.184	.284	15.00	5.00	15.411	1.940	1.914	2.359	9.570	.339
101	9106	.184	.245	10.00	10.00	16.205	2.018	1.970	2.365	8.250	.339
102	9110	.184	.010	8.00	10.00	11.786	1.695	1.684	2.476	.330	.339
103	9112	.183	.050	8.00	10.00	12.752	1.755	1.754	2.475	1.650	.341
104	9118	.184	.199	8.00	10.00	13.049	1.780	1.748	2.449	6.600	.339
105	9202	.220	.098	15.00	10.00	15.392	2.198	2.040	2.848	3.930	.479

106	9203	.249	.098	15.00	10.00	12.356	2.116	1.870	3.187	4.460	.610
107	9208	.280	.097	15.00	10.00	10.453	2.003	1.695	3.520	4.980	.762
108	9210	.295	.010	15.00	10.00	8.931	1.412	1.410	3.672	.530	.842
109	9213	.294	.024	15.00	10.00	9.335	1.515	1.488	3.596	1.310	.831
110	9214	.292	.049	15.00	10.00	9.624	1.706	1.546	3.567	2.620	.821
111	9217	.290	.098	15.00	10.00	9.905	2.073	1.633	3.550	5.240	.812
112	9218	.283	.151	15.00	10.00	10.367	2.169	1.758	3.451	7.860	.773
113	9221	.302	.010	10.00	10.00	8.685	1.403	1.395	3.673	.544	.876
114	9222	.302	.024	10.00	10.00	9.004	1.562	1.476	3.660	1.340	.876
115	9223	.302	.048	10.00	10.00	9.038	1.675	1.525	3.652	2.680	.876
116	9302	.302	.096	10.00	10.00	9.063	1.839	1.574	3.659	5.360	.876
117	9307	.302	.145	10.00	10.00	9.135	1.855	1.606	3.671	8.040	.877
118	10022	.301	.098	12.00	10.00	9.053	1.893	1.567	3.770	5.360	.878
119	10101	.265	.110	20.00	10.00	11.212	2.150	1.796	3.303	5.360	.688
120	10104	.302	.048	12.00	8.00	8.963	1.651	1.494	3.711	2.680	.877
121	10105	.302	.097	12.00	8.00	8.964	1.753	1.550	3.694	5.360	.878
122	10108	.296	.125	12.00	8.00	9.290	1.965	1.590	3.636	6.810	.847
123	10113	.302	.010	15.00	5.00	8.950	1.386	1.376	3.897	.530	.876
124	10114	.295	.025	15.00	5.00	9.480	1.478	1.460	3.801	1.340	.841
125	10118	.291	.102	15.00	5.00	9.860	1.762	1.594	3.749	5.360	.823
126	10120	.294	.151	15.00	5.00	9.635	1.872	1.600	3.785	8.040	.843
127	10123	.293	.202	15.00	5.00	9.843	1.961	1.678	3.759	10.720	.832
128	10202	.301	.010	10.00	5.00	9.008	1.362	1.361	3.858	.536	.877
129	10203	.301	.025	10.00	5.00	9.078	1.378	1.373	3.847	1.340	.877
130	10204	.300	.049	10.00	5.00	9.336	1.476	1.456	3.827	2.680	.870
131	10207	.302	.074	10.00	5.00	9.282	1.501	1.466	3.885	4.020	.877
132	10208	.300	.099	10.00	5.00	9.357	1.529	1.501	3.860	5.360	.870
133	10211	.300	.149	10.00	5.00	9.428	1.563	1.518	3.863	8.040	.870
134	10212	.300	.198	10.00	5.00	9.413	1.633	1.566	3.851	10.720	.870
135	10218	.300	.010	5.00	5.00	5.824	1.124	1.122	3.933	.530	.880
136	10221	.301	.099	5.00	5.00	5.828	1.115	1.111	3.925	5.360	.878
137	10222	.301	.198	5.00	5.00	6.094	1.128	1.114	3.912	10.720	.878
138	10303	.301	.099	5.00	10.00	9.213	1.568	1.522	3.911	5.360	.877
139	10305	.301	.099	3.80	10.00	9.237	1.489	1.489	3.911	5.360	.877
140	10309	.301	.099	2.80	10.00	8.941	1.414	1.401	3.896	5.360	.877
141	12020	.270	.001	20.00	10.00	9.019	1.387	1.379	3.491	.050	.718
142	12102	.302	.001	5.00	10.00	8.846	1.378	1.378	3.820	.050	.882
143	12109	.279	.001	6.00	10.00	9.492	1.427	1.423	3.486	.050	.756
144	12118	.262	.001	20.00	10.00	8.857	1.370	1.370	3.247	.050	.676
145	12203	.231	.001	20.00	10.00	9.570	1.457	1.443	2.887	.045	.531
146	12208	.244	.001	7.00	10.00	10.901	1.561	1.553	3.270	.045	.587
147	12300	.204	.001	20.00	10.00	11.005	1.570	1.567	2.707	.040	.421
148	12305	.169	.001	20.00	10.00	10.339	1.537	1.527	2.253	.033	.292
149	12310	.186	.001	7.00	10.00	10.500	1.530	1.524	2.469	.033	.350
150	13021	.108	.002	7.00	10.00	8.873	1.415	1.409	1.503	.033	.120
151	13107	.105	.002	20.00	10.00	8.185	1.321	1.315	1.421	.033	.113
152	13115	.068	.003	20.00	10.00	7.160	1.262	1.256	.919	.033	.048
153	13120	.072	.003	5.00	10.00	7.120	1.242	1.237	.962	.033	.053
154	13205	.036	.003	5.00	10.00	5.627	1.126	1.105	.489	.017	.014
155	13217	.036	.003	20.00	10.00	4.658	1.117	1.068	.486	.017	.013
156	13222	.276	.001	20.00	10.00	9.478	1.454	1.447	3.657	.050	.749
157	13303	.247	.001	7.00	10.00	11.015	1.565	1.563	3.298	.045	.603
158	13308	.215	.001	7.00	10.00	11.535	1.639	1.638	2.884	.040	.461
159	13310	.216	.001	7.00	10.00	11.512	1.640	1.635	2.885	.040	.466
160	13313	.181	.001	7.00	10.00	9.241	1.468	1.468	2.405	.033	.332
161	13321	.294	.001	7.00	10.00	9.469	1.368	1.368	3.741	.050	.839
162	14019	.183	.050	15.00	10.00	10.989	1.913	1.699	2.454	1.650	.339
163	14021	.182	.100	15.00	10.00	11.534	2.086	1.831	2.434	3.300	.336
164	14023	.182	.150	15.00	10.00	11.969	2.163	1.939	2.427	4.950	.335
165	14104	.183	.050	15.00	10.00	10.942	1.902	1.686	2.449	1.650	.338
166	14106	.184	.099	15.00	10.00	11.494	2.060	1.816	2.449	3.300	.340
167	14108	.183	.149	15.00	10.00	11.880	2.157	1.913	2.443	4.950	.339
168	14117	.293	.026	15.00	10.00	10.502	1.551	1.508	3.843	1.354	.837
169	14119	.293	.051	15.00	10.00	10.614	1.700	1.575	3.818	2.680	.836

170	14200	.294	.025	15.00	10.00	10.507	1.534	1.508	3.822	1.340	.843
171	14202	.293	.051	15.00	10.00	10.670	1.718	1.580	3.793	2.680	.839
172	14208	.291	.102	15.00	10.00	10.976	1.956	1.671	3.764	5.360	.828
173	14210	.292	.101	15.00	10.00	10.848	1.942	1.650	3.760	5.360	.832
174	14218	.292	.025	15.00	10.00	9.546	1.683	1.509	3.763	1.340	.830
175	14219	.291	.051	15.00	10.00	9.664	1.820	1.565	3.736	2.680	.824
176	14220	.287	.103	15.00	10.00	9.973	2.062	1.657	3.683	5.360	.805
177	15218	.290	.099	15.00	10.00	.000	-.005	1.657	3.679	5.240	.818
178	10117	.295	.050	15.00	5.00	9.570	1.608	1.510	3.803	2.680	.843
179	7202	.302	.050	12.00	5.00	8.947	1.499	1.465	3.861	2.700	.877
180	7222	.298	.051	10.00	5.00	9.379	1.462	1.461	3.975	2.700	.876
ref#	case	avem	k	alpha0	alpha1	Cp Max	Cl max	Cl at	Re(mil)	freq	aveQ

The AMES 01 Airfoil (ames)

ref#	case	avem	k	alpha0	alpha1	Cp Max	Cl max	Cl at	Re(mil)	freq	aveQ
1	26020	.301	.000	-5.00	.00	3.628	-.509	-.509	3.922	.000	.880
2	26022	.302	.000	-2.00	.00	1.545	-.160	-.160	3.908	.000	.881
3	26023	.302	.000	.00	.00	.634	.089	.089	3.901	.000	.882
4	26101	.302	.000	2.00	.00	.950	.313	.313	3.879	.000	.878
5	26107	.302	.000	4.00	.00	1.357	.547	.547	3.839	.000	.879
6	26108	.302	.000	8.00	.00	2.979	.987	.987	3.840	.000	.880
7	26109	.302	.000	10.00	.00	4.505	1.212	1.212	3.827	.000	.879
8	26114	.303	.000	12.00	.00	6.210	1.399	1.399	3.832	.000	.884
9	26122	.298	.000	13.00	.00	6.973	1.465	1.465	3.737	.000	.857
10	26200	.293	.000	13.50	.00	7.330	1.495	1.495	3.668	.000	.833
11	26205	.298	.000	14.00	.00	4.439	1.034	1.034	3.721	.000	.857
12	26207	.302	.000	15.00	.00	4.261	.976	.976	3.754	.000	.882
13	26209	.300	.000	16.00	.00	4.365	.968	.968	3.716	.000	.870
14	26215	.290	.000	18.00	.00	4.396	.941	.941	3.590	.000	.815
15	26216	.282	.000	20.00	.00	4.426	.911	.911	3.497	.000	.778
16	26218	.252	.000	25.00	.00	5.187	1.035	1.035	3.129	.000	.626
17	26219	.281	.000	20.00	.00	4.427	.928	.928	3.466	.000	.773
18	26220	.293	.000	16.00	.00	4.358	.980	.980	3.592	.000	.832
19	26300	.302	.000	14.00	.00	4.686	1.101	1.101	3.703	.000	.878
20	26301	.293	.000	13.00	.00	6.668	1.425	1.425	3.591	.000	.828
21	26302	.302	.000	11.00	.00	5.328	1.289	1.289	3.694	.000	.879
22	26306	.303	.000	5.00	.00	1.666	.685	.685	3.706	.000	.883
23	26307	.302	.000	.00	.00	.673	.102	.102	3.693	.000	.878
24	26313	.250	.000	-5.00	.00	3.523	-.512	-.512	3.126	.000	.614
25	26315	.250	.000	-2.00	.00	1.489	-.167	-.167	3.113	.000	.612
26	26318	.250	.000	.00	.00	.598	.059	.059	3.132	.000	.616
27	26320	.249	.000	2.00	.00	.894	.274	.274	3.119	.000	.614
28	26321	.250	.000	4.00	.00	1.260	.513	.513	3.113	.000	.612
29	26414	.250	.000	8.00	.00	3.120	.999	.999	3.371	.000	.618
30	26415	.249	.000	10.00	.00	4.647	1.217	1.217	3.346	.000	.612
31	26417	.249	.000	12.00	.00	6.193	1.401	1.401	3.336	.000	.614
32	26419	.251	.000	13.00	.00	7.147	1.502	1.502	3.345	.000	.621
33	26421	.249	.000	14.00	.00	7.896	1.573	1.573	3.328	.000	.615
34	27020	.250	.000	15.00	.00	5.206	1.168	1.168	3.308	.000	.617
35	27022	.250	.000	16.00	.00	4.533	1.025	1.025	3.293	.000	.616
36	27100	.250	.000	18.00	.00	4.510	.967	.967	3.281	.000	.616
37	27101	.250	.000	20.00	.00	4.543	.937	.937	3.281	.000	.618
38	27103	.249	.000	25.00	.00	4.450	.994	.994	3.256	.000	.613
39	27107	.252	.000	20.00	.00	4.521	.933	.933	3.304	.000	.630
40	27108	.249	.000	16.00	.00	4.468	1.015	1.015	3.260	.000	.615
41	27109	.250	.000	14.00	.00	7.872	1.585	1.585	3.265	.000	.617
42	27110	.249	.000	13.00	.00	6.870	1.486	1.486	3.248	.000	.611
43	27111	.249	.000	11.10	.00	5.280	1.304	1.304	3.247	.000	.612

44	27116	.248	.000	5.00	.00	1.599	.653	.653	3.242	.000	.607
45	27117	.249	.000	.00	.00	.623	.078	.078	3.259	.000	.615
46	27123	.185	.000	-5.00	.00	3.531	-.508	-.508	2.449	.000	.344
47	27201	.184	.000	-2.00	.00	1.505	-.151	-.151	2.441	.000	.343
48	27202	.184	.000	.00	.00	.605	.083	.083	2.429	.000	.340
49	27204	.184	.000	2.00	.00	.889	.288	.288	2.437	.000	.343
50	27205	.185	.000	4.00	.00	1.287	.540	.540	2.438	.000	.343
51	27211	.185	.000	8.00	.00	2.918	.963	.963	2.460	.000	.347
52	27212	.185	.000	10.00	.00	4.329	1.171	1.171	2.444	.000	.344
53	27214	.185	.000	12.00	.00	5.813	1.357	1.357	2.441	.000	.345
54	27216	.184	.000	13.00	.00	6.547	1.440	1.440	2.430	.000	.342
55	27218	.184	.000	14.00	.00	7.439	1.519	1.519	2.419	.000	.340
56	27220	.186	.000	14.90	.00	5.957	1.341	1.341	2.445	.000	.347
57	27301	.185	.000	16.00	.00	4.600	1.035	1.035	2.441	.000	.344
58	27303	.184	.000	18.00	.00	4.546	.980	.980	2.430	.000	.343
59	27304	.185	.000	20.00	.00	4.675	.941	.941	2.429	.000	.343
60	27306	.184	.000	25.00	.00	1.145	.866	.866	2.422	.000	.342
61	27307	.184	.000	20.00	.00	1.080	.823	.823	2.419	.000	.342
62	27308	.184	.000	16.00	.00	4.740	1.096	1.096	2.422	.000	.342
63	27309	.184	.000	14.00	.00	7.526	1.527	1.527	2.422	.000	.342
64	27310	.185	.000	13.00	.00	6.666	1.459	1.459	2.427	.000	.343
65	27311	.184	.000	11.00	.00	5.029	1.272	1.272	2.422	.000	.341
66	27317	.184	.000	5.00	.00	1.504	.635	.635	2.433	.000	.339
67	27318	.184	.000	.00	.00	.620	.070	.070	2.435	.000	.342
68	27400	.109	.000	-5.00	.00	3.466	-.492	-.492	1.539	.000	.121
69	27402	.110	.000	-2.00	.00	1.570	-.155	-.155	1.550	.000	.123
70	27403	.108	.000	.00	.00	.733	.069	.069	1.534	.000	.121
71	27405	.109	.000	2.00	.00	.930	.289	.289	1.536	.000	.122
72	27406	.109	.000	4.00	.00	1.335	.553	.553	1.532	.000	.122
73	27413	.110	.000	8.00	.00	3.084	.986	.986	1.527	.000	.122
74	27414	.109	.000	10.00	.00	4.305	1.203	1.203	1.522	.000	.121
75	27416	.110	.000	12.00	.00	5.730	1.388	1.388	1.526	.000	.122
76	28019	.109	.000	13.00	.00	6.566	1.399	1.399	1.491	.000	.121
77	28021	.109	.000	14.00	.00	7.372	1.479	1.479	1.485	.000	.121
78	28023	.114	.000	15.00	.00	4.303	1.038	1.038	1.542	.000	.132
79	28101	.112	.000	16.00	.00	4.460	1.007	1.007	1.527	.000	.129
80	28106	.110	.000	18.00	.00	4.729	.948	.948	1.498	.000	.124
81	28107	.110	.000	20.00	.00	4.926	.939	.939	1.492	.000	.124
82	28109	.109	.000	25.00	.00	1.212	.874	.874	1.479	.000	.122
83	28110	.109	.000	20.00	.00	.880	.708	.708	1.488	.000	.124
84	28115	.109	.000	14.00	.00	7.393	1.413	1.413	1.476	.000	.122
85	28116	.110	.000	13.00	.00	6.459	1.375	1.375	1.474	.000	.123
86	28117	.109	.000	11.00	.00	4.846	1.218	1.218	1.467	.000	.121
87	28119	.110	.000	.00	.00	.673	.022	.022	1.476	.000	.123
88	28120	.108	.000	14.50	.00	7.779	1.506	1.506	1.460	.000	.121
89	28207	.184	.000	.00	.00	.613	.034	.034	2.441	.000	.341
90	28209	.183	.000	5.00	.00	1.540	.622	.622	2.425	.000	.338
91	28211	.184	.000	10.00	.00	4.316	1.146	1.146	2.439	.000	.342
92	28213	.185	.000	12.00	.00	5.782	1.320	1.320	2.440	.000	.343
93	28215	.185	.000	13.00	.00	6.274	1.388	1.388	2.439	.000	.343
94	28217	.184	.000	14.00	.00	7.270	1.457	1.457	2.432	.000	.342
95	28222	.185	.000	15.00	.00	3.986	.982	.982	2.428	.000	.341
96	28300	.184	.000	16.00	.00	3.658	.903	.903	2.427	.000	.342
97	28302	.184	.000	20.00	.00	3.077	.839	.839	2.424	.000	.342
98	28304	.185	.000	.00	.00	.615	.040	.040	2.426	.000	.343
99	28312	.301	.000	.00	.00	.631	.061	.061	3.957	.000	.878
100	28314	.303	.000	5.00	.00	1.593	.653	.653	3.960	.000	.886
101	28316	.302	.000	10.00	.00	4.448	1.208	1.208	3.940	.000	.884
102	28321	.301	.000	12.00	.00	5.957	1.371	1.371	3.914	.000	.878
103	28323	.298	.000	13.00	.00	6.778	1.455	1.455	3.864	.000	.860
104	28401	.292	.000	14.00	.00	7.273	1.496	1.496	3.779	.000	.827
105	28403	.298	.000	15.00	.00	3.505	.943	.943	3.838	.000	.859
106	28408	.298	.000	16.00	.00	3.738	.967	.967	3.842	.000	.857
107	28410	.302	.000	.00	.00	.630	.064	.064	3.887	.000	.882

108	24022	.296	.025	15.00	10.00	9.725	1.805	1.747	3.840	1.310	.850
109	24100	.290	.050	15.00	10.00	10.331	2.043	1.871	3.733	2.620	.814
110	24105	.289	.100	15.00	10.00	10.398	2.303	1.925	3.715	5.240	.813
111	24109	.283	.153	15.00	10.00	10.786	2.405	1.999	3.625	7.860	.779
112	24117	.280	.098	15.00	10.00	10.915	2.391	1.961	3.598	4.980	.765
113	24201	.248	.099	15.00	10.00	13.476	2.472	2.153	3.211	4.460	.609
114	24209	.220	.098	15.00	10.00	16.265	2.484	2.205	2.846	3.930	.480
115	24217	.184	.099	15.00	10.00	17.657	2.632	2.314	2.396	3.300	.340
116	24302	.184	.049	7.50	10.00	11.422	1.754	1.754	2.396	1.650	.340
117	24306	.184	.197	7.50	10.00	11.844	1.803	1.775	2.395	6.600	.341
118	24314	.110	.099	15.00	10.00	16.945	2.648	2.282	1.504	1.960	.123
119	24323	.073	.099	15.00	10.00	15.434	2.567	2.201	.995	1.300	.054
120	25022	.302	.025	10.00	10.00	9.631	1.788	1.726	3.845	1.340	.881
121	25102	.302	.049	10.00	10.00	9.871	1.960	1.831	3.832	2.680	.881
122	25104	.302	.098	10.00	10.00	9.940	2.104	1.873	3.817	5.360	.880
123	25109	.302	.147	10.00	10.00	10.069	2.189	1.909	3.811	8.040	.879
124	25117	.303	.024	10.00	5.00	8.794	1.617	1.609	3.829	1.340	.884
125	25118	.302	.049	10.00	5.00	9.020	1.649	1.637	3.803	2.680	.879
126	25119	.303	.097	10.00	5.00	9.346	1.694	1.680	3.805	5.360	.883
127	25121	.302	.147	10.00	5.00	9.592	1.715	1.712	3.813	8.040	.881
128	25122	.303	.146	10.00	5.00	9.616	1.725	1.715	3.820	8.040	.884
129	25123	.303	.195	10.00	5.00	9.805	1.762	1.757	3.817	10.720	.885
130	29023	.291	.025	15.00	10.00	10.449	1.776	1.710	3.698	1.310	.820
131	29101	.288	.050	15.00	10.00	11.155	1.963	1.832	3.640	2.620	.805
132	29106	.288	.100	15.00	10.00	11.317	2.209	1.899	3.646	5.240	.806
133	29115	.184	.049	15.00	10.00	12.313	2.050	1.872	2.418	1.650	.340
134	29117	.184	.099	15.00	10.00	14.488	2.315	2.080	2.418	3.300	.341
135	29119	.184	.148	15.00	10.00	15.831	2.452	2.216	2.417	4.950	.341
136	29205	.301	.010	5.00	10.00	8.820	1.605	1.595	3.947	.530	.876
137	29207	.301	.050	5.00	10.00	9.343	1.682	1.673	3.919	2.680	.877
138	29211	.301	.099	5.00	10.00	9.589	1.706	1.696	3.903	5.360	.877
139	29213	.301	.148	5.00	10.00	9.863	1.738	1.722	3.896	8.040	.879
140	29215	.301	.148	5.00	10.00	9.860	1.739	1.724	3.891	8.040	.879
141	29223	.301	.196	13.50	2.00	9.672	1.712	1.706	3.812	10.720	.876
142	29304	.300	.197	14.50	2.00	9.868	1.853	1.781	3.777	10.720	.870
143	29309	.296	.199	16.50	2.00	7.274	1.620	1.607	3.722	10.720	.852
144	29317	.035	.102	15.00	10.00	10.695	2.339	1.995	.472	.650	.013
145	30019	.298	.010	15.00	10.00	8.964	1.619	1.615	3.857	.520	.865
146	30020	.298	.010	15.00	10.00	9.070	1.634	1.629	3.828	.520	.864
147	30105	.301	.010	10.00	10.00	8.817	1.609	1.603	3.845	.530	.880
148	30110	.301	.010	15.00	5.00	8.442	1.565	1.563	3.818	.530	.877
149	30119	.300	.010	10.00	5.00	8.262	1.559	1.550	3.819	.530	.874
150	30201	.301	.010	11.00	5.00	8.302	1.564	1.562	3.814	.538	.877
151	30206	.301	.010	14.00	2.00	8.275	1.546	1.544	3.819	.530	.876
152	30215	.183	.010	7.50	10.00	9.906	1.650	1.650	2.416	.330	.338
153	31102	.302	.025	10.00	10.00	9.430	1.814	1.717	3.880	1.340	.877
154	31104	.302	.049	10.00	10.00	9.725	1.958	1.799	3.860	2.680	.878
155	31110	.302	.147	10.00	10.00	9.918	2.184	1.896	3.842	8.040	.880
156	31112	.302	.147	10.00	10.00	9.912	2.184	1.898	3.832	8.040	.880
157	31119	.303	.024	5.00	10.00	8.800	1.609	1.603	3.856	1.340	.884
158	31121	.302	.049	5.00	10.00	9.066	1.651	1.646	3.827	2.680	.880
159	31123	.303	.098	5.00	10.00	9.381	1.696	1.684	3.824	5.360	.884
160	31201	.303	.146	5.00	10.00	9.592	1.722	1.710	3.817	8.040	.883
161	31209	.184	.099	15.00	10.00	17.616	2.530	2.307	2.421	3.300	.341
162	31215	.184	.049	7.50	10.00	11.336	1.755	1.751	2.425	1.650	.341
163	31217	.185	.197	7.50	10.00	11.720	1.797	1.780	2.423	6.600	.341
164	31302	.297	.199	14.50	2.00	9.854	1.866	1.800	3.766	10.720	.852
165	31310	.298	.148	14.50	2.00	9.707	1.771	1.729	3.732	8.040	.854
166	25204	.301	.025	15.00	5.00	9.358	1.728	1.680	3.973	1.340	.877
167	25205	.301	.050	15.00	5.00	9.745	1.845	1.771	3.953	2.680	.878
168	25208	.301	.099	15.00	5.00	10.043	1.962	1.854	3.951	5.360	.878
169	25209	.298	.151	15.00	5.00	10.331	2.117	1.928	3.887	8.040	.857
170	25210	.297	.201	15.00	5.00	10.231	2.236	1.949	3.865	10.720	.852
171	25214	.302	.049	11.00	5.00	9.441	1.688	1.684	3.926	2.680	.880

172	25216	.302	.099	11.00	5.00	9.786	1.756	1.755	3.910	5.360	.883
173	25301	.302	.098	5.00	5.00	4.496	1.218	1.214	3.904	5.360	.884
174	25303	.303	.196	5.00	5.00	4.781	1.246	1.232	3.879	10.720	.885
175	25311	.302	.098	5.00	10.10	9.603	1.719	1.709	3.853	5.360	.881
176	25319	.302	.098	5.50	10.00	9.712	1.736	1.736	3.834	5.360	.881
ref#	case	avem	k	alpha0	alpha1	Cp Max	Cl max	Cl at	Re(mil)	freq	aveQ

The Hughes02 Airfoil (HH02)

ref#	case	avem	k	alpha0	alpha1	Cp Max	Cl max	Cl at	Re(mil)	freq	aveQ
1	40018	.110	.000	-5.00	.00	4.220	-.495	-.495	1.509	.000	.122
2	40019	.109	.000	.00	.00	.610	.079	.079	1.503	.000	.121
3	40020	.110	.000	5.00	.00	1.440	.667	.667	1.512	.000	.123
4	40101	.110	.000	10.00	.00	4.840	1.200	1.200	1.512	.000	.123
5	40102	.109	.000	12.00	.00	6.678	1.356	1.356	1.491	.000	.120
6	40103	.111	.000	14.00	.00	6.564	1.266	1.266	1.515	.000	.125
7	40104	.109	.000	14.50	.00	4.988	.987	.987	1.502	.000	.123
8	40105	.110	.000	15.00	.00	5.548	1.101	1.101	1.499	.000	.122
9	40106	.109	.000	15.50	.00	1.000	.919	.919	1.494	.000	.121
10	40107	.109	.000	16.00	.00	1.001	.899	.899	1.487	.000	.121
11	40108	.110	.000	20.00	.00	.932	.816	.816	1.497	.000	.122
12	40114	.185	.000	-5.00	.00	4.251	-.522	-.522	2.477	.000	.342
13	40115	.185	.000	.00	.00	.564	.073	.073	2.469	.000	.341
14	40117	.185	.000	4.90	.00	1.383	.655	.655	2.470	.000	.341
15	40201	.185	.000	10.00	.00	5.001	1.185	1.185	2.478	.000	.341
16	40203	.185	.000	12.00	.00	6.926	1.385	1.385	2.480	.000	.343
17	40205	.185	.000	14.00	.00	8.421	1.483	1.483	2.474	.000	.341
18	40207	.186	.000	14.50	.00	7.721	1.349	1.349	2.484	.000	.344
19	40212	.185	.000	15.00	.00	6.227	1.190	1.190	2.474	.000	.340
20	40213	.185	.000	16.00	.00	6.786	1.304	1.304	2.473	.000	.340
21	40215	.185	.000	20.00	.00	.941	.862	.862	2.474	.000	.342
22	40222	.302	.000	8.00	.00	3.697	1.041	1.041	4.130	.000	.879
23	40223	.301	.000	10.00	.00	5.430	1.239	1.239	4.103	.000	.874
24	40301	.300	.000	12.00	.00	7.899	1.434	1.434	4.086	.000	.875
25	40303	.299	.000	13.00	.00	8.696	1.472	1.472	4.052	.000	.869
26	40308	.301	.000	13.50	.00	8.546	1.440	1.440	4.060	.000	.878
27	40310	.301	.000	14.00	.00	7.627	1.338	1.338	4.042	.000	.878
28	40312	.302	.000	14.50	.00	6.723	1.254	1.254	4.040	.000	.883
29	40314	.303	.000	15.00	.00	6.839	1.268	1.268	4.032	.000	.884
30	40319	.288	.000	18.00	.00	5.771	1.073	1.073	3.854	.000	.806
31	40321	.270	.000	20.00	.00	6.604	1.232	1.232	3.619	.000	.715
32	40322	.301	.000	14.00	.00	7.855	1.362	1.362	4.009	.000	.881
33	40323	.299	.000	13.00	.00	8.549	1.463	1.463	3.980	.000	.869
34	40400	.300	.000	12.50	.00	8.066	1.432	1.432	3.981	.000	.871
35	40406	.301	.000	5.00	.00	1.486	.673	.673	4.024	.000	.877
36	40407	.301	.000	.00	.00	.583	.081	.081	4.023	.000	.878
37	41019	.300	.000	-5.00	.00	4.457	-.510	-.510	4.149	.000	.874
38	41021	.300	.000	-2.00	.00	1.590	-.148	-.148	4.124	.000	.874
39	41100	.300	.000	.00	.00	.593	.087	.087	4.107	.000	.872
40	41102	.300	.000	2.00	.00	.792	.314	.314	4.097	.000	.875
41	41103	.301	.000	5.00	.00	1.491	.683	.683	4.091	.000	.877
42	41110	.248	.000	-5.00	.00	4.438	-.528	-.528	3.410	.000	.610
43	41111	.248	.000	-2.00	.00	1.678	-.171	-.171	3.397	.000	.610
44	41112	.248	.000	.00	.00	.612	.072	.072	3.394	.000	.610
45	41113	.248	.000	2.00	.00	.777	.294	.294	3.392	.000	.611
46	41114	.248	.000	5.00	.00	1.457	.666	.666	3.381	.000	.609
47	41119	.248	.000	8.00	.00	3.628	1.024	1.024	3.361	.000	.610
48	41120	.248	.000	10.00	.00	5.182	1.229	1.229	3.343	.000	.609
49	41121	.248	.000	12.00	.00	7.300	1.419	1.419	3.337	.000	.609

50	41122	.249	.000	13.00	.00	8.443	1.504	1.504	3.338	.000	.612
51	41123	.249	.000	13.50	.00	9.080	1.538	1.538	3.341	.000	.614
52	41200	.249	.000	14.00	.00	9.339	1.543	1.543	3.329	.000	.611
53	41201	.248	.000	14.50	.00	9.019	1.501	1.501	3.322	.000	.610
54	41202	.248	.000	15.00	.00	6.098	1.180	1.180	3.316	.000	.609
55	41205	.248	.000	18.00	.00	5.850	1.102	1.102	3.317	.000	.608
56	41206	.248	.000	20.00	.00	5.484	1.017	1.017	3.306	.000	.608
57	41207	.249	.000	14.00	.00	8.984	1.521	1.521	3.322	.000	.614
58	41208	.248	.000	13.00	.00	8.348	1.486	1.486	3.310	.000	.609
59	41209	.249	.000	12.50	.00	7.890	1.462	1.462	3.319	.000	.613
60	41214	.249	.000	5.00	.00	1.475	.665	.665	3.342	.000	.613
61	41215	.249	.000	.00	.00	.567	.085	.085	3.332	.000	.611
62	41221	.299	.000	.00	.00	.565	.090	.090	4.054	.000	.875
63	41223	.300	.000	5.00	.00	1.501	.693	.693	4.026	.000	.874
64	41301	.300	.000	10.00	.00	5.410	1.258	1.258	4.012	.000	.877
65	41303	.300	.000	12.00	.00	6.899	1.395	1.395	3.995	.000	.873
66	41305	.296	.000	13.00	.00	7.262	1.423	1.423	3.950	.000	.858
67	41307	.300	.000	13.50	.00	5.887	1.277	1.277	3.987	.000	.879
68	41312	.300	.000	14.00	.00	5.381	1.185	1.185	3.991	.000	.876
69	41314	.287	.000	16.00	.00	3.710	.991	.991	3.822	.000	.811
70	41401	.182	.000	.00	.00	.557	.078	.078	2.505	.000	.336
71	41403	.184	.000	5.00	.00	1.418	.662	.662	2.517	.000	.340
72	41405	.183	.000	10.00	.00	5.059	1.220	1.220	2.510	.000	.339
73	41407	.182	.000	12.00	.00	6.520	1.361	1.361	2.496	.000	.336
74	41409	.183	.000	13.00	.00	7.262	1.425	1.425	2.499	.000	.337
75	41411	.182	.000	13.50	.00	7.536	1.458	1.458	2.499	.000	.338
76	41413	.181	.000	14.00	.00	5.885	1.286	1.286	2.489	.000	.334
77	41415	.183	.000	14.50	.00	5.391	1.234	1.234	2.503	.000	.339
78	41417	.182	.000	16.00	.00	4.219	1.045	1.045	2.496	.000	.338
79	41419	.182	.000	.00	.00	.597	.074	.074	2.496	.000	.338
80	42019	.292	.025	15.00	10.00	7.408	1.717	1.520	3.955	1.310	.836
81	42021	.289	.051	15.00	10.00	8.062	1.979	1.625	3.884	2.620	.821
82	42100	.283	.104	15.00	10.00	8.834	2.258	1.768	3.786	5.240	.788
83	42108	.183	.051	15.00	10.00	11.200	2.065	1.883	2.530	1.650	.339
84	42110	.183	.101	15.00	10.00	11.617	2.383	2.009	2.527	3.300	.338
85	42113	.183	.152	15.00	10.00	11.856	2.606	2.068	2.532	4.950	.340
86	42121	.072	.101	15.00	10.00	16.851	2.467	2.331	1.028	1.300	.054
87	42206	.290	.026	15.00	10.00	9.320	1.766	1.616	3.981	1.310	.823
88	42208	.292	.051	15.00	10.00	9.153	1.960	1.641	3.978	2.620	.834
89	42210	.288	.103	15.00	10.00	9.739	2.248	1.736	3.912	5.240	.813
90	42212	.283	.156	15.00	10.00	10.035	2.370	1.830	3.830	7.850	.786
91	42217	.283	.156	15.00	10.00	10.002	2.363	1.824	3.833	7.860	.786
92	42218	.278	.101	15.00	10.00	10.287	2.280	1.740	3.756	4.980	.759
93	42302	.183	.101	15.00	10.00	16.949	2.545	2.206	2.526	3.300	339
94	42309	.218	.101	15.00	10.00	15.256	2.408	2.045	2.981	3.930	.476
95	42313	.246	.101	15.00	10.00	12.201	2.295	1.879	3.328	4.460	.604
96	42321	.108	.101	15.00	10.00	18.512	2.572	2.492	1.511	1.960	.120
97	43019	.297	.010	10.00	10.00	8.929	1.522	1.519	3.898	.540	.858
98	43106	.301	.025	10.00	10.00	8.932	1.636	1.570	3.930	1.340	.870
99	43108	.302	.050	10.00	10.00	8.893	1.910	1.604	3.927	2.680	.876
100	43114	.299	.150	10.00	10.00	9.111	2.176	1.731	3.899	8.040	.861
101	43117	.297	.151	10.00	10.00	9.249	2.186	1.732	3.887	8.040	.849
102	43202	.301	.025	3.80	10.00	8.942	1.516	1.504	3.968	1.340	.874
103	43112	.302	.099	10.00	10.00	8.965	2.120	1.678	3.946	5.360	.876
104	43204	.302	.050	3.80	10.00	8.953	1.574	1.569	3.963	2.680	.877
105	43206	.302	.099	3.80	10.00	9.020	1.604	1.587	3.955	5.360	.876
106	43209	.302	.149	3.80	10.00	9.006	1.610	1.597	3.956	8.040	.878
107	43215	.302	.010	3.80	10.00	8.924	1.503	1.486	4.061	.540	.876
108	43219	.303	.100	4.00	10.00	9.114	1.641	1.628	4.046	5.360	.879
109	43303	.296	.025	15.00	5.00	9.246	1.540	1.536	3.918	1.340	.845
110	43304	.292	.051	15.00	5.00	9.462	1.677	1.609	3.842	2.680	.821
111	43305	.291	.103	15.00	5.00	9.619	1.949	1.672	3.823	5.360	.817
112	43309	.289	.207	15.00	5.00	9.637	2.351	1.784	3.777	10.720	.805
113	43314	.302	.025	11.00	5.00	8.974	1.530	1.522	3.934	1.340	.876

114	43315	.302	.049	11.00	5.00	8.863	1.585	1.564	3.922	2.650	.877
115	43316	.302	.099	11.00	5.00	8.993	1.746	1.612	3.909	5.360	.875
116	44019	.301	.010	10.00	5.00	8.616	1.457	1.452	3.960	.540	.869
117	44021	.302	.025	10.00	5.00	8.927	1.523	1.511	3.951	1.340	.876
118	44023	.302	.050	10.00	5.00	8.930	1.580	1.573	3.944	2.680	.876
119	44104	.303	.099	10.00	5.00	8.953	1.648	1.601	3.996	5.360	.881
120	44106	.303	.149	10.00	5.00	8.979	1.715	1.632	3.991	8.040	.880
121	44112	.303	.199	10.00	5.00	8.932	1.831	1.660	4.003	10.720	.880
122	44118	.302	.100	10.00	5.00	9.153	1.665	1.635	4.038	5.360	.880
123	44119	.302	.025	10.00	5.00	9.090	1.549	1.531	4.019	1.340	.876
124	44120	.302	.200	10.00	5.00	9.065	1.858	1.688	4.007	10.720	.878
125	44202	.301	.100	14.00	2.00	9.082	1.585	1.573	4.004	5.360	.875
126	44204	.301	.200	14.00	2.00	9.065	1.871	1.632	3.987	10.720	.872
127	44209	.282	.213	17.50	2.00	9.303	1.952	1.548	3.757	10.720	.773
128	44212	.297	.010	15.50	2.00	8.760	1.444	1.444	3.961	.540	.854
129	44214	.297	.025	15.50	2.00	8.406	1.431	1.429	3.917	1.340	.851
130	44215	.296	.051	15.50	2.00	8.562	1.457	1.456	3.904	2.680	.849
131	44216	.293	.102	15.50	2.00	9.037	1.621	1.525	3.855	5.360	.829
132	44217	.291	.154	15.50	2.00	9.224	1.765	1.558	3.827	8.040	.820
133	44218	.292	.205	15.50	2.00	9.266	1.985	1.604	3.832	10.720	.824
134	44221	.301	.010	12.50	2.00	8.787	1.473	1.470	3.957	.540	.871
135	44222	.302	.025	12.50	2.00	8.896	1.493	1.484	3.946	1.340	.877
136	44223	.301	.050	12.50	2.00	9.022	1.530	1.517	3.926	2.680	.871
137	44300	.301	.099	12.50	2.00	9.040	1.581	1.574	3.930	5.360	.874
138	44303	.302	.149	12.50	2.00	9.010	1.605	1.584	3.952	8.040	.877
139	44304	.302	.198	12.50	2.00	8.953	1.672	1.597	3.946	10.720	.878
140	43308	.290	.155	15.00	5.00	9.641	2.088	1.692	3.809	8.040	.813
ref#	case	avem	k	alpha0	alpha1	Cp Max	Cl max	Cl at	Re(mil)	freq	aveQ

The NLR1 Airfoil (nlr1)

ref#	case	avem	k	alpha0	alpha1	Cp Max	Cl max	Cl at	Re(mil)	freq	aveQ
1	61018	.109	.000	-5.00	.00	1.855	-.396	-.396	1.524	.000	.122
2	61019	.110	.000	.00	.00	.650	.088	.088	1.534	.000	.123
3	61020	.110	.000	5.00	.00	1.731	.691	.691	1.529	.000	.122
4	61101	.111	.000	10.00	.00	5.257	1.164	1.164	1.537	.000	.125
5	61102	.109	.000	12.00	.00	7.014	1.277	1.277	1.518	.000	.122
6	61103	.110	.000	14.00	.00	9.295	1.411	1.411	1.522	.000	.122
7	61104	.110	.000	15.00	.00	2.553	1.010	1.010	1.518	.000	.122
8	61105	.110	.000	14.60	.00	2.339	.994	.994	1.512	.000	.122
9	61106	.109	.000	16.50	.00	.966	.752	.752	1.502	.000	.121
10	61107	.110	.000	18.00	.00	.866	.771	.771	1.511	.000	.123
11	61108	.110	.000	20.00	.00	.856	.741	.741	1.509	.000	.122
12	61114	.185	.000	-5.00	.00	2.428	-.406	-.406	2.467	.000	.341
13	61115	.185	.000	.00	.00	.640	.095	.095	2.469	.000	.342
14	61117	.184	.000	5.00	.00	1.613	.638	.638	2.462	.000	.341
15	61201	.184	.000	10.00	.00	5.422	1.178	1.178	2.434	.000	.341
16	51203	.185	.000	12.00	.00	7.660	1.352	1.352	2.440	.000	.345
17	61205	.186	.000	14.00	.00	8.749	1.480	1.480	2.430	.000	.344
18	61208	.184	.000	15.40	.00	10.015	1.526	1.526	2.407	.000	.338
19	61212	.185	.000	16.50	.00	.902	.831	.831	2.420	.000	.342
20	61213	.184	.000	18.00	.00	.860	.797	.797	2.414	.000	.341
21	61215	.184	.000	20.00	.00	.826	.741	.741	2.408	.000	.342
22	61221	.250	.000	-5.00	.00	2.533	-.424	-.424	3.195	.000	.612
23	61222	.250	.000	-2.00	.00	1.714	-.098	-.098	3.198	.000	.614
24	61223	.250	.000	.00	.00	.611	.088	.088	3.194	.000	.613
25	61300	.250	.000	2.00	.00	.799	.295	.295	3.191	.000	.612
26	61301	.250	.000	5.00	.00	1.641	.634	.634	3.188	.000	.612
27	61306	.251	.000	8.00	.00	3.608	.958	.958	3.401	.000	.616
28	61307	.251	.000	10.00	.00	5.492	1.164	1.164	3.402	.000	.619
29	61308	.249	.000	12.00	.00	7.987	1.355	1.355	3.381	.000	.613

30	61309	.250	.000	12.50	.00	8.574	1.395	1.395	3.381	.000	.614
31	61310	.249	.000	13.00	.00	9.103	1.425	1.425	3.365	.000	.610
32	61311	.251	.000	14.00	.00	7.855	1.310	1.310	3.386	.000	.619
33	61312	.249	.000	15.00	.00	6.916	1.210	1.210	3.361	.000	.611
34	61315	.249	.000	16.00	.00	4.547	.883	.883	3.363	.000	.611
35	61316	.250	.000	20.00	.00	4.329	.881	.881	3.358	.000	.612
36	61317	.250	.000	25.00	.00	.896	.815	.815	3.345	.000	.612
37	61318	.250	.000	14.00	.00	7.708	1.297	1.297	3.349	.000	.612
38	61319	.250	.000	12.50	.00	8.600	1.400	1.400	3.357	.000	.614
39	61400	.249	.000	5.00	.00	1.684	.627	.627	3.373	.000	.613
40	61401	.250	.000	.00	.00	.635	.095	.095	3.365	.000	.612
41	61407	.301	.000	-5.00	.00	2.037	-.432	-.432	3.982	000	.876
42	61409	.302	.000	-2.00	.00	1.734	-.110	-.110	3.971	.000	.878
43	61410	.302	.000	.00	.00	.775	.062	.062	3.963	.000	.877
44	61412	.302	.000	2.00	.00	.832	.299	.299	3.955	.000	.877
45	61413	.303	.000	5.00	.00	1.667	.642	.642	3.954	.000	.879
46	61421	.302	.000	8.00	.00	3.627	.950	.950	3.954	.000	.878
47	61422	.300	.000	10.00	.00	5.502	1.151	1.151	3.921	.000	.869
48	61500	.301	.000	12.00	.00	8.119	1.327	1.327	3.911	.000	.872
49	61502	.302	.000	12.50	.00	8.213	1.322	1.322	3.915	.000	.879
50	61508	.302	.000	12.50	.00	8.448	1.334	1.334	4.030	.000	.882
51	61510	.302	.000	13.00	.00	7.346	1.275	1.275	4.003	.000	.882
52	61512	.302	.000	14.00	.00	5.994	1.167	1.167	3.982	.000	.879
53	61513	.302	.000	16.00	.00	4.532	.879	.879	3.969	.000	.877
54	61519	.275	.000	20.00	.00	1.557	.859	.859	3.622	.000	.736
55	61521	.263	.000	25.00	.00	.873	.812	.812	3.460	.000	.677
56	61522	.302	.000	14.00	.00	6.586	1.190	1.190	3.940	.000	.880
57	61523	.300	.000	12.50	.00	8.580	1.345	1.345	3.914	.000	.870
58	61605	.302	.000	5.00	.00	1.678	.626	.626	3.966	.000	.879
59	61606	.302	.000	.00	.00	.637	.094	.094	3.961	.000	.880
60	64221	.185	.000	.00	.00	.584	.084	.084	2.353	.000	.341
61	64223	.184	.000	5.00	.00	1.429	.601	.601	2.345	.000	.339
62	64301	.185	.000	10.00	.00	4.603	1.110	1.110	2.350	.000	.342
63	64303	.185	.000	12.00	.00	6.012	1.267	1.267	2.347	.000	.341
64	64305	.185	.000	13.00	.00	6.662	1.312	1.312	2.344	.000	.341
65	64307	.187	.000	14.00	.00	3.476	.998	.998	2.370	.000	.348
66	64309	.185	.000	16.00	.00	2.413	.776	.776	2.346	.000	.342
67	64311	.186	.000	.00	.00	.553	.088	.088	2.356	.000	.344
68	65019	.301	.000	-11.00	.00	1.426	-.665	-.665	3.814	.000	.875
69	65020	.301	.000	-9.00	.00	1.706	-.677	-.677	3.804	.000	.876
70	65021	.301	.000	-7.00	.00	2.533	-.601	-.601	3.798	.000	.875
71	65022	.301	.000	-6.00	.00	4.553	-.558	-.558	3.791	.000	.874
72	65023	.301	.000	-5.00	.00	4.546	-.447	-.447	3.792	.000	.876
73	65100	.301	.000	.00	.00	.663	.084	.084	3.787	.000	.875
74	65101	.302	.000	5.00	.00	1.588	.638	.638	3.783	.000	.878
75	65103	.301	.000	10.00	.00	4.937	1.131	1.131	3.765	.000	.875
76	65107	.295	.000	11.80	.00	6.347	1.259	1.259	3.697	.000	.842
77	65109	.298	.000	13.00	.00	4.143	1.074	1.074	3.722	.000	.858
78	65112	.294	.000	14.00	.00	3.244	.946	.946	3.665	.000	.839
79	65113	.288	.000	16.00	.00	2.502	.801	.801	3.575	.000	.800
80	65115	.302	.000	.00	.00	.603	.103	.103	3.746	.000	.879
81	62020	.073	.099	15.00	10.00	10.065	1.966	1.618	.968	1.300	.054
82	62104	.109	.099	15.00	10.00	14.676	2.246	1.828	1.446	1.960	.121
83	62112	.184	.100	15.00	10.00	14.964	2.424	1.893	2.513	3.300	.340
84	62114	.199	.100	15.00	10.00	13.072	2.400	1.837	2.699	3.570	.396
85	62121	.200	.171	10.00	10.00	12.983	2.252	1.831	2.557	6.250	398
86	62201	.200	.283	15.00	5.00	12.931	2.265	1.858	2.540	10.350	.398
87	62202	.199	171	15.00	5.00	12.674	2.243	1.789	2.534	6.250	.396
88	62208	.220	.097	15.00	10.00	10.680	2.325	1.717	2.778	3.930	.480
89	62210	.250	.097	15.00	10.00	10.413	2.195	1.638	3.113	4.460	.612
90	62218	.280	.097	15.00	10.00	9.405	2.033	1.555	3.442	4.980	760
91	62302	.295	.025	15.00	10.00	8.934	1.503	1.447	3.859	1.310	.838
92	62304	.294	.050	15.00	10.00	9.011	1.704	1.514	3.817	2.620	.834
93	62307	.294	.099	15.00	10.00	9.108	2.028	1.583	3.811	5.240	.835

94	62309	.287	.152	15.00	10.00	9.410	2.239	1.665	3.699	7.860	.796
95	62317	.301	.010	10.00	10.00	8.367	1.397	1.383	3.726	.540	.872
96	62320	.302	.024	10.00	10.00	8.497	1.507	1.429	3.704	1.340	.874
97	62322	.301	.048	10.00	10.00	8.607	1.676	1.471	3.685	2.680	.873
98	62400	.302	.097	10.00	10.00	8.582	1.940	1.534	3.686	5.360	.878
99	62403	.303	.116	10.00	10.00	8.603	2.012	1.557	3.701	6.430	.881
100	62405	.300	.146	10.00	10.00	8.716	1.990	1.588	3.657	8.040	.866
101	63018	.297	.010	15.00	5.00	8.452	1.340	1.340	3.913	.540	.855
102	63019	.299	.025	15.00	5.00	8.732	1.473	1.398	3.886	1.340	.862
103	63020	.299	.050	15.00	5.00	8.766	1.566	1.427	3.871	2.680	.862
104	63021	.297	.100	15.00	5.00	8.931	1.767	1.483	3.836	5.360	.850
105	63100	.296	.121	15.00	5.00	8.958	1.799	1.513	3.831	6.430	.848
106	63101	.295	.151	15.00	5.00	9.075	1.870	1.521	3.801	8.040	.839
107	63102	.289	.205	15.00	5.00	9.238	2.104	1.622	3.730	10.720	.812
108	63108	.303	.024	10.00	5.00	8.475	1.409	1.371	3.797	1.340	.881
109	63112	.301	.098	10.00	5.00	8.553	1.595	1.430	3.755	5.360	.873
110	63114	.302	.195	10.00	5.00	8.562	1.757	1.538	3.748	10.720	.876
111	63122	.300	.117	12.00	8.00	8.534	1.897	1.500	3.740	6.430	.868
112	63208	.286	.208	16.40	2.00	9.078	1.752	1.430	3.675	10.720	.789
113	63213	.286	.052	17.00	2.00	5.694	1.160	1.147	3.653	2.680	.790
114	63215	.284	.187	17.00	2.00	8.482	1.623	1.389	3.611	9.600	.780
115	63220	.294	.050	15.00	2.00	7.482	1.316	1.271	3.729	2.680	.833
116	63302	.300	.049	11.10	2.00	8.522	1.332	1.329	3.789	2.680	.866
117	63304	.302	.195	11.10	2.00	8.513	1.430	1.412	3.791	10.720	.876
118	63312	.302	.010	2.50	10.00	8.038	1.280	1.280	3.763	.540	.874
119	63314	.302	.024	2.50	10.00	8.259	1.313	1.312	3.741	1.340	.877
120	63318	.303	.049	2.50	10.00	8.304	1.339	1.335	3.756	2.680	.879
121	63320	.303	.097	2.50	10.00	8.333	1.351	1.346	3.740	5.360	.878
122	63323	.303	.097	2.70	10.00	8.351	1.366	1.366	3.747	5.360	.880
123	64019	.296	.025	15.00	10.00	6.898	1.509	1.362	3.865	1.310	.844
124	64021	.295	.049	15.00	10.00	7.132	1.729	1.436	3.814	2.620	.840
125	64023	.292	.100	15.00	10.00	7.285	2.008	1.509	3.752	5.240	.821
126	64107	.185	.050	15.00	10.00	8.751	1.862	1.602	2.449	1.650	.340
127	64109	.184	.099	15.00	10.00	9.453	2.141	1.729	2.439	3.300	.340
128	64111	.185	.148	15.00	10.00	9.753	2.317	1.835	2.440	4.950	.341
129	64119	.302	.010	2.50	10.00	6.506	1.294	1.291	3.823	.540	.876
130	64121	.302	.024	2.50	10.00	6.759	1.349	1.324	3.785	1.340	.875
131	64202	.303	.049	2.50	10.00	6.833	1.346	1.335	3.795	2.680	.879
132	64204	.302	.097	2.50	10.00	6.883	1.345	1.344	3.774	5.360	.878
133	64212	.302	.010	-2.00	10.00	4.982	.911	-.547	3.718	.540	.877
134	64213	.303	.024	-2.00	10.00	5.229	.917	-.546	3.695	1.340	.878
135	64214	.302	.048	-2.00	10.00	5.651	.903	-.633	3.685	2.680	.878
136	64215	.303	.096	-2.00	10.00	6.011	.881	-.707	3.684	5.360	.880
137	65121	.300	.010	-2.00	10.00	4.692	.936	-.472	3.717	.540	.869
138	65122	.301	.024	-2.00	10.00	5.084	.941	-.532	3.700	1.340	.873
139	65123	.301	.049	-2.00	10.00	5.442	.932	-.617	3.695	2.680	.874
140	65200	.302	.097	-2.00	10.00	5.886	.917	-.683	3.695	5.360	.877
141	65207	.199	.100	15.00	10.00	13.427	2.362	1.830	2.647	3.570	.395
142	65209	.292	.102	15.00	10.00	9.339	2.077	1.578	3.778	5.360	.828
143	65223	.109	.025	7.00	5.00	6.867	1.297	1.295	1.475	.490	.121
144	65300	.109	.200	7.00	5.00	6.404	1.268	1.255	1.473	3.920	.121
145	65311	.301	.197	7.00	5.00	8.622	1.376	1.359	3.863	10.720	.879
146	65309	.301	.010	7.00	5.00	8.093	1.291	1.291	3.889	.540	.876
147	63222	.291	.203	15.00	2.00	8.976	1.783	1.483	3.676	10.720	.818
ref#	case	avem	k	alpha0	alpha1	Cp Max	Cl max	Cl at	Re(mil)	freq	aveQ

The NLR7301 Airfoil (7301)

ref#	case	avem	k	alpha0	alpha1	Cp Max	Cl max	Cl at	Re(mil)	freq	aveQ
1	66019	.300	.000	-5.00	.00	2.369	-.370	-.370	4.004	.000	.872

2	66021	.300	.000	-2.00	.00	1.195	-.011	-.011	3.999	.000	.876
3	66022	.301	.000	.00	.00	1.059	.226	.226	3.992	.000	.874
4	66100	.302	.000	2.00	.00	1.690	.480	.480	4.000	.000	.883
5	66101	.301	.000	5.00	.00	2.829	.860	.860	3.988	.000	.881
6	66109	.300	.000	8.00	.00	4.326	1.194	1.194	3.982	.000	.877
7	66110	.300	.000	10.00	.00	5.554	1.404	1.404	3.968	.000	.876
8	66112	.299	.000	12.00	.00	6.842	1.568	1.568	3.933	.000	.867
9	66114	.281	.000	14.00	.00	7.826	1.703	1.703	3.704	.000	.772
10	66116	.270	.000	16.00	.00	8.862	1.830	1.830	3.564	.000	.717
11	66118	.267	.000	17.60	.00	9.413	1.873	1.873	3.518	.000	.701
12	66120	.274	.000	18.30	.00	8.669	1.761	1.761	3.589	.000	.733
13	66122	.274	.000	20.00	.00	8.150	1.669	1.669	3.591	.000	.737
14	66200	.267	.000	17.00	.00	9.338	1.885	1.885	3.500	.000	.702
15	66201	.269	.000	16.00	.00	8.766	1.828	1.828	3.515	.000	.709
16	66208	.300	.000	5.00	.00	2.834	.856	.856	3.933	.000	.877
17	66209	.300	.000	.00	.00	1.046	.234	.234	3.923	.000	.875
18	66214	.248	.000	-5.00	.00	2.304	-.361	-.361	3.281	.000	.609
19	66215	.248	.000	.00	.00	1.053	.233	.233	3.275	.000	.609
20	66216	.248	.000	5.00	.00	2.728	.848	.848	3.270	.000	.608
21	66221	.248	.000	8.00	.00	4.179	1.179	1.179	3.272	.000	.608
22	66222	.248	.000	10.00	.00	5.357	1.388	1.388	3.268	.000	.610
23	66223	.247	.000	12.00	.00	6.497	1.561	1.561	3.252	.000	.606
24	66300	.248	.000	14.00	.00	7.510	1.697	1.697	3.246	.000	.607
25	66301	.247	.000	16.00	.00	8.481	1.810	1.810	3.236	.000	.608
26	66302	.248	.000	17.20	.00	8.907	1.857	1.857	3.236	.000	.610
27	66303	.249	.000	20.00	.00	1.135	.912	.912	3.235	.000	.612
28	66304	.247	.000	25.00	.00	1.219	.962	.962	3.196	.000	.602
29	66305	.248	.000	17.00	.00	1.140	.839	.839	3.218	.000	.608
30	66306	.249	.000	15.00	.00	7.912	1.760	1.760	3.229	.000	.612
31	66307	.249	.000	14.00	.00	7.562	1.715	1.715	3.229	.000	.612
32	66308	.248	.000	12.00	.00	6.513	1.572	1.572	3.227	.000	.610
33	66313	.248	.000	5.00	.00	2.712	.838	.838	3.256	.000	.608
34	66314	.247	.000	.00	.00	1.035	.233	.233	3.250	.000	.606
35	66320	.184	.000	-5.00	.00	2.202	-.343	-.343	2.469	.000	.340
36	66321	.183	.000	.00	.00	1.033	.230	.230	2.461	.000	.339
37	66323	.184	.000	5.00	.00	2.677	.833	.833	2.464	.000	.341
38	66405	.183	.000	8.00	.00	4.059	1.163	1.163	2.464	.000	.339
39	66406	.183	.000	10.00	.00	5.074	1.334	1.334	2.458	.000	.339
40	66408	.184	.000	12.00	.00	6.136	1.510	1.510	2.459	.000	.340
41	66410	.184	.000	14.00	.00	7.152	1.643	1.643	2.457	.000	.340
42	66412	.183	.000	16.00	.00	7.964	1.750	1.750	2.453	.000	.339
43	66414	.184	.000	17.40	.00	8.494	1.827	1.827	2.456	.000	.341
44	66421	.183	.000	20.00	.00	1.038	.783	.783	2.456	.000	.338
45	66423	.183	.000	25.00	.00	.899	.875	.875	2.448	.000	.338
46	66500	.183	.000	17.00	.00	.927	.807	.807	2.451	.000	.339
47	66501	.183	.000	15.00	.00	1.002	.787	.787	2.452	.000	.339
48	66502	.183	.000	14.00	.00	.991	.775	.775	2.449	.000	.337
49	66503	.183	.000	13.00	.00	1.075	.798	.798	2.450	.000	.338
50	66504	.183	.000	12.00	.00	6.142	1.515	1.515	2.452	.000	.339
51	66510	.183	.000	5.00	.00	2.743	.847	.847	2.554	.000	.338
52	66511	.183	.000	.00	.00	1.311	.246	.246	2.556	.000	.339
53	66516	.108	.000	-5.00	.00	2.222	-.339	-.339	1.534	.000	.121
54	66517	.109	.000	.00	.00	1.097	.243	.243	1.536	.000	.122
55	66518	.109	.000	5.00	.00	2.750	.825	.825	1.534	.000	.121
56	66600	.109	.000	10.00	.00	4.977	1.311	1.311	1.528	.000	.122
57	66601	.109	.000	12.00	.00	5.893	1.417	1.417	1.519	.000	.120
58	66602	.109	.000	14.00	.00	6.784	1.541	1.541	1.517	.000	.120
59	66603	.108	.000	16.00	.00	7.700	1.654	1.654	1.516	.000	.121
60	66604	.109	.000	16.50	.00	7.777	1.681	1.681	1.518	.000	.121
61	66605	.109	.000	20.00	.00	.957	.773	.773	1.517	.000	.122
62	66606	.109	.000	25.00	.00	.981	.908	.908	1.520	.000	.122
63	66607	.109	.000	17.00	.00	.886	.698	.698	1.519	.000	.122
64	66608	.108	.000	15.00	.00	.839	.650	.650	1.514	.000	.121
65	66609	.109	.000	13.00	.00	.896	.632	.632	1.513	.000	.121

66	66610	.109	.000	12.00	.00	1.084	.863	.863	1.520	.000	.122
67	66611	.109	.000	11.50	.00	5.759	1.432	1.432	1.518	.000	.122
68	66616	.109	.000	5.00	.00	2.682	.822	.822	1.516	.000	.121
69	66617	.110	.000	.00	.00	1.118	.262	.262	1.529	.000	.124
70	66623	.183	.000	.00	.00	1.078	.234	.234	2.469	.000	.337
71	66701	.183	.000	5.00	.00	2.698	.837	.837	2.463	.000	.338
72	66703	.182	.000	10.00	.00	5.100	1.347	1.347	2.456	.000	.338
73	66705	.182	.000	12.00	.00	6.164	1.510	1.510	2.456	.000	.338
74	66707	.182	.000	14.70	.00	7.460	1.670	1.670	2.454	.000	.338
75	66709	.184	.000	15.50	.00	5.031	1.360	1.360	2.472	.000	.343
76	66711	.183	.000	17.00	.00	6.389	1.515	1.515	2.450	.000	.337
77	66716	.183	.000	18.00	.00	6.402	1.516	1.516	2.456	.000	.338
78	66718	.183	.000	20.00	.00	4.782	1.468	1.468	2.453	.000	.338
79	66720	.183	.000	25.00	.00	3.457	1.384	1.384	2.446	.000	.337
80	66722	.184	.000	17.00	.00	5.592	1.456	1.456	2.465	.000	.343
81	66800	.183	.000	14.70	.00	7.423	1.669	1.669	2.453	.000	.339
82	66802	.184	.000	.00	.00	1.011	.245	.245	2.460	.000	.341
83	66810	.299	.000	.00	.00	1.051	.225	.225	3.979	.000	.871
84	66812	.300	.000	5.00	.00	2.853	.863	.863	3.963	.000	.873
85	66814	.300	.000	8.00	.00	4.330	1.199	1.199	3.953	.000	.875
86	66818	.294	.000	12.00	.00	6.731	1.559	1.559	3.862	.000	.845
87	66820	.290	.000	13.00	.00	7.402	1.638	1.638	3.796	.000	.820
88	66822	.300	.000	.00	.00	1.055	.238	.238	3.915	.000	.874
89	67019	.183	.025	15.00	10.00	8.994	1.928	1.896	2.439	.830	.339
90	67021	.184	.099	15.00	10.00	11.018	2.308	2.230	2.433	3.300	.340
91	67023	.183	.198	15.00	10.00	11.665	2.436	2.384	2.428	6.600	.340
92	67108	.301	.024	10.00	5.00	8.214	1.678	1.678	3.809	1.340	.880
93	67110	.298	.049	10.00	5.00	8.511	1.714	1.706	3.754	2.680	.862
94	67112	.298	.099	10.00	5.00	8.711	1.742	1.737	3.744	5.360	.860
95	67120	.110	.099	15.00	10.00	11.227	2.306	2.244	1.482	1.960	.122
96	67201	.110	.099	10.00	10.00	9.750	1.988	1.970	1.483	1.960	.122
97	67208	.184	.025	10.00	10.00	9.338	1.898	1.894	2.462	.830	.341
98	67210	.185	.099	10.00	10.00	10.552	2.090	2.082	2.459	3.300	.343
99	67212	.184	.198	10.00	10.00	10.931	2.148	2.124	2.453	6.600	.341
100	67218	.184	.025	15.00	10.00	10.032	2.009	2.009	2.458	.830	.341
101	67220	.184	.099	15.00	10.00	12.536	2.356	2.346	2.455	3.300	.342
102	67222	.184	.198	15.00	10.00	13.919	2.471	2.460	2.454	6.600	.342
103	67305	.248	.099	15.00	10.00	13.272	2.362	2.311	3.254	4.460	.609
104	67310	.250	.099	10.00	10.00	11.751	2.127	2.114	3.264	4.460	.613
105	68019	.287	.011	15.00	5.00	9.679	1.846	1.833	3.792	.540	.803
106	68100	.288	.026	15.00	5.00	9.662	1.840	1.830	3.774	1.340	.806
107	68102	.286	.052	15.00	5.00	9.983	1.909	1.871	3.726	2.680	.796
108	68104	.287	.104	15.00	5.00	10.324	2.016	2.015	3.730	5.360	.803
109	68109	.291	.154	15.00	5.00	10.110	2.121	2.063	3.788	8.040	.822
110	68111	.293	.203	15.00	5.00	10.019	2.201	2.100	3.793	10.720	.833
111	68119	.297	.010	10.00	5.00	8.342	1.706	1.704	3.814	.540	.853
112	68121	.298	.025	10.00	5.00	8.384	1.713	1.713	3.793	1.340	.860
113	68123	.299	.049	10.00	5.00	8.569	1.751	1.743	3.791	2.680	.863
114	68201	.300	.098	10.00	5.00	8.717	1.779	1.767	3.805	5.360	.872
115	68203	.302	.196	10.00	5.00	9.059	1.865	1.851	3.824	10.720	.882
116	68211	.299	.198	5.00	5.00	5.579	1.356	1.347	3.843	10.720	.869
117	68219	.295	.050	12.00	2.00	7.961	1.675	1.675	3.767	2.680	.843
118	68221	.293	.101	12.00	2.00	8.099	1.699	1.694	3.726	5.360	.834
119	68304	.293	.201	12.00	2.00	8.491	1.744	1.735	3.722	10.720	.835
120	69019	.299	.010	10.00	10.00	8.793	1.737	1.726	3.950	.540	.871
121	69100	.300	.025	10.00	10.00	9.028	1.810	1.780	3.919	1.340	.873
122	69102	.300	.050	10.00	10.00	9.237	1.911	1.911	3.900	2.680	.876
123	69105	.301	.099	10.00	10.00	9.435	2.065	2.020	3.904	5.360	.877
124	69107	.300	.148	10.00	10.00	9.521	2.133	2.059	3.884	8.040	.876
125	69119	.273	.027	16.80	2.00	9.621	1.857	1.853	3.492	1.340	.727
126	69121	.270	.055	16.80	2.00	9.668	1.881	1.880	3.431	2.680	.710
127	69123	.268	.110	16.80	2.00	10.000	1.930	1.926	3.397	5.360	.700
128	69201	.267	.221	16.80	2.00	10.890	2.018	2.008	3.367	10.720	.692
129	69206	.275	.027	17.20	2.00	8.973	1.787	1.782	3.461	1.340	.734

130	69208	.277	.053	17.20	2.00	7.113	1.622	1.593	3.469	2.680	.745
131	69211	.270	.109	17.20	2.00	10.243	1.939	1.937	3.371	5.360	.709
132	69213	.272	.162	17.20	2.00	1.306	.985	.966	3.388	8.040	.719
133	69215	.279	.210	17.20	2.00	5.972	1.518	1.432	3.460	10.720	.755
134	69221	.273	.054	17.50	2.00	9.836	1.871	1.868	3.405	2.680	.726
135	69223	.265	.221	17.50	2.00	1.272	.994	.993	3.287	10.720	.684
136	69304	.266	.055	18.50	2.00	1.391	.928	.901	3.289	2.680	.688
137	69310	.262	.055	16.50	2.00	9.422	1.863	1.863	3.218	2.680	.671
138	70019	.185	.024	9.40	10.00	9.138	1.879	1.871	2.344	.830	.341
139	70021	.185	.097	9.40	10.00	10.202	2.046	2.032	2.339	3.300	.340
140	70023	.185	.195	9.40	10.00	10.584	2.112	2.083	2.337	6.600	.340
141	70107	.301	.010	5.70	10.00	8.730	1.764	1.758	3.916	.560	.875
142	70109	.301	.025	5.70	10.00	8.845	1.808	1.802	3.876	1.340	.876
143	70113	.300	.049	5.70	10.00	9.105	1.840	1.822	3.862	2.680	.872
144	70115	.301	.099	5.70	10.00	9.357	1.902	1.891	3.855	5.360	.875
145	70117	.301	.148	5.70	10.00	9.443	1.915	1.908	3.844	8.040	.874
ref#	case	avem	k	alpha0	alpha1	Cp Max	Cl max	Cl at	Re(mil)	freq	aveQ

The Sikorsky Airfoil (siky)

ref#	case	avem	k	alpha0	alpha1	Cp Max	Cl max	Cl at	Re(mil)	freq	aveQ
1	34022	.301	.000	.00	.00	.652	.110	.110	3.985	.000	.878
2	34100	.301	.000	5.00	.00	1.986	.715	.715	3.977	.000	.880
3	34102	.303	.000	10.00	.00	4.850	1.281	1.281	3.969	.000	.884
4	34107	.302	.000	12.00	.00	6.350	1.427	1.427	3.962	.000	.879
5	34109	.302	.000	13.00	.00	3.807	1.167	1.167	3.947	.000	.883
6	34111	.297	.000	14.00	.00	3.661	1.114	1.114	3.868	.000	.856
7	34113	.287	.000	16.00	.00	3.599	1.111	1.111	3.735	.000	.806
8	34115	.301	.000	.00	.00	.644	.110	.110	3.903	.000	.880
9	34200	.184	.000	.00	.00	.619	.095	.095	2.464	.000	.341
10	34202	.184	.000	5.00	.00	1.822	.675	.675	2.464	.000	.342
11	34204	.184	.000	10.00	.00	4.555	1.198	1.198	2.455	.000	.342
12	34208	.184	.000	13.00	.00	6.914	1.467	1.467	2.449	.000	.342
13	34210	.184	.000	14.00	.00	3.885	1.142	1.142	2.448	.000	.342
14	34212	.184	.000	16.00	.00	3.788	1.099	1.099	2.441	.000	.341
15	34214	.184	.000	.00	.00	.630	.118	.118	2.445	.000	.341
16	35021	.301	.000	-5.00	.00	3.059	-.523	-.523	3.836	.000	.880
17	35023	.301	.000	-2.00	.00	1.062	-.152	-.152	3.820	.000	.878
18	35100	.301	.000	.00	.00	.684	.094	.094	3.816	.000	.877
19	35102	.301	.000	2.00	.00	1.158	.335	.335	3.820	.000	.880
20	35103	.301	.000	5.00	.00	1.995	.693	.693	3.812	.000	.877
21	35111	.302	.000	8.00	.00	3.465	1.081	1.081	4.009	.000	.881
22	35112	.302	.000	10.00	.00	5.123	1.293	1.293	3.991	.000	.879
23	35114	.301	.000	12.00	.00	6.983	1.470	1.470	3.960	.000	.877
24	35116	.295	.000	13.00	.00	8.117	1.549	1.549	3.868	.000	.845
25	35118	.293	.000	13.50	.00	8.788	1.581	1.581	3.836	.000	.836
26	35123	.302	.000	14.00	.00	5.059	1.247	1.247	3.928	.000	.879
27	35200	.293	.000	16.00	.00	4.172	1.075	1.075	3.809	.000	.832
28	35206	.301	.000	14.00	.00	5.395	1.294	1.294	3.893	.000	.874
29	35207	.291	.000	13.00	.00	7.977	1.538	1.538	3.761	.000	.822
30	35208	.295	.000	12.50	.00	7.324	1.488	1.488	3.802	.000	.845
31	35213	.302	.000	5.00	.00	1.979	.691	.691	3.895	.000	.878
32	35214	.302	.000	.00	.00	.668	.104	.104	3.895	.000	.883
33	35220	.249	.000	-5.00	.00	3.074	-.508	-.508	3.240	.000	.610
34	35221	.249	.000	-2.00	.00	.953	-.135	-.135	3.232	.000	.611
35	35222	.250	.000	.00	.00	.680	.097	.097	3.234	.000	.613
36	35223	.249	.000	2.00	.00	1.163	.336	.336	3.228	.000	.612
37	35300	.250	.000	5.00	.00	1.989	.688	.688	3.229	.000	.613
38	35305	.249	.000	8.00	.00	3.267	1.042	1.042	3.194	.000	.612
39	35306	.249	.000	10.00	.00	4.945	1.260	1.260	3.195	.000	.614
40	35307	.249	.000	12.00	.00	6.747	1.450	1.450	3.176	.000	.610

41	35308	.248	.000	13.00	.00	7.707	1.534	1.534	3.168	.000	.609
42	35309	.247	.000	13.50	.00	7.426	1.489	1.489	3.151	.000	.605
43	35310	.250	.000	14.10	.00	5.000	1.257	1.257	3.175	.000	.615
44	35313	.249	.000	16.00	.00	4.211	1.079	1.079	3.172	.000	.614
45	35314	.249	.000	18.00	.00	3.944	.978	.978	3.155	.000	.611
46	35315	.248	.000	20.00	.00	3.920	.952	.952	3.139	.000	.609
47	35316	.250	.000	25.00	.00	1.144	.893	.893	3.136	.000	.612
48	35317	.249	.000	14.00	.00	5.238	1.295	1.295	3.143	.000	.611
49	35318	.250	.000	13.00	.00	7.674	1.522	1.522	3.143	.000	.612
50	35319	.249	.000	12.50	.00	7.241	1.486	1.486	3.140	.000	.611
51	35400	249	.000	5.00	.00	1.939	.677	.677	3.166	.000	.614
52	35401	.249	.000	.00	.00	.657	.101	.101	3.154	.000	.611
53	36019	.184	.000	-5.00	.00	2.912	-.466	-.466	2.510	.000	.342
54	36020	.185	.000	.00	.00	.646	.125	.125	2.503	.000	.341
55	36022	.185	.000	5.00	.00	1.883	.704	.704	2.494	.000	.341
56	36106	.185	.000	10.00	.00	4.815	1.246	1.246	2.468	.000	.341
57	36108	.185	.000	12.00	.00	6.436	1.426	1.426	2.462	.000	.341
58	36110	.184	.000	13.50	.00	7.843	1.555	1.555	2.452	.000	.340
59	36112	.185	.000	14.00	.00	8.326	1.585	1.585	2.448	.000	.341
60	36117	.183	.000	15.00	.00	5.938	1.330	1.330	2.428	.000	.338
61	36118	.184	.000	16.00	.00	5.101	1.192	1.192	2.432	.000	.340
62	36120	.185	.000	20.00	.00	4.074	.951	.951	2.425	.000	.341
63	36202	.110	.000	-5.00	.00	2.870	-.441	-.441	1.457	.000	.123
64	36203	.111	.000	.00	.00	.637	.143	.143	1.462	.000	.124
65	36204	.110	.000	5.00	.00	1.923	.704	.704	1.455	.000	.123
66	36209	.110	.000	10.00	.00	4.670	1.193	1.193	1.429	.000	.122
67	36210	.109	.000	12.00	.00	6.226	1.397	1.397	1.421	.000	.121
68	36211	.110	.000	13.50	.00	7.373	1.504	1.504	1.428	.000	.122
69	36212	.110	.000	14.00	.00	7.892	1.550	1.550	1.431	.000	.124
70	36213	.110	.000	15.00	.00	4.401	1.163	1.163	1.421	.000	.122
71	36216	.110	.000	15.50	.00	5.165	1.274	1.274	1.425	.000	.123
72	36217	.109	.000	16.00	.00	4.606	1.157	1.157	1.413	.000	.121
73	36218	.109	.000	20.00	.00	4.208	1.027	1.027	1.409	.000	.120
74	33022	.073	.099	15.00	10.00	15.381	2.520	2.247	.975	1.300	.054
75	33106	.110	.098	15.00	10.00	16.264	2.496	2.242	1.462	1.960	.124
76	33110	.183	.099	15.00	10.00	16.937	2.573	2.306	2.400	3.300	.339
77	33118	.182	.050	6.20	10.00	10.914	1.735	1.734	2.391	1.650	.334
78	33121	.184	.198	6.20	10.00	10.832	1.733	1.704	2.409	6.600	.340
79	33205	.219	.099	15.00	10.00	15.376	2.436	2.178	2.838	3.930	.479
80	33207	.249	.098	15.00	10.00	13.261	2.392	2.074	3.185	4.460	.612
81	33215	.279	.100	15.00	10.00	11.822	2.395	1.998	3.745	4.980	.762
82	33217	.297	.025	15.00	10.00	10.480	1.902	1.808	3.921	1.310	.855
83	33222	.296	.049	15.00	10.00	10.804	2.095	1.878	3.887	2.620	.852
84	33300	.292	.100	15.00	10.00	11.101	2.303	1.935	3.817	5.240	.832
85	34223	.292	.025	15.00	10.00	7.674	1.819	1.720	3.739	1.310	.826
86	34306	.292	.050	15.00	10.00	9.978	2.058	1.822	3.876	2.620	.828
87	34308	.288	.102	15.00	10.00	10.920	2.372	1.950	3.800	5.240	.807
88	34318	.184	.050	15.00	10.00	11.152	2.149	1.868	2.482	1.650	.340
89	34321	.184	.100	15.00	10.00	12.591	2.437	2.050	2.476	3.300	.341
90	34323	.184	.150	15.00	10.00	13.443	2.573	2.163	2.472	4.950	.341
91	34409	.279	.156	15.00	10.00	11.248	2.443	2.029	3.601	7.860	.762
92	34418	.302	.098	4.40	10.00	9.665	1.689	1.681	3.865	5.360	.881
93	37023	.300	.025	10.00	10.00	9.896	1.820	1.754	3.936	1.350	.866
94	37101	.301	.050	10.00	10.00	10.250	2.033	1.865	3.929	2.680	.876
95	37107	.302	.099	10.00	10.00	10.512	2.173	1.908	3.915	5.360	.880
96	37109	.302	.148	10.00	10.00	10.636	2.229	1.947	3.894	8.040	.879
97	37119	.302	.049	4.10	10.00	9.461	1.646	1.642	3.867	2.680	.879
98	37121	.303	.098	4.10	10.00	9.617	1.673	1.664	3.860	5.360	.886
99	37123	.302	.147	4.10	10.00	9.885	1.698	1.683	3.836	8.040	.879
100	37207	.302	.024	10.00	5.00	9.200	1.603	1.602	3.784	1.340	.879
101	37208	.301	.049	10.00	5.00	9.634	1.662	1.661	3.750	2.680	.871
102	37210	.302	.097	10.00	5.00	9.898	1.727	1.714	3.760	5.360	.879
103	37213	.303	.145	10.00	5.00	10.127	1.768	1.752	3.780	8.040	.885
104	37215	.303	.194	10.00	5.00	10.325	1.887	1.815	3.764	10.720	.883

105	37219	.301	.049	11.00	5.00	9.779	1.720	1.680	3.753	2.680	.871
106	37221	.302	.097	11.00	5.00	10.077	1.879	1.779	3.753	5.360	.878
107	37304	.301	.050	12.00	8.00	10.204	1.968	1.822	4.001	2.680	.878
108	37305	.301	.100	12.00	8.00	10.555	2.110	1.891	3.984	5.360	.878
109	37306	.301	.127	12.00	8.00	10.594	2.247	1.949	3.970	6.810	.876
110	38021	.302	.025	15.00	5.00	9.544	1.733	1.669	3.955	1.340	.879
111	38022	.299	.050	15.00	5.00	9.992	1.886	1.771	3.894	2.680	.865
112	38102	.294	.101	15.00	5.00	10.652	2.069	1.884	3.785	5.360	.840
113	38103	.293	.152	15.00	5.00	10.903	2.152	1.924	3.747	8.040	.830
114	38104	.289	.205	15.00	5.00	11.097	2.292	2.014	3.688	10.720	.808
115	38119	.300	.198	14.00	2.00	10.334	1.960	1.832	3.854	10.720	.870
116	38201	.301	.197	12.30	2.00	9.648	1.667	1.662	3.876	10.720	.876
117	38216	.183	.010	6.20	10.00	9.855	1.690	1.688	2.469	.330	.339
118	38300	.298	.010	15.00	10.00	9.318	1.711	1.660	3.951	.540	.862
119	38306	.299	.010	10.00	10.00	9.253	1.652	1.631	3.932	.530	.869
120	39021	.300	.010	4.10	10.00	8.553	1.579	1.579	3.812	.530	.875
121	39104	.297	.010	15.00	5.00	9.399	1.643	1.626	3.927	.530	.856
122	39110	.299	.010	11.00	5.00	9.064	1.599	1.596	3.897	.530	.869
123	39115	.298	.010	14.00	2.00	8.873	1.574	1.573	3.839	.540	.865
124	38110	.293	.202	16.00	2.00	8.952	1.857	1.754	3.755	10.720	.832
125	39107	.300	.010	10.00	5.00	9.186	1.611	1.611	3.939	.530	.876
ref#	case	avem	k	alpha0	alpha1	Cp Max	Cl max	Cl at	Re(mil)	freq	aveQ

The Vr7 Airfoil (Vr07)

ref#	case	avem	k	alpha0	alpha1	Cp Max	Cl max	Cl at	Re(mil)	freq	aveQ
1	46018	.108	.000	-5.00	.00	2.066	-.421	-.421	1.551	.000	.121
2	46019	.108	.000	.00	.00	.896	.182	.182	1.546	.000	.121
3	46020	.109	.000	5.00	.00	1.659	.841	.841	1.558	.000	.123
4	46101	.107	.000	10.00	.00	4.432	1.440	1.440	1.513	.000	.118
5	46102	.109	.000	12.00	.00	6.067	1.522	1.522	1.540	.000	.122
6	46103	.109	.000	12.50	.00	6.260	1.534	1.534	1.548	.000	.123
7	46104	.109	.000	13.00	.00	6.519	1.547	1.547	1.544	.000	.123
8	46105	.109	.000	13.50	.00	6.518	1.511	1.511	1.542	.000	.123
9	46106	.109	.000	14.00	.00	6.479	1 502	1.502	1.536	.000	.122
10	46107	.109	.000	15.00	.00	6.606	1.429	1.429	1.538	.000	.122
11	46108	.109	.000	17.00	.00	6.425	1.305	1.305	1.541	.000	.123
12	46109	.109	.000	20.00	.00	6.481	1.194	1.194	1.534	.000	.122
13	46110	.108	.000	25.00	.00	1.201	.988	.988	1.523	.000	.120
14	46116	.184	.000	-5.00	.00	2.021	-.417	-.417	2.551	.000	.341
15	46117	.183	.000	.00	.00	.795	.185	.185	2.553	.000	.342
16	46119	.183	.000	5.00	.00	1.529	.781	.781	2.547	.000	.341
17	46203	.184	.000	10.00	.00	4.245	1.370	1.370	2.562	.000	.343
18	46205	.183	.000	12.00	.00	6.132	1.504	1.504	2.551	.000	.341
19	46207	.183	.000	12.50	.00	6.387	1.511	1.511	2.553	.000	.342
20	46209	.184	.000	13.00	.00	6.349	1.486	1.486	2.554	.000	.342
21	46211	.183	.000	13.50	.00	6.414	1.474	1.474	2.551	.000	.341
22	46217	.183	.000	14.00	.00	6.688	1.493	1.493	2.638	.000	.342
23	46219	.183	.000	15.00	.00	6.687	1.443	1.443	2.630	.000	.341
24	46221	.183	.000	17.00	.00	6.173	1.243	1.243	2.624	.000	.340
25	46223	.183	.000	20.00	.00	6.179	1.134	1.134	2.623	.000	.340
26	46301	.183	.000	25.00	.00	5.640	1.056	1.056	2.615	.000	.340
27	46307	.248	.000	-5.00	.00	2.088	-.421	-.421	3.482	.000	.612
28	46308	.249	.000	-2.00	.00	2.076	-.062	-.062	3.477	.000	.613
29	46309	.248	.000	.00	.00	.814	.195	.195	3.469	.000	.612
30	46310	.248	.000	2.00	.00	.990	.424	.424	3.461	.000	.611
31	46311	.248	.000	5.00	.00	1.570	.811	.811	3.463	.000	.614
32	46317	.249	.000	8.00	.00	2.819	1.176	1.176	3.458	.000	.615
33	46318	.248	.000	10.00	.00	4.163	1.380	1.380	3.435	.000	.611
34	46319	.248	.000	12.00	.00	6.261	1.548	1.548	3.433	.000	.613
35	46320	.249	.000	12.50	.00	6.700	1.571	1.571	3.430	.000	.615
36	46321	.248	.000	13.00	.00	6.539	1.533	1.533	3.419	.000	.612
37	46322	.248	.000	13.50	.00	6.603	1.543	1.543	3.410	.000	.610

38	46323	.249	.000	14.00	.00	6.604	1.538	1.538	3.418	.000	.613
39	46400	.249	.000	15.00	.00	6.827	1.523	1.523	3.413	.000	.613
40	46403	.249	.000	17.00	.00	6.016	1.230	1.230	3.428	.000	.616
41	46404	.249	.000	20.00	.00	5.855	1.121	1.121	3.412	.000	.615
42	46405	.248	.000	25.00	.00	5.581	1.049	1.049	3.397	.000	.614
43	46406	.249	.000	13.00	.00	6.473	1.512	1.512	3.399	.000	.613
44	46407	.248	.000	12.00	.00	6.235	1.536	1.536	3.392	.000	.610
45	46412	.248	.000	.00	.00	.779	.179	.179	3.394	.000	.614
46	46418	.300	.000	-5.00	.00	1.964	-.409	-.409	3.996	.000	.877
47	46420	.301	.000	-2.00	.00	2.027	-.056	-.056	3.986	.000	.878
48	46423	.300	.000	2.00	.00	.960	.434	.434	3.967	.000	.875
49	46500	.300	.000	5.00	.00	1.553	.810	.810	3.966	.000	.877
50	46508	.300	.000	8.00	.00	2.752	1.171	1.171	4.162	.000	.878
51	46509	.298	.000	10.00	.00	4.080	1.387	1.387	4.126	.000	.870
52	46511	.299	.000	12.00	.00	6.176	1.558	1.558	4.119	.000	.876
53	46513	.299	.000	12.50	.00	6.474	1.562	1.562	4.100	.000	.874
54	46515	.298	.000	13.00	.00	6.376	1.534	1.534	4.071	.000	.867
55	46517	.300	.000	13.50	.00	6.256	1.525	1.525	4.088	.000	.879
56	46519	.300	.000	14.00	.00	6.363	1.516	1.516	4.077	.000	.878
57	46600	.299	.000	15.00	.00	6.374	1.461	1.461	4.089	.000	.873
58	46602	.300	.000	17.00	.00	5.688	1.220	1.220	4.078	.000	.878
59	46604	.291	.000	20.00	.00	5.676	1.133	1.133	3.956	.000	.831
60	46608	.265	.000	25.00	.00	5.096	1.039	1.039	3.627	.000	.690
61	46609	.299	.000	13.00	.00	6.276	1.529	1.529	4.071	.000	.876
62	46610	.299	.000	12.00	.00	6.058	1.542	1.542	4.055	.000	.872
63	46615	.300	.000	.00	.00	.788	.192	.192	4.097	.000	.881
64	46621	.183	.000	.00	.00	.784	.179	.179	2.523	.000	.340
65	46623	.183	.000	5.00	.00	1.519	.790	.790	2.515	.000	.340
66	46701	.183	.000	10.00	.00	3.789	1.325	1.325	2.513	.000	.340
67	46703	.183	.000	12.00	.00	5.177	1.377	1.377	2.515	.000	.341
68	46705	.183	.000	13.00	.00	5.093	1.313	1.313	2.506	.000	.340
69	46707	.182	.000	14.00	.00	5.263	1.322	1.322	2.502	.000	.338
70	46712	.183	.000	15.00	.00	5.496	1.332	1.332	2.518	.000	.340
71	46714	.184	.000	16.00	.00	4.387	1.036	1.036	2.517	.000	.341
72	46716	.184	.000	20.00	.00	3.625	.906	.906	2.518	.000	.343
73	46718	.183	.000	.00	.00	.772	.180	.180	2.519	.000	.342
74	46802	.300	.000	.00	.00	.785	.193	.193	4.205	.000	.881
75	46804	.300	.000	5.00	.00	1.537	.815	.815	4.185	.000	.881
76	46806	.301	.000	10.00	.00	3.913	1.376	1.376	4.171	.000	.886
77	46808	.300	.000	12.00	.00	4.878	1.420	1.420	4.148	.000	.882
78	46810	.301	.000	13.00	.00	4.980	1.444	1.444	4.140	.000	.883
79	46815	.300	.000	14.00	.00	4.871	1.369	1.369	4.137	.000	.881
80	46817	.300	.000	15.00	.00	4.495	1.180	1.180	4.108	.000	.877
81	46819	.299	.000	16.00	.00	3.899	1.049	1.049	4.091	.000	.877
82	46821	.287	.000	20.00	.00	3.440	.953	.953	3.898	.000	.806
83	46823	.300	.000	.00	.00	.785	.191	.191	4.085	.000	.881
84	45019	.300	.025	15.00	10.00	9.990	1.814	1.810	4.062	1.310	.873
85	45021	.292	.051	15.00	10.00	11.709	2.107	2.089	3.938	2.620	.830
86	45023	.293	.101	15.00	10.00	11.845	2.330	2.147	3.931	5.240	.835
87	45101	.285	.155	15.00	10.00	12.436	2.489	2.216	3.825	7.860	.793
88	45109	.301	.010	10.00	10.00	8.442	1.655	1.649	4.033	.540	.873
89	45111	.301	.025	10.00	10.00	9.776	1.770	1.770	4.011	1.340	.875
90	45113	.301	.050	10.00	10.00	10.836	2.001	1.999	4.010	2.680	.878
91	45117	.301	.100	10.00	10.00	11.149	2.204	2.072	4.019	5.360	.875
92	45119	.302	.150	10.00	10.00	11.127	2.292	2.116	4.015	8.040	.879
93	45203	.300	.010	15.00	5.00	7.329	1.591	1.568	4.019	.540	.869
94	45205	.301	.025	15.00	5.00	8.772	1.674	1.665	4.008	1.340	.876
95	45207	.301	.050	15.00	5.00	9.919	1.812	1.812	4.006	2.680	.877
96	45209	.300	.100	15.00	5.00	11.003	2.061	2.053	3.986	5.360	.871
97	45211	.298	.151	15.00	5.00	11.309	2.204	2.089	3.957	8.040	.860
98	45213	.295	.204	15.00	5.00	11.612	2.321	2.141	3.909	10.720	.841
99	45221	.302	.025	10.00	5.00	8.227	1.645	1.636	4.054	1.340	.878
100	45223	.301	.050	10.00	5.00	9.030	1.699	1.691	4.033	2.680	.877
101	45300	.301	.100	10.00	5.00	9.667	1.776	1.767	4.032	5.360	.878

102	45302	.302	.150	10.00	5.00	10.055	1.822	1.811	4.030	8.040	.879
103	45303	.301	.200	10.00	5.00	10.444	1.874	1.859	4.027	10.720	.878
104	47020	.299	.025	15.00	10.00	7.632	1.659	1.651	4.059	1.310	.859
105	47100	.292	.101	15.00	10.00	11.275	2.333	2.164	3.929	5.240	.820
106	47110	.184	.051	15.00	10.00	11.486	1.835	1.830	2.578	1.650	.338
107	47112	.185	.101	15.00	10.00	16.100	2.259	2.198	2.586	3.300	.342
108	47114	.185	.151	15.00	10.00	19.502	2.609	2.502	2.581	4.950	.342
109	47123	.073	.101	15.00	10.00	15.198	2.476	2.332	1.031	1.300	.054
110	47206	.110	.101	15.00	10.00	16.313	2.412	2.263	1.553	1.960	.123
111	47213	.185	.102	15.00	10.00	18.228	2.361	2.290	2.607	3.300	.340
112	47217	.221	.101	15.00	10.00	16.968	2.478	2.286	3.036	3.930	.479
113	47301	.250	.101	15.00	10.00	14.465	2.386	2.236	3.408	4.460	.610
114	47305	.281	.100	15.00	10.00	12.415	2.368	2.165	3.784	4.980	.760
115	54019	.183	.026	10.00	10.00	10.272	1.733	1.713	2.633	.830	.340
116	54022	.183	.051	10.00	10.00	12.652	1.890	1.866	2.616	1.650	.340
117	54101	.183	.102	10.00	10.00	15.857	2.100	2.091	2.607	3.300	.339
118	54110	.184	.153	10.00	10.00	17.367	2.186	2.164	2.598	4.950	.341
119	54113	.184	.203	10.00	10.00	18.073	2.232	2.210	2.588	6.600	.341
120	54116	.184	.254	10.00	10.00	18.668	2.269	2.247	2.581	8.250	.341
121	54216	.184	.151	15.00	10.00	20.706	2.652	2.491	2.548	4.950	.340
122	48019	.299	.010	4.10	10.00	7.744	1.626	1.608	4.216	.540	.874
123	48023	.300	.025	4.10	10.00	8.446	1.678	1.665	4.190	1.340	.880
124	48101	.299	.051	4.10	10.00	9.129	1.728	1.720	4.160	2.680	.877
125	48103	.300	.102	4.10	10.00	9.581	1.777	1.764	4.154	5.360	.879
126	48116	.299	.025	13.00	2.00	7.716	1.622	1.606	4.085	1.340	.878
127	48118	.299	.050	13.00	2.00	8.477	1.653	1.643	4.059	2.680	.878
128	48122	.299	.101	13.00	2.00	9.288	1.721	1.716	4.058	5.360	.876
129	48209	.298	.203	16.00	2.00	10.388	1.868	1.829	4.059	10.720	.870
130	48215	.300	.050	14.00	2.00	8.170	1.652	1.648	4.058	2.680	.877
131	48216	.300	.101	14.00	2.00	9.265	1.736	1.734	4.048	5.360	.879
132	48217	.300	.201	14.00	2.00	10.389	1.848	1.848	4.038	10.720	.879
133	48300	.300	.010	12.50	2.00	7.004	1.579	1.576	4.033	.540	.878
134	48301	.300	.025	12.50	2.00	7.532	1.614	1.604	4.012	1.340	.878
135	48302	.301	.050	12.50	2.00	8.134	1.653	1.641	4.009	2.680	.881
136	48303	.299	.100	12.50	2.00	8.879	1.695	1.689	3.986	5.360	.874
137	48304	.299	.151	12.50	2.00	9.264	1.724	1.716	3.980	8.040	.873
138	48308	.300	.201	12.50	2.00	9.533	1.753	1.742	3.998	10.720	.875
139	49110	.184	.026	15.00	10.00	10.487	1.751	1.728	2.634	.830	.339
140	49117	.185	.051	15.00	10.00	13.496	1.947	1.938	2.620	1.650	342
141	49120	.185	.101	15.00	10.00	18.147	2.333	2.270	2.600	3.300	.340
142	49203	.185	.152	15.00	10.00	20.917	2.673	2.510	2.593	4.950	.341
143	49206	.185	.202	15.00	10.00	22.491	2.890	2.714	2.585	6.600	.341
144	49216	.184	.025	4.70	10.00	8.283	1.619	1.609	2.560	.830	.340
145	49300	.184	.101	4.70	10.00	9.343	1.719	1.701	2.536	3.300	.338
146	49307	.185	.201	4.70	10.00	9.275	1.708	1.680	2.549	6.600	.342
147	49310	.185	.250	4.70	10.00	9.359	1.716	1.675	2.544	8.250	.343
148	49023	.184	.010	15.00	10.00	8.565	1.571	1.555	2.543	.330	.338
149	50116	.183	.010	4.70	10.00	7.362	1.556	1.550	2.531	.330	.339
150	57018	.184	.152	15.00	10.00	20.935	2.662	2.519	2.555	4.950	.340
151	58018	.183	.150	15.00	10.00	20.554	2.700	2.546	2.438	4.950	.338
152	58102	.037	.098	15.00	10.00	12.243	2.363	2.330	.497	.650	.014
153	58111	.109	.101	15.00	10.00	16.684	2.436	2.299	1.529	1.960	.121
154	58120	.184	.151	15.00	10.00	21.218	2.766	2.612	2.536	4.950	.340
155	58121	.184	.101	15.00	10.00	18.361	2.426	2.362	2.532	3.300	.340
156	47022	.296	.050	15.00	10.00	9.995	1.900	1.900	3.990	2.620	.841
157	48200	.301	.201	13.00	2.00	9.883	1.792	1.785	4.062	10.720	.884
ref#	case	avem	k	alpha0	alpha1	Cp Max	Cl max	Cl at	Re(mil)	freq	aveQ

The Wortmann Airfoil (wort)

ref#	case	avem	k	alpha0	alpha1	Cp Max	Cl max	Cl at	Re(mil)	freq	aveQ

1	17208	.301	.000	.00	.00	.711	.168	.168	3.975	.000	.877
2	17212	.301	.000	5.00	.00	1.632	.749	.749	3.929	.000	.880
3	17220	.302	.000	10.00	.00	5.387	1.266	1.266	3.911	.000	.879
4	17303	.296	.000	12.00	.00	7.173	1.372	1.372	3.802	.000	.847
5	17305	.300	.000	13.00	.00	6.221	1.255	1.255	3.836	.000	.870
6	17310	.299	.000	14.00	.00	5.953	1.241	1.241	3.820	.000	.866
7	17312	.299	.000	15.00	.00	4.460	1.046	1.046	3.806	.000	.866
8	17314	.292	.000	16.00	.00	3.212	.953	.953	3.710	.000	.828
9	18019	.184	.000	.00	.00	.668	.172	.172	2.399	.000	.341
10	18102	.185	.000	5.00	.00	1.538	.699	.699	2.401	.000	.343
11	18106	.184	.000	10.00	.00	5.081	1.207	1.207	2.379	.000	.339
12	18108	.185	.000	12.00	.00	7.147	1.346	1.346	2.389	.000	.343
13	18115	.185	.000	13.00	.00	7.993	1.363	1.363	2.395	.000	.346
14	18117	.185	.000	14.00	.00	4.056	.875	.875	2.389	.000	.345
15	18119	.184	.000	15.00	.00	6.154	1.211	1.211	2.375	.000	.341
16	18121	.184	.000	16.00	.00	4.730	1.031	1.031	2.368	.000	.340
17	18123	.184	.000	19.90	.00	6.335	1.229	1.229	2.371	.000	.342
18	18206	.184	.000	.00	.00	.627	.132	.132	2.380	.000	.341
19	18215	.110	.000	-5.00	.00	3.388	-.395	-.395	1.500	.000	.122
20	18217	.110	.000	-2.00	.00	1.375	-.057	-.057	1.502	.000	.123
21	18218	.109	.000	.00	.00	.708	.156	.156	1.488	.000	.121
22	18220	.110	.000	2.00	.00	.985	.388	.388	1.494	.000	.122
23	18221	.109	.000	4.00	.00	1.377	.633	.633	1.487	.000	.121
24	18304	.109	.000	8.00	.00	3.494	1.042	1.042	1.480	.000	.121
25	18305	.110	.000	10.00	.00	5.353	1.230	1.230	1.483	.000	.122
26	18307	.109	.000	12.00	.00	7.616	1.401	1.401	1.476	.000	.122
27	18312	.109	.000	13.00	.00	8.791	1.439	1.439	1.467	.000	.121
28	18319	.109	.000	13.50	.00	8.489	1.371	1.371	1.470	.000	.123
29	18321	.110	.000	14.00	.00	7.316	1.310	1.310	1.474	.000	.124
30	18323	.110	.000	15.00	.00	6.402	1.078	1.078	1.464	.000	.122
31	18401	.109	.000	16.00	.00	5.806	.975	.975	1.461	.000	.122
32	18410	.111	.000	18.00	.00	1.119	.770	.770	1.460	.000	.124
33	18411	.110	.000	20.00	.00	1.087	.765	.765	1.448	.000	.123
34	18413	.109	.000	25.00	.00	1.221	1.017	1.017	1.445	.000	.123
35	18414	.110	.000	20.00	.00	1.086	.805	.805	1.440	.000	.122
36	18421	.109	.000	16.00	.00	1.048	.815	.815	1.446	.000	.123
37	18422	.110	.000	14.00	.00	7.500	1.317	1.317	1.438	.000	.122
38	18423	.109	.000	13.00	.00	7.785	1.348	1.348	1.440	.000	.122
39	18500	.110	.000	11.00	.00	6.370	1.285	1.285	1.438	.000	.122
40	18501	.109	.000	5.00	.00	1.545	.751	.751	1.436	.000	.122
41	18502	.110	.000	.00	.00	.658	.165	.165	1.440	.000	.122
42	19020	.185	.000	-5.00	.00	3.525	-.413	-.413	2.455	.000	.342
43	19022	.184	.000	-2.00	.00	1.382	-.066	-.066	2.448	.000	.342
44	19023	.185	.000	.00	.00	.602	.199	.199	2.441	.000	.340
45	19101	.185	.000	2.00	.00	.827	.436	.436	2.444	.000	.341
46	19110	.185	.000	4.00	.00	1.172	.653	.653	2.400	.000	.340
47	19116	.185	.000	8.00	.00	3.444	1.109	1.109	2.379	.000	.341
48	19117	.185	.000	10.00	.00	5.247	1.290	1.290	2.373	.000	.340
49	19119	.185	.000	12.00	.00	7.493	1.448	1.448	2.380	.000	.343
50	19121	.183	.000	13.00	.00	8.394	1.417	1.417	2.355	.000	.338
51	19123	.185	.000	13.50	.00	8.834	1.513	1.513	2.371	.000	.343
52	19204	.185	.000	14.00	.00	8.080	1.370	1.370	2.362	.000	.340
53	19206	.185	.000	15.00	.00	6.720	1.285	1.285	2.365	.000	.342
54	19208	.185	.000	16.00	.00	5.750	1.050	1.050	2.361	.000	.342
55	19213	.185	.000	18.00	.00	1.318	.934	.934	2.366	.000	.341
56	19214	.185	.000	20.00	.00	1.138	.848	.848	2.358	.000	.340
57	19216	.184	.000	25.00	.00	1.024	.967	.967	2.351	.000	.341
58	19217	.185	.000	20.00	.00	1.100	.869	.869	2.348	.000	.340
59	19221	.185	.000	16.00	.00	5.928	1.078	1.078	2.359	.000	.341
60	19222	.186	.000	14.00	.00	7.716	1.428	1.428	2.365	.000	.343
61	19223	.185	.000	13.00	.00	8.361	1.473	1.473	2.353	.000	.340
62	19300	.185	.000	11.00	.00	6.134	1.346	1.346	2.354	.000	.341
63	19305	.185	.000	5.00	.00	1.482	.767	.767	2.357	.000	.340
64	19308	.185	.000	.00	.00	.566	.192	.192	2.355	.000	.340

65	19314	.250	.000	-5.00	.00	3.631	-.411	-.411	3.151	.000	.614
66	19316	.250	.000	-2.00	.00	1.324	-.089	-.089	3.138	.000	.611
67	19317	.250	.000	.00	.00	.610	.144	.144	3.138	.000	.612
68	19401	.251	.000	2.00	.00	.909	.384	.384	3.301	.000	.616
69	19402	.251	.000	4.00	.00	1.274	.628	.628	3.297	.000	.616
70	19405	.251	.000	8.00	.00	3.184	1.066	1.066	3.288	.000	.617
71	19406	.250	.000	10.00	.00	5.356	1.288	1.288	3.276	.000	.614
72	19411	.251	.000	12.00	.00	7.905	1.459	1.459	3.278	.000	.617
73	19413	.251	.000	13.00	.00	8.630	1.503	1.503	3.268	.000	.618
74	19415	.251	.000	13.50	.00	8.119	1.428	1.428	3.265	.000	.620
75	19423	.250	.000	14.00	.00	7.743	1.387	1.387	3.236	.000	.613
76	19504	.250	.000	15.00	.00	6.603	1.199	1.199	3.233	.000	.613
77	19506	.250	.000	16.00	.00	5.773	1.027	1.027	3.229	.000	.613
78	19508	.248	.000	18.00	.00	4.870	1.057	1.057	3.195	.000	.602
79	20019	.249	.000	25.00	.00	.984	.873	.873	3.162	.000	.610
80	20020	.250	.000	20.00	.00	4.353	1.129	1.129	3.159	.000	.612
81	20021	.250	.000	16.00	.00	5.915	1.039	1.039	3.163	.000	.614
82	20022	.250	.000	14.00	.00	7.710	1.385	1.385	3.164	.000	.614
83	20103	.249	.000	13.00	.00	8.674	1.459	1.459	3.155	.000	.610
84	20104	.249	.000	11.00	.00	6.382	1.322	1.322	3.151	.000	.609
85	20109	.250	.000	5.00	.00	1.503	.716	.716	3.157	.000	.613
86	20112	.250	.000	.00	.00	.671	.170	.170	3.152	.000	.615
87	20118	.304	.000	-5.00	.00	3.880	-.417	-.417	3.775	.000	.883
88	20122	.303	.000	-2.00	.00	1.381	-.091	-.091	3.777	.000	.883
89	20123	.302	.000	.00	.00	.647	.150	.150	3.759	.000	.877
90	20203	.303	.000	2.00	.00	.872	.375	.375	3.749	.000	.879
91	20204	.302	.000	4.00	.00	1.284	.614	.614	3.742	.000	.876
92	20210	.303	.000	8.00	.00	3.484	1.036	1.036	3.769	.000	.878
93	20211	.302	.000	10.00	.00	5.211	1.249	1.249	3.764	.000	.880
94	20213	.299	.000	12.00	.00	7.201	1.388	1.388	3.709	.000	.860
95	20222	.291	.000	13.00	.00	8.716	1.487	1.487	3.821	.000	.821
96	20300	.295	.000	13.50	.00	8.328	1.416	1.416	3.849	.000	.841
97	20302	.301	.000	14.00	.00	6.954	1.314	1.314	3.916	.000	.875
98	20307	.299	.000	15.00	.00	5.693	1.043	1.043	3.904	.000	.866
99	20309	.302	.000	16.00	.00	5.766	1.033	1.033	3.913	.000	.877
100	20311	.294	.000	18.00	.00	5.829	.970	.970	3.812	.000	.835
101	20312	.275	.000	20.00	.00	1.468	.902	.902	3.577	.000	.737
102	20317	.261	.000	25.00	.00	.906	.850	.850	3.411	.000	.668
103	20318	.275	.000	20.00	.00	1.248	.866	.866	3.578	.000	.740
104	20319	.302	.000	16.00	.00	5.551	.994	.994	3.892	.000	.881
105	20320	.302	.000	14.00	.00	6.726	1.290	1.290	3.889	.000	.882
106	20321	.300	.000	13.00	.00	8.007	1.399	1.399	3.850	.000	.867
107	20322	.302	.000	11.00	.00	6.627	1.375	1.375	3.875	.000	.879
108	16019	.036	.101	15.00	10.00	7.680	2.159	1.583	.488	.657	.013
109	16105	.074	.097	15.00	10.00	17.546	2.367	2.063	.986	1.300	.056
110	16114	.110	.098	15.00	10.00	20.332	2.473	2.228	1.463	1.960	.123
111	16200	.185	.098	15.00	10.00	20.967	2.422	2.177	2.430	3.300	.343
112	16213	.184	.050	6.50	10.00	14.515	1.776	1.770	2.502	1.650	.340
113	16215	.184	.200	6.50	10.00	14.994	1.789	1.761	2.495	6.600	.340
114	16300	.220	.099	15.00	10.00	17.431	2.340	2.053	2.891	3.930	.481
115	16308	.249	.099	15.00	10.00	14.001	2.312	1.851	3.229	4.460	.612
116	17100	.184	.050	15.00	10.00	12.805	1.872	1.732	2.457	1.650	.340
117	17103	.184	.099	15.00	10.00	13.654	2.227	1.861	2.453	3.300	.341
118	17109	.184	.149	15.00	10.00	13.852	2.368	1.896	2.453	4.950	.342
119	17117	.293	.025	15.00	10.00	9.515	1.563	1.533	3.772	1.310	.830
120	17119	.291	.050	15.00	10.00	10.201	1.836	1.646	3.725	2.620	.823
121	17200	.290	.100	15.00	10.00	10.669	2.160	1.660	3.702	5.240	.814
122	21100	.291	.010	15.00	10.00	9.955	1.517	1.510	3.719	.520	.823
123	21107	.299	.010	10.00	10.00	9.524	1.495	1.492	3.792	.530	.867
124	21200	.301	.010	10.00	5.00	9.381	1.486	1.486	3.932	.530	.875
125	21208	.302	.010	3.30	10.00	8.999	1.492	1.470	3.899	.530	.882
126	21219	.184	.010	6.50	10.00	11.028	1.531	1.528	2.455	.326	.339
127	22023	.293	.025	15.00	10.00	9.638	1.572	1.564	3.728	1.310	.827
128	22103	.294	.049	15.00	10.00	10.600	1.815	1.667	3.749	2.620	.837

129	22201	.285	.101	15.00	10.00	11.393	2.144	1.772	3.554	5.240	.785
130	22206	.279	.154	15.00	10.00	11.825	2.222	1.835	3.477	7.860	.754
131	22208	.281	.097	15.00	10.00	11.704	2.231	1.729	3.484	4.980	.763
132	22216	.302	.024	10.00	10.00	10.192	1.597	1.577	3.732	1.340	.875
133	22217	.302	.049	10.00	10.00	10.170	1.780	1.619	3.720	2.680	.875
134	22218	.300	.098	10.00	10.00	10.324	2.001	1.687	3.685	5.360	.862
135	22219	.294	.149	10.00	10.00	10.837	2.091	1.753	3.619	8.040	.835
136	22307	.301	.025	10.00	5.00	9.942	1.525	1.520	3.854	1.340	.875
137	22308	.303	.049	10.00	5.00	10.185	1.592	1.592	3.857	2.680	.880
138	22309	.303	.098	10.00	5.00	10.375	1.694	1.662	3.853	5.360	.881
139	22311	.302	.148	10.00	5.00	10.446	1.738	1.676	3.850	8.040	.877
140	22312	.303	.196	10.00	5.00	10.278	1.838	1.721	3.849	10.720	.882
141	23021	.298	.025	15.00	5.00	10.044	1.550	1.550	3.792	1.340	.858
142	23022	.297	.050	15.00	5.00	10.444	1.665	1.637	3.750	2.680	.851
143	23023	.295	.100	15.00	5.00	10.762	1.863	1.724	3.717	5.360	.840
144	23100	.292	.152	15.00	5.00	11.026	1.993	1.765	3.671	8.040	.822
145	23107	.300	.099	5.00	5.00	5.128	1.244	1.242	3.803	5.360	.867
146	23109	.300	.197	5.00	5.00	5.549	1.268	1.255	3.789	10.720	.867
147	23117	.300	.098	5.00	10.00	10.449	1.733	1.671	3.803	5.360	.869
148	23201	.299	.100	3.80	10.00	10.600	1.683	1.682	3.948	5.360	.866
149	23206	.299	.050	3.30	10.00	10.286	1.613	1.603	3.924	2.680	.866
150	23208	.300	.100	3.30	10.00	10.443	1.645	1.640	3.914	5.360	.871
151	23211	.300	.149	3.30	10.00	10.624	1.651	1.650	3.896	8.040	.870
152	23219	.299	.199	12.00	2.00	10.622	1.696	1.692	3.866	10.720	.864
153	23305	.298	.200	14.00	2.00	10.617	1.877	1.714	3.832	10.720	.858
154	23310	.294	.201	16.00	2.00	9.812	1.769	1.589	3.769	10.720	.839
155	21112	.301	.010	15.00	5.00	9.332	1.478	1.473	3.940	.530	.873
156	23101	.287	.205	15.00	5.00	11.254	2.177	1.833	3.617	10.720	.800
ref#	case	avem	k	alpha0	alpha1	Cp Max	Cl max	Cl at	Re(mil)	freq	aveQ

Appendix B. Lorber and Carta data

Glossary:

ref#	Case number for this study
case	case number from UTRC
avem	average Mach number
Pitch rate	pitching rate of airfoil, $(\partial\alpha/\partial t)c/(2U)$
alpha0	maximum angle for ramp up mean angle for sinusoidal
alpha1	initial angle for ramp up amplitude of oscillation for sinusoidal
$C_{p_{Max}}$	Maximum suction peak
$C_{\ell max}$	Maximum lift coefficient
C_ℓ at	lift Coefficient at $C_{p_{Max}}$

The Airfoil is Sikorsky SSC-A09

ref#	case	avem	Pitch rate	alpha0	alpha1	$C_{p_{Max}}$	$C_{\ell max}$	C_ℓ at
1	8.01	.200	.001	10.00	.00	12.044	19.431	6.056
2	8.02	.200	.003	10.00	.00	11.418	19.431	6.978
3	8.03	.200	.005	10.00	.00	11.878	19.565	8.360
4	8.04	.200	.010	10.00	.00	12.412	19.565	10.295
5	9.04	.200	.001	15.00	.00	12.535	29.508	1.231
6	9.05	.200	.003	15.00	.00	11.738	29.685	.837
7	9.06	.200	.005	15.00	.00	12.451	29.685	1.952
8	9.07	.200	.010	15.00	.00	12.682	29.685	4.016
9	15.02	.200	.020	15.00	.00	13.644	29.685	8.797
10	10.01	.200	.005	15.00	.00	12.621	29.724	3.538
11	10.02	.200	.001	15.00	.00	11.967	29.724	.061
12	20.05	.400	.001	10.00	.00	†	†	†
13	21.02	.400	.003	10.00	.00	5.636	29.724	3.153
14	21.01	.400	.005	10.00	.00	5.460	29.724	5.154
15	21.03	.400	.010	10.00	.00	5.599	29.724	5.031
16	22.03	.300	.005	10.00	.00	8.626	29.724	7.989
17	22.04	.300	.010	15.00	.00	8.976	29.724	4.121
18	22.01	.300	.054	12.00	8.00	8.428	29.724	11.531
19	22.02	.300	.110	9.00	8.00	9.029	29.724	15.017
ref#	case	avem	Pitch rate	alpha0	alpha1	$C_{p_{Max}}$	$C_{\ell max}$	C_ℓ at

† Values were not consistent with other cases.